Synthesis and characterization of cyclic polyethers with controlled orientation of the dipolar moment along the chain contour

Jordan Ochs

Departamento de Física de Materiales

Thesis Director: Fabienne Barroso-Bujans

Tutor: Angel Alegria

eman ta zabal zazu

Universidad del País Vasco   Euskal Herriko Unibertsitatea

Resumen

La síntesis de macromoléculas con estructuras bien controladas ha sido el foco de muchas investigaciones en química de polímeros. Las propiedades físicas y químicas de un material dependen de sus características moleculares, como el peso molecular, la polidispersidad, los grupos funcionales y la topología. El desarrollo de rutas sintéticas que permitan el control sobre las características moleculares ha llevado a la preparación de materiales cada vez más complejos como por ejemplo cepillos poliméricos, polímeros en estrella y escalera, dendrímeros, polímeros hiperramificados, redes y polímeros cíclicos. Se han realizado amplios estudios para vincular las propiedades físicas (i.e., temperatura de transición vítrea y de fusión, viscosidad intrínseca y de fundido, termoestabilidad, solubilidad, propiedades reológicas y viscoelásticas) y las propiedades químicas (i.e., reactividad y estabilidad) a la estructura covalente de un material.

Los grupos finales de un polímero tienen una gran influencia sobre las propiedades mencionadas anteriormente, lo que hace que los polímeros cíclicos sean únicos, debido a su ausencia de grupos finales. A pesar de sus interesantes propiedades reológicas y térmicas, hasta la fecha se han desarrollado pocas aplicaciones que utilicen polímeros cíclicos. La dificultad para producir polímeros cíclicos puros en gran cantidad ha hecho que, por el momento, estos materiales sean de bajo interés para la industria. Por esta razón una gran cantidad de estudios se han enfocado en mejorar las técnicas sintéticas para producir polímeros cíclicos altamente puros. Además, ejemplos de moléculas cíclicas naturales como las proteínas cíclicas, los péptidos cíclicos o el ADN cíclico han

fomentado una investigación más profunda de sus propiedades únicas conferidas por la ausencia de extremos de cadena.

A pesar de un enorme esfuerzo en el estudio de las relaciones estructura-propiedad en polímeros cíclicos, la microestructura dipolar de dichos materiales ha quedado fuera del alcance de la gran mayoría de esos trabajos. Debido a que esta propiedad está relacionada con el momento dipolar asociado a la cadena principal ($\overrightarrow{P_A}$), la microestructura dipolar depende principalmente de la regioquímica, es decir, de la orientación de las unidades de monómero dentro de la cadena del polímero, y de la topología, es decir, de la configuración general de una estructura macromolecular. En el caso de polímeros que presentan un componente de momento dipolar neto a lo largo del contorno de la cadena, esta propiedad puede vincularse con sus características arquitectónicas. En este caso, la identificación de la microestructura dipolar puede proporcionar información importante sobre la pureza topológica y las propiedades dinámicas de una cadena de polímero.

El estudio de la microestructura dipolar de polímeros sintéticos no es sencillo y requiere de muestras con estructura precisa y con una alta pureza. El objetivo de esta tesis es la preparación de polímeros cíclicos regio-regulares que tengan microestructuras dipolares y pesos moleculares controlados y una baja polidispersidad. Se eligió el poli(glicidil fenil éter) (PGPE) como muestra de estudio ya que es un polímero que presenta señales dieléctricas intensas y por tanto permite el estudio de los modos dieléctricos segmentales y de cadena de forma adecuada.

En esta tesis se sintetizaron muestras de PGPE cíclicos con microestructuras dipolares controladas mediante la técnica de cierre de anillo. Una parte importante de este trabajo se centró en la caracterización de los precursores lineales para garantizar la fidelidad de sus grupos finales de cadena ya que es un parámetro esencial para la síntesis de cadenas monocíclicas puras a través de la técnica de cierre de anillo. La

polimerización aniónica de apertura de anillo del glicidil fenil éter (GPE) se eligió como estrategia para la síntesis de precursores lineales de PGPE. Para verificar la composición de los grupos finales de cadenas se utilizó la desorción/ionización láser asistida por una matriz con detección de masas por tiempo de vuelo (MALDI-ToF MS) y la resonancia magnética nuclear (RMN).

Se estudiaron dos casos principales. Primero, los polímeros que tienen cada unidad de monómero alineada en la misma dirección dando como resultado una microestructura dipolo no invertida. En segundo lugar, las cadenas de polímeros que presentan una inversión del dipolo en el medio de la cadena. Para la primera serie de muestras se consiguió obtener α-azida, ω-hidroxi PGPE con una gran fidelidad de grupo final mediante la utilización de azida de tetrabutilamonio y el conocido activador de monómero triisobutilaluminio (iBu$_3$Al), el cual fue necesario para evitar reacciones de transferencia al monómero durante la polimerización. Sin embargo, para la segunda serie de polímeros, con inversión del dipolo, la utilización del iBu$_3$Al fue inapropiada. De hecho, se descubrió que para la síntesis de PGPE mediante la iniciación con etilenglicol y una base de fosfaceno, t-BuP$_4$, el iBu$_3$Al promovía varias reacciones secundarias que no daban lugar a la formación de cadenas terminadas en dos grupos hidroxilos y por tanto, la síntesis resultaba en poca fidelidad de grupos finales. En este caso, las reacciones de transferencia al monómero se eliminaron ajustando la relación de GPE / t-BuP$_4$ > 50. Finalmente se evaluó la orientación del dipolo a lo largo del contorno de la cadena mediante la espectroscopía dieléctrica de banda ancha (BDS).

Los polímeros cíclicos sin inversión de dipolo se prepararon mediante cicloadición azida-alquino catalizada con cobre (I) y aquellos con inversión de dipolo mediante acoplamiento alquino-alquino (i.e., Glaser coupling). Para esto, los grupos terminales hidroxilo de los precursores lineales fueron inicialmente transformados en grupos alquinos mediante reacción de propargilación. La formación de las estructuras cíclicas

y su pureza topológica se evaluaron mediante cromatografía de exclusión por tamaños (SEC), además de las técnicas de MALDI-ToF MS y BDS.

La formación de cadenas de alto peso molecular por acoplamiento intermolecular es una de las principales fuentes de impurezas durante la ciclación mediante la técnica de cierre de anillo. Para abordar este problema se realizó una serie de experimentos con el objetivo de evaluar la influencia de los diferentes parámetros de la reacción de ciclación sobre la pureza cíclica. Finalmente se destacó la importancia del estado de oxidación del catalizador de cobre tanto en las reacciones de acoplamiento como en las condiciones experimentales óptimas para la preparación de cadenas monocíclicas puras.

Finalmente, el estudio mediante BDS de la relajación dieléctrica alfa y del modo normal de los polímeros regio-regulares cíclicos sintetizados permitió identificar la formación de las microestructuras dipolares deseadas. En los polímeros cíclicos con dipolos no invertidos, el momento dipolar a lo largo de la cadena se cancela dando lugar a la desaparición del modo normal. Estos resultados se utilizaron para validar la pureza cíclica de estos polímeros, lo que además mostró por primera vez la utilidad del BDS para este propósito no convencional. En el caso de los polímeros con inversión de dipolo, éstos presentan una relajación dieléctrica del modo normal que refleja específicamente las fluctuaciones del diámetro del anillo. Esta importante característica permitió evaluar la dinámica del anillo, lo que resultó en una relajación 1,5 veces más lenta que la relajación análoga en el precursor lineal a la temperatura de transición vítrea. Estos resultados muestran el potencial de los macrociclos con dipolo invertido en el estudio de problemas físicos fundamentales en polímeros cíclicos.

Chapter I

Introduction

Table of Contents

1. <u>Motivations</u>

The synthesis of macromolecules with well controlled structures has been the focus of many investigations in polymer chemistry. Both physical and chemical properties of a material depend on its molecular characteristics such as molecular weight, polydispersity, functional groups and topology. The development of synthetic routes allowing control over molecular characteristics have led to the preparation of more and more complex materials including polymer brushes, star polymers, ladder polymers, dendrimers, hyperbranched polymers, networks and cyclic polymers. Extensive studies have been made to link physical properties (i.e. glass transition temperature (T_g), melt temperature, intrinsic and melt viscosities, thermostability, solubility, rheological and viscoelastic properties) and chemical properties (i.e. reactivity and stability) to the covalent structure of a material.

The end groups of a polymer have a large influence over the abovementioned properties, making the cyclic polymers unique, because of their absence of end groups. Despite their interesting rheological and thermal properties, few applications using cyclic polymers have been developed to date. The difficulty to produce high quantity of pure cyclic polymers has made those materials of low interest for the industry. For these reasons, better synthetic techniques to yield highly pure cyclic polymers have been the focus of a large number of studies. Moreover, examples of natural cyclic molecules such as cyclic proteins,[1] cyclic peptides[2] or cyclic DNA[3] have encouraged deeper investigation of their unique properties conferred by the absence of chain ends.

Because of the extra constrains imposed by their ring structure, cyclic polymers have a more compact coil conformation. This property was demonstrated in early works by Kramers[4] and Stockmayer,[5] where the authors found that the radius of gyration of cyclic chains was approximately half of that of linear chains with similar molecular weights. This is due to the lower conformational degree of freedom in cyclic chains[6] resulting in a lower hydrodynamic volume. As a result, cyclic polymers exhibit lower intrinsic viscosity compared to their linear analogues.[7] The rheological properties are also affected by the cyclic topology. For example, the melt viscosity of rings is inherently smaller than that of linear chains.[8,9] Extensive studies have demonstrated the influence of the cyclic topology over the thermal properties of a polymer. For example, cyclic polymers exhibit a higher values of T_g compared to their linear counterparts.[10,11] For certain polymers, the same trends have been observed for crystallization temperatures[12,13] and melting temperatures.[14] However, some studies have shown the exact opposite effect.[15,16] Additionally, cyclic polymers were found to have a much weaker dependence of the T_g with the molecular weight.[17] Interestingly, a decrease of T_g with the increase of molecular weight has been observed for cyclic poly(dimethylsiloxane).[18] This unique behavior was interpreted as the higher stiffness of cyclic chains of lower degree of polymerization.[19] Additionally, new structural features arise from the "endless" structure of ring polymers, such as the presence of knots[20,21] and concatenated structures.[22]

Despite an enormous effort in the study of structure-property relationships in cyclic polymers, the dipolar microstructure of such materials has remained out of the scope of the large majority of those works. Because it is related with the dipole moment associated to the main chain $(\overrightarrow{P_A})$, the dipolar microstructure is a property that mainly

depends on the regiochemistry, i.e. the orientation of the monomer units within the polymer chain, and the topology, i.e. the overall configuration of a macromolecular structure. In the case of polymers presenting a net dipole moment component along the chain contour, this property can be linked to the architectural features of a polymer chain. In this case, identification of the dipolar microstructure can give important information over the topological purity and dynamic properties of a polymer chain.

The study of the dipolar microstructure of synthetic polymers is not straightforward and requires samples with precise structures and high purity. The aim of this thesis is the preparation of regio-regular cyclic polymers having controlled dipolar microstructures, controlled molecular weights and low polydispersity.

2. <u>Polymers with controlled dipolar microstructure</u>

According to Stockmayer,[23] type A polymers present fix dipole moments of the monomeric unit parallel to the main chain backbone.[24] In the case of linear regio-regular polymers (Figure 1a), where every monomer unit is aligned in the same direction, the dipole moment associated to the main chain $(\overrightarrow{P_A})$ is proportional to the end-to-end vector $(\overrightarrow{R_N})$. In the following sections, a polymer displaying this dipolar microstructure will be referred to as linear 1-arm polymer (l-1a-polymer).

If a polymer is composed of two symmetric subchains with monomers oriented in the same direction within each subchain but with opposite direction between the subchains, a linear polymer with a distinct dipolar microstructure, here referred to as linear 2-arm polymer (*l*-2a-polymer), is obtained (Figure 1b). In this case, each subchain presents a resulting dipole moment that is proportional to the end-to-end vector of the subchain or "arm" $\overrightarrow{R_{N/2}}$.

On the other hand, the chain topology imposes additional features to the resulting dipole moment $\overrightarrow{P_A}$. Upon cyclization of a *l*-1a-polymer, $\overrightarrow{P_A}$ cancels because the end-to-end vector is now equal to zero. Here after, a cyclic polymer characterized by this dipolar microstructure will be referred to as cyclic 1-arm polymer (*c*-1a-polymer). The cyclization of a *l*-2a-polymer will result in a cyclic polymer characterized by $\overrightarrow{P_A} \propto \overrightarrow{R_{N/2}}$ (Figure 1d). A polymer displaying such dipolar microstructure will be referred to as cyclic 2-arm polymer (*c*-2a-polymer).

If the monomer orientation is not controlled during polymerization, regio-irregular structures are formed and the dipolar microstructures presented in Figure 1e and 1f are obtained. Both structures are characterized by $\overrightarrow{P_A} \neq 0$.[25] However, the module of the resulting dipole moment is small and its direction different for each synthesized macromolecule.
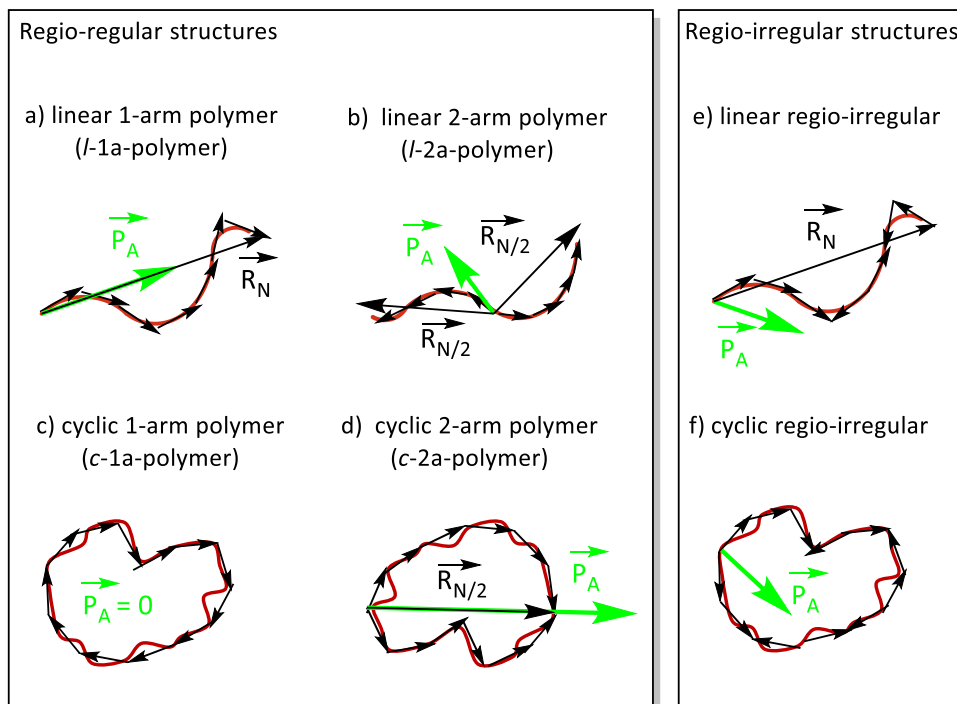
Figure 1. Schematic representation of polymers having different dipolar microstructures.

By monitoring the fluctuations of $\overrightarrow{P_A}$, it is possible to evaluate the dipolar microstructure of a polymer sample after synthesis. Moreover, important information over cyclic purity (Figure 1a) or cyclic dynamics (Figure 1d and 1f) can be obtained. The most adequate technique to evaluate such structures is broadband dielectric spectroscopy (BDS), as explained further below.

3. <u>Ring opening polymerization of epoxides</u>

Specific synthetic routes must be followed to prepare polymers having distinct dipolar microstructures. For example, a *l*-1a-polymer, as depicted in Figure 1a, can be prepared using a monofunctional initiator throughout a polymerization mechanism allowing the alignment of the monomer units in a single direction. If instead a bifunctional initiator is used, a *l*-2a-polymer will be obtained (Figure 1b). Monosubstituted epoxy monomers are characterized by large dipole moment of the monomer unit.[25] Therefore they are good candidates for the preparation of polymers chains presenting a dipolar moment associated to the main chain. Moreover, they can be polymerized under mild conditions due to their high reactivity.

Ring-opening polymerization (ROP) is a chain-growth polymerization in which the terminal end group of a polymer chain acts as a reactive center propagating the polymerization reaction. A large number of monomers can be polymerized by ROP including epoxides, cyclic esters, cyclic amines, cyclic sulfides and cyclic olefins.[26,27] Polymerization is favored thermodynamically for all ring monomers of 3 to 8 atoms, with the exception of 6-membered rings where polymerization is generally not observed.[28] Cyclic monomers can polymerize due to the loss of enthalpy associated with the loss of ring strain, which is considerable in the case of three-membered rings.[29] Moreover, the polarization of the CO bound increases the reactivity of epoxide monomers towards ROP.[30]

During ROP of monosubstituted epoxides, regio-errors can frequently occur.[31] The attack on the epoxy ring can occur on the methine (1) or the methylene group (2) (Figure 2). If only one process occurs, then only head-to-tail linkage or tail-to-head linkage will be formed. However, in the case of occurring both processes, head-to-head and tail-to-tail linkage will be formed leading to regio-irregular structures. Analysis of the triad regiosequence by ^{13}C nuclear magnetic resonance (NMR) gives information about the polymer microstructure. The percentage of the type of linkage present in a polymer can be obtained by integration of the corresponding signals.[32]
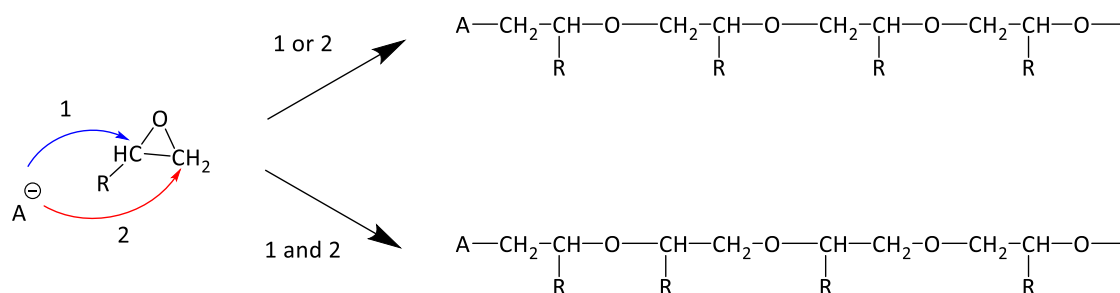

Figure 2. Nucleophilic attack leading to regio-regular and regio-irregular polyethers.

When a nucleophilic attack on a heterocyclic monomer initiates the reaction, the polymerization is described as anionic ring opening polymerization (AROP). During AROP of monosubstituted epoxides, the nucleophile attack of the alkoxide chain end generally proceeds selectively on the methylene carbon.[33] Therefore, the presence of regio-errors within the chain is greatly reduced compared to cationic ROP.

3.1. <u>Anionic ring opening polymerization</u>

3.1.1. Conventional anionic ring opening of epoxide monomers

With the exception of some four-membered ring oxetanes, three membered ring epoxides are the only cyclic ethers that can be polymerized by anionic polymerization. Larger rings are exclusively polymerized by a cationic ring opening mechanism. Typically, the anionic polymerization of monosubstituted epoxides follows three steps (Figure 3): a bimolecular initiation to form an alkoxide species, propagation via the alkoxide group and termination.
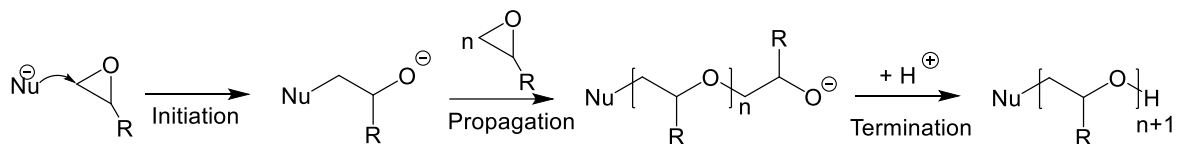
Figure 3. AROP of epoxides initiated by a nucleophile.

Monomers such as ethylene oxide,[34] lactide[35] and hexamethylcyclotrisiloxane[36] have been successfully polymerized by AROP. Alkali metals derivatives, especially sodium, potassium and cesium have been extensively used for the AROP of epoxides.[37,38] Although higher polymerization rates are obtained when larger counterions are used,[39,40] conventional AROP of epoxide monomers is generally limited by slow kinetics.

For that reason, other initiation systems have been developed. Notably, the addition of crown ethers[41] and aluminum-based catalysts,[42] as well as organic initiators[43,44] have allowed faster polymerization.

3.1.2. Initiation by phosphazene bases

Among organic initiators, phosphazene bases[45] are of particular interest for the AROP of epoxides monomers. These strong Brönsted bases are highly hindered with pKa ranging from 26.9 to 42.6, with t-BuP$_4$ being the most basic (Figure 4).[46]
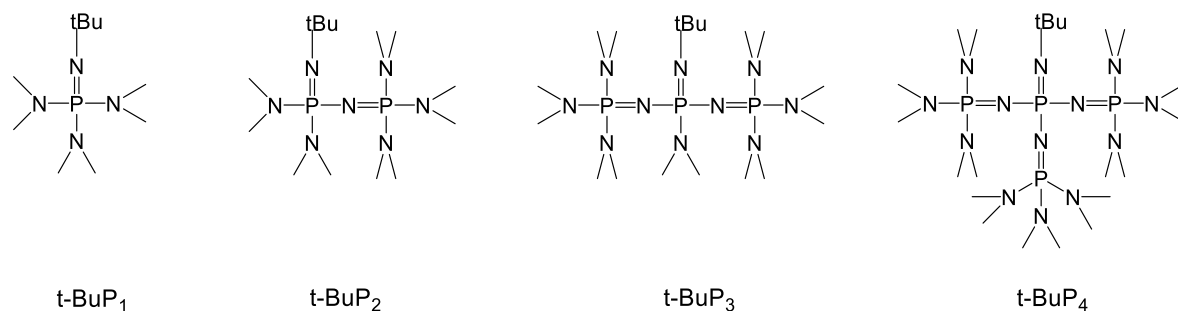

Figure 4. Structures of the different phosphazene bases reported by Schwesinger et al.[45]

Due to their high basicity, phosphazene bases are able to deprotonate alcohols,[47] amides[48] and carboxylic acids[49] to form alkoxides, azanides and carboxylates,

respectively, which are capable to initiate the ring opening of epoxide monomers. This strategy offers the possibility to incorporate a wide range of functional groups at one end of the polymer chain (Figure 5).
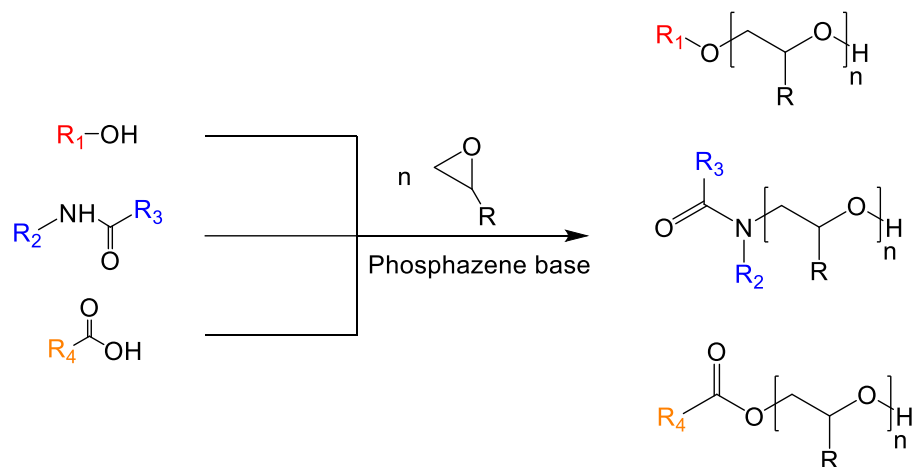

Figure 5. Combination of phosphazene base with alcohols, amides and carboxylic acids for the AROP of epoxide monomers.

When used for the AROP of epoxides, phosphazene bases form soft and highly delocalized counterions. Due to their large size, the distance between the charges of the counterion and the chain end is larger, helping to reduce aggregation phenomena during polymerization.[50] Moreover, the use of soft counterions increases the reactivity of the active chain end, increasing the polymerization rate.[51] The synthesis of poly(methyl methacrylate),[52] poly(butylene oxide),[53] poly(glycidyl ether)[54,55] and many other polymers[56] has been successfully achieved using phosphazene bases as counterions.

Zhang et al.[57] used phosphazene bases to partially deprotonate mono- and multifunctional alcohols such as 2-(allyloxy)ethan-1-ol, 1,4-phenylenedimethanol and 2,2-bis(hydroxymethyl)propane-1,3-diol for the AROP of ethylene oxide, propylene oxide, butylene oxide as well as vinyl glycidyl ether and tert-butyl glycidyl ether. The use of an initiator having multiple functional groups allowed the formation of star polymers having two, three and four arms. A fast proton exchange between the base and the active chain end allowed controlled polymerization even at phosphazene concentration as low as 5 % with respect to the alcohol.

In 2013 Kakuchi et al. reported the use of 2,2-bis((6-azidohexyloxy)methy)- propane-1,3-diol in combination with t-BuP$_4$ for the synthesis of four-arm star polymers.[53] The obtained polymer had two arms terminated in azide groups while the two others were terminated in hydroxyls, which were further modified into alkynes. Under high dilution, the azide and alkyne end groups were linked via intramolecular coupling to form eight-shaped polymers. This reaction is known as the copper(I)-catalyzed alkyne-azide cycloaddition (CuCAA) and will be further explained in the following section. The obtained star and eight-shaped polymers had controlled molecular arm length, molecular weights and polydispersity. Later, an initiator having two azide groups and two hydroxyls groups was used in combination with t-BuP$_4$ for the preparation of block copolymers of 2-(2-(2-methoxyethoxy)ethoxy)ethyl glycidyl ether as a hydrophilic monomer and decyl glycidyl ether as a hydrophobic monomer.[58] After modification of the hydroxyl end groups into alkynes, the copper(I)-catalyzed alkyne-azide cycloaddition reaction was performed under high dilution for the preparation of four-armed caged shaped amphiphilic polymers with controlled molecular characteristics.

Those works are great examples of the use of phosphazene bases in AROP of epoxides for the preparation of polymers with controlled topologies.

3.1.3. Transfer to monomer

During AROP of monosubstituted epoxides, such as propylene oxide (POx), side reactions can frequently occur leading to a poor control over the molecular weight, polydispersity and chemical structure of the obtained polymer. In the case of POx, the abstraction of a proton from the methyl group can take place and lead to transfer to monomer (Figure 6). This side reaction can drastically limit the molecular weight of final polymer chains.[59]
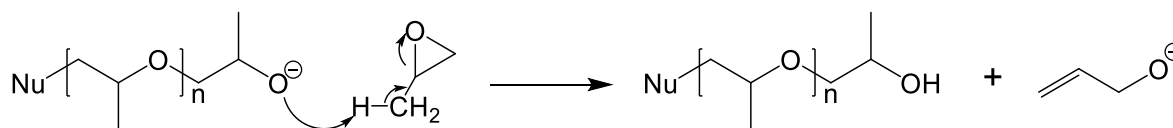

Figure 6. Transfer to monomer reaction during AROP of propylene oxide.

Deffieux et al.[60] reported the synthesis of propylene oxide initiated by alkali metal and an excess of triisobutylaluminium (iBu$_3$Al). The authors demonstrated the absence of transfer reactions in the presence of the Lewis acid. It is believed that iBu$_3$Al is forming

a 1:1 "ate" complex with the initiator while simultaneously activates the monomer (Figure 7). Activation of the monomer makes the epoxy ring much more likely to undergo a nucleophilic attack from the propagating chain and, at the same time, reduces the basicity of the propagating chain end thus limiting the proton abstraction on the methyl group leading to transfer to monomer reactions.
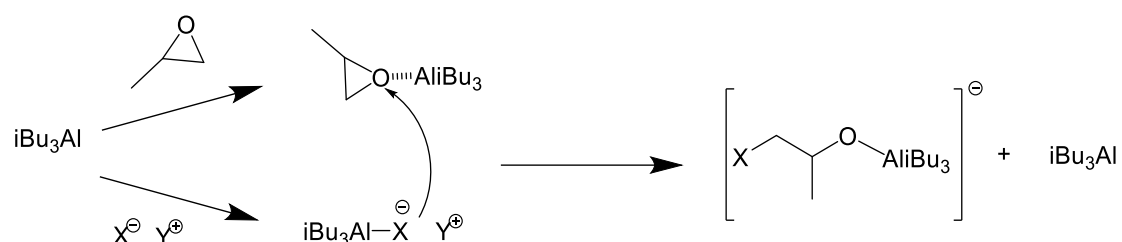

Figure 7. Monomer activation by iBu_3Al in the AROP of propylene oxide with a metal alkoxide (X^-Y^+).[61]

Later, the kinetics of polymerization using chloro(tert-butyl)phenylphosphine, sodium isopropoxide or tetraoctylammonium bromide as initiator, and iBu_3Al as monomer activator was studied.[61] The authors demonstrated that the polymerization rate was higher in the presence of iBu_3Al for all onium salts, although faster kinetics was observed with tetraoctylammonium bromide. The same authors also demonstrated the conservation of the living character of the polymerization in the presence of iBu_3Al.[62]

Another transfer to monomer mechanism for glycidyl phenyl ether was observed by Stolarzewicz[63] (Figure 8). In this case, the proton of the methine group is abstracted to

yield a carbanion able to initiate the AROP of epoxide monomers. According to the author, this mechanism could also occur during AROP of POx. Fortunately, the addition of iBu₃Al was efficient to prevent transfer to monomer via both mechanisms described in Figure 6 and 8.
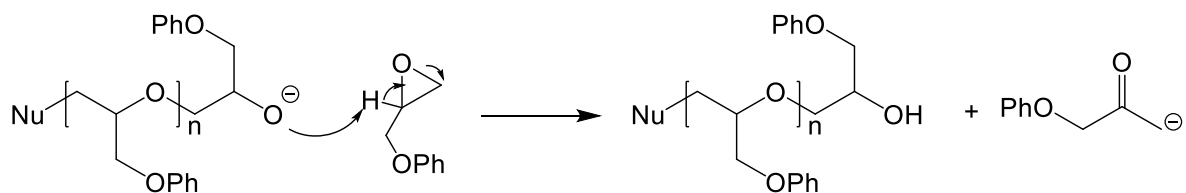

Figure 8. Second type of transfer to monomer reaction in the case of poly(glycidyl phenyl ether).

AROP of epoxides is a suitable synthetic route for the preparation of polyethers with controlled structure. By playing with the functionality of the initiator, different architectures can be obtained. Moreover, AROP allows the synthesis of polymers with controlled regio-order, regiochemistry and controlled tacticity. for optically pure monomers.

4. <u>Synthesis of cyclic polymers</u>

Cyclic polymers have been prepared by different strategies. The first examples of cyclic polymers were those synthesized by ring chain equilibration.[64] However, only low molecular weight rings were obtained with high polydispersity. The linear precursor could not be properly isolated making the characterization of the cyclic chains complicated. To that respect, the ring expansion polymerization and the ring closure strategies are more appropriated for the synthesis of well-defined macrocyclic structures.[65–68] Examples of cyclic polymers prepared by these strategies are presented in Appendix 1.

4.1. <u>Ring expansion polymerization</u>

Ring expansion polymerization (REP) allows the synthesis of cyclic polymers through the use of a cyclic monomer or a cyclic initiator.[68] During propagation, monomer units are incorporated into the cyclic structure through a weak labile bond (e.g. organometallic or electrostatic). At the end of the reaction, the catalyst is either retained or expelled from the macrocycle (Figure 9). Because the cyclic structure is maintained throughout the whole polymerization, this method does not suffer the entropic penalties associated to the ring closure by reaction between two end groups. Since neither linear precursors nor high dilution conditions are needed to form macrocyclic polymers, high

molecular weights are accessible and the reaction can be scale up to obtain high amounts of cyclic product. However, complications can occur if the components of the reaction are not chosen carefully. Because the formation of the stable ring polymer is based on rates of polymerization, depolymerization and backbiting, high polydispersity can be obtained and removal of the catalyst from the polymer sample can be a challenge.
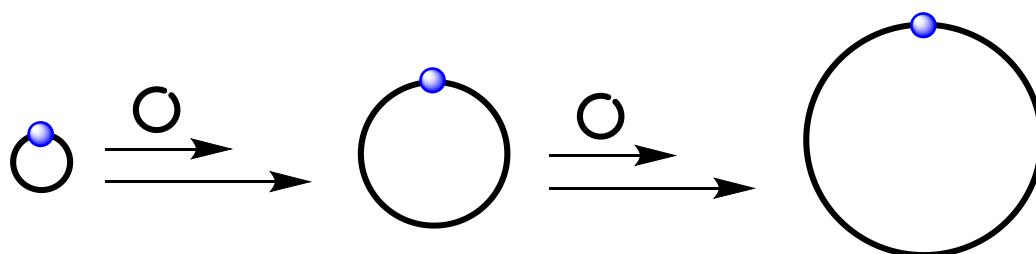
○ = weak labile bound

Figure 9. Schematic representation of the ring expansion polymerization.

4.2. __Ring closure strategy__

The ring closure strategy relies on intramolecular coupling of the end-groups of a previously synthesized linear precursor. The use of predesigned linear polymers as precursors for the preparation of cyclic polymers allows high control over the molecular characteristics of the obtained rings. This strategy can be further divided into three different approaches: bimolecular homodifunctional coupling, unimolecular

homodifunctional coupling and unimolecular heterodifunctional coupling (Figure 10).[66] These strategies will be discussed in detail below.
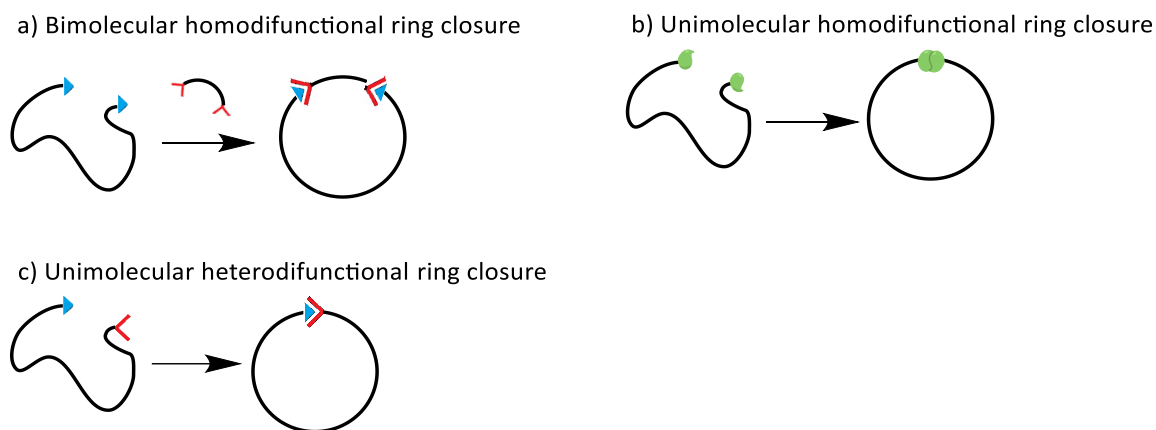
a) Bimolecular homodifunctional ring closure

b) Unimolecular homodifunctional ring closure

c) Unimolecular heterodifunctional ring closure

Figure 10. Schematic representation of ring closure strategies.

Based on the works of Paul Ruggli[69] and Karl Ziegler,[70] showing that high dilution favored the intramolecular coupling of small organic molecules, cyclization via ring closure technique is performed under high dilution and on small scales to avoid intermolecular coupling. The entropic penalty, associated to the localization of the two chain ends into a space small enough to promote intramolecular coupling,[71] only allows cyclization of relatively low molecular weight chains (< 25000 g/mol).

The probability of cyclization, can be described by the well-known Jacobson-Stockmayer equations.[71]

$$P_c = \left(\frac{3}{2\pi}\right)^{3/2} \frac{v_s}{\langle r^2 \rangle^{3/2}} \qquad \text{Eq.1}$$

$$P_l = 2N\frac{v_s}{V} = \frac{2N_Ac}{M}v_s \qquad\qquad \text{Eq.2}$$

P_c is the probability of reaction when two ends of the same chain are within the capture volume, v_s; P_l is the probability of reaction when two ends from two different chains are within the capture volume; $\langle r^2 \rangle$ is the mean square of the end-to-end distance of a chain; N is the total number of molecules in a total volume V; N_A is the Avogadro number; M is the molecular weight of the polymer and c is the polymer concentration in g/mL.

The ratio P_c/P_l is defined as follows:

$$\frac{P_c}{P_l} = \left(\frac{3}{2\pi\langle r^2\rangle}\right)^{3/2}\frac{2000}{N_A[P]} \qquad\qquad \text{Eq.3}$$

[P] is the polymer concentration in mol/L.

The theoretical percentage of monocyclic chains can be calculated as follows:

$$\%cyclic = \frac{P_c}{P_c + P_l} \times 100 \qquad\qquad \text{Eq.4}$$

From this set of equations, it is clear that a decrease in the concentration of the linear precursor [P] increases P_c/P_l, and therefore the probability of cyclization. Since the intramolecular coupling is a unimolecular process, it is not influenced by the dilution.

20

Contrarily, the intermolecular coupling, which is a bimolecular process, is largely reduced upon dilution.[69,70] Experimentally, it is possible to obtain a high percentage of cyclic chains by adding the previously synthesized linear precursor into a catalyst solution at a slow rate. In that way, the concentration of linear precursor is maintained as low as possible (pseudo-high-diluted conditions) and the active end-groups are consumed during intramolecular coupling.[72,73] The second important prediction of the Jacobson-Stockmayer theory is the decreasing probability of intramolecular coupling with the chain length. Indeed, the probability for the two ends of the same chain to be within the capture volume decreases with the chain length. This is why high molecular cyclic polymers are not achievable via ring closure.

Although high molecular weights are not achievable as opposed to the ring expansion technique, ring closure stays the most versatile choice for the preparation of ring polymers. The use of highly activated coupling reaction allows the synthesis of well-defined cyclic polymers with a large scope of chemical compositions.[74]

4.2.1. Ring closure by bimolecular approach

The bimolecular ring closure approach relies on the coupling between a difunctional polymer chain and a difunctional coupling agent in dilute solution. The cyclization takes place in two distinct steps, first the intermolecular coupling between the polymer chain and the coupling agent complementary functional groups, and second the intramolecular coupling between the remaining complementary functional group of the

polymer chain and coupling agent. Because the homodifunctional bimolecular cyclization reaction is first order in both polymer and coupling agent, the stoichiometry between the polymer chain and the coupling agent must be respected to obtain a high percentage of cyclic products. If this condition is not met, linear polymers will be obtained. In the case of an excess of polymer over the coupling agent, oligomerization will occur (Figure 11). For an excess of coupling agent over the polymer chains, high molecular weight chains composed by a number of linear precursors will be formed. For that reason, extra care must be taken in the stoichiometry when preparing cyclic polymers via bimolecular ring closure.
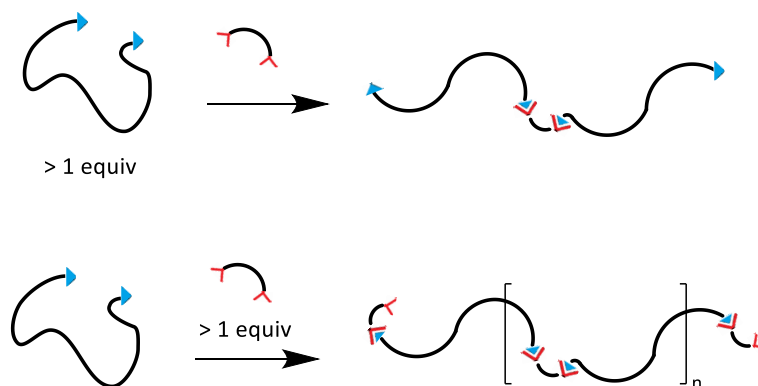

Figure 11. Consequence of incorrect stoichiometry during bimolecular cyclization.

The second and biggest limitation concerning this approach is the combination of two steps requiring opposite conditions. Indeed, the first intermolecular reaction between the polymer chain and the coupling agent is favored by low dilution for the two

molecules to meet. However, the second intramolecular reaction to produce cyclic chains is favored by high dilution. Because the reaction is a one pot process, the concentration of both components must be kept as low as possible to avoid the formation of linear impurities. As a result, the intermolecular coupling occurring during the first step is very slow. To palliate the slow kinetics of the first step, highly efficient coupling reactions must be used. However, in most cases cyclization via bimolecular ring closure is contaminated by acyclic products.

4.2.2. Ring closure by unimolecular approach

The unimolecular strategy presents the advantage to link complementary end groups present on the same polymer chain (Figure 12). Consequently, high dilution will minimize intermolecular oligomerization without reducing the rate of intramolecular coupling. Moreover, stoichiometry between two reactants is no longer needed eliminating a great source of impurities.
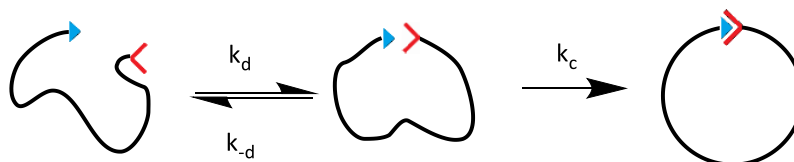

Figure 12. Competition between diffusion and coupling during ring closure by unimolecular approach.

Prior to the coupling reaction, the two reactive chain ends have to diffuse within a capture volume. This step is characterized by a diffusion constant rate, k_d. Then, the coupling reaction can occur to form the cyclic polymer. This is characterized by a cyclization constant rate, k_c. If the coupling reaction does not occur, the chain ends will diffuse away from each other with a constant rate k_{-d}. In the case of $k_c \gg k_{-d}$ the ring closure reaction will be under diffusion control. In the reverse case $k_c \ll k_{-d}$ the ring closure will be driven by its equilibrium kinetics.

4.2.2.1. Homodifunctional unimolecular ring closure

Although the number of homocoupling reactions is limited in organic chemistry, the homodifunctional unimolecular approach is motivated by the need to incorporate a unique functional group at both ends of a polymer chain.

One of the earliest examples of oxidative homocoupling is the reaction between two alkynes to form a diyne bound, also known as Glaser coupling.[75] In 1869, Glaser reported the formation of diphenyldiacetylene when mixing phenylacetylene, copper (I) chloride and ammonium hydroxide in ethanol under air. Years later, Hay proposed a crucial modification by adding a nitrogen ligand such as N,N,N',N'-tetramethylethylenediamine thus allowing the reaction to occur under mild conditions.[76] Glaser coupling is now known to be catalyzed by metal salts, usually copper (I) and copper (II) through a complex mechanism.[77,78]

Cyclic poly(ethylene oxide) and cyclic polystyrene have been synthesized via Glaser coupling of alkyne terminated linear precursors.[79] A solution of linear polymer was added slowly to a copper catalyst solution to generate cyclic polymers in high yields >95 % (Figure 13). The reaction proceeded under air and at room temperature, which makes Glaser coupling suitable for the cyclization of a large range of polymer backbones. The disappearance of alkyne groups and the formation of the diyne bound was confirmed by ^{1}H NMR and Fourier-transform infrared (FTIR) spectroscopy. Additionally, the loss of two protons was confirmed by matrix assisted laser desorption ionization - time of flight mass spectrometry (MALDI-ToF MS) and the reduction of the hydrodynamic volume of polymer chains was demonstrated by a clear shit toward higher retention times in size exclusion chromatography (SEC) measurements. As pyridine is a good solvent for a large majority of synthetic polymers, the authors chose this solvent to carry out the Glaser coupling reaction. However, its high boiling point makes it difficult to remove completely after reaction, and additionally, pyridine requires extra cares during manipulation due to its toxicity.
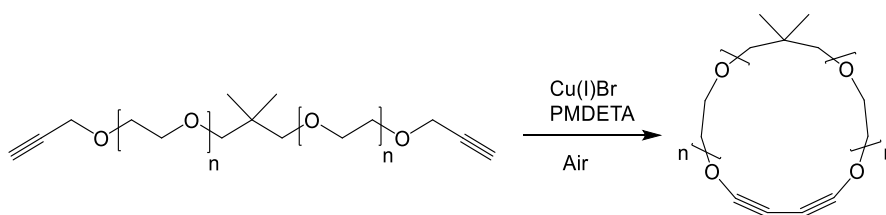

Figure 13. Synthesis of poly(ethylene oxide) via Glaser coupling.

Other homocoupling reactions can be found in the literature for the synthesis of a large number of cyclic polymers such as cyclic polystyrene,[80] cyclic poly(propylene oxide),[81] cyclic poly(ethylene oxide)[82] or cyclic poly(methyl acrylate).[83]

4.2.2.2. Heterodifunctional unimolecular ring closure

The coupling of heterodifunctional polymers is the most efficient way to produce cyclic polymers with high purity. Although the synthesis of α,ω-heterofunctional polymers is more challenging compared to α,ω-homofunctional polymers, the amounts of impurities generated during cyclization is notably reduced in heterodifunctional unimolecular ring closure reactions. This is because the rate of intermolecular coupling is reduced by a factor of two since the effective concentration of complimentary reactive groups is reduced by two.

In 2001 the concept of "click" chemistry was introduced by Sharpless et al.[84] In order to be qualified as "click" reaction, the reaction must be modular, wide in scope and have a very high yield. In the case of the formation of byproducts, they must be inoffensive and removable by non-chromatographic methods. Additionally, the reaction conditions must be simple (i.e. readily available reagents, easily removable solvent and purification by non-chromatographic methods). Finally, the product must be stable under physiological conditions. One of the most popular "click" reaction is the Huisgen dipolar cycloaddition[85,86] of an azide and an alkyne group, to form both 1,4 and 1,5-substitued [1,2,3]-triazole ring. Later, the research groups of Folkin et al.[87] and Meldal et al.[88]

reported simultaneously the use of a copper (I) catalyst, allowing the reaction to proceed at room temperature and giving access to one specific regioisomer, the 1,4-substituted [1,2,3]-triazole. Since then, the copper catalyzed azide alkyne cycloaddition (CuAAC) has been extensively used in polymer chemistry.[89-90]

In 2006 Laurent and Grayson combined CuAAC with controlled radical polymerization to prepare cyclic poly(styrene)s.[72] This use of "click" chemistry constituted a great breakthrough for the synthesis of cyclic polymers. Linear polystyrene chains were first synthesized by atom transfer radical polymerization (ATRP) with propargyl 2-bromoisobutyrate as initiator (Figure 14). After modification of the terminal bromide into azide, a solution of the obtained polymer was added dropwise into a copper catalyst solution under inert atmosphere. The consumption of the two complementary end-groups to form triazole rings was confirmed by ^{1}H NMR and FTIR. The clear shift in retention time observed in SEC measurements demonstrated the formation of cyclic chains.
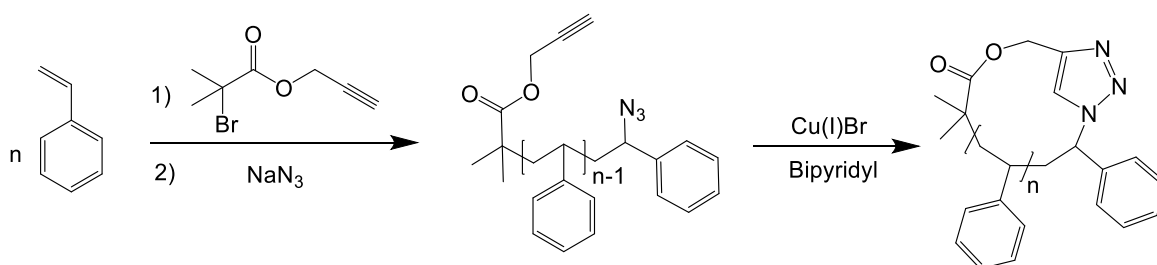

Figure 14. Cyclization of poly(styrene) via CuAAC "click" reaction.

In the following years, the same strategy was employed for the synthesis of cyclic poly(N-isopropylacrylamide),[91] cyclic poly(tert-butyl acrylate)[92] and cyclic poly(4-vinylbenzyl)carba-zole).[93] Polymers of about 8000 Da with low polydispersity index (< 1.1) were obtained. Since then, the use of reactions considered as "click" chemistry has been greatly reported for the preparation of macrocyclic chains with high purity and in high yields.

5. Main characterization techniques used in this thesis

5.1. Size Exclusion Chromatography

In the 1950s Porath and Flodin successfully separated water-soluble compounds using crosslinked dextrane gels.[94] In 1964 Moore[95] introduced the gel permeation chromatography (GPC) for the separation of non-water soluble polymers. Since then, GPC, sometimes referred to as SEC, has become one of the most popular methods for the determination of molecular masses. During SEC measurements, a dilute solution of the sample is injected through a column packed with small particles of a porous material. The space among particles is filled with a mobile phase consisting of the same solvent used for the preparation of the sample solution. The sample molecules are eluted from the column and separated

according to their hydrodynamic volumes. The smallest molecules, which are capable of entering into smaller pores, will elute at longer retention times than the larger molecules which are excluded rapidly from the column. SEC does not only give molar mass averages but also a complete description of the molar mass distribution.

Different detectors can be used to monitor the elution of the analyzed samples. Two of the most commonly used detectors are ultra-violet (UV) detector and refractive index (RI) detector. Both are concentration-sensitive detectors and their signals are only proportional to the concentration of sample in the eluate. The UV detector measures the absorbance of the eluate in the ultra-violet region. Its use is therefore reserved for polymers absorbing at those particular wavelengths. On the other hand, RI detector measures the variation of the refractive index of the eluate and can be used universally for all compounds. SEC can also be equipped with a viscosity detector (VIS). This detector measures the specific viscosity of the eluate. When coupled to a concentration-sensitive detector, the intrinsic viscosity [η] can be obtained. [η] is a measure of the solute contribution to the solution viscosity and is one of the fundamental characteristics of a polymer.

The disadvantage of SEC in its conventional form is that the determination of molecular weight depends on calibration. Retention times are compared to standards, usually polystyrene, to determine relative molecular weight values. For that reason, light scattering (LS) detectors represent the most powerful detection in SEC since they eliminate the use of calibration curves, allow the determination of absolute molecular weights and are very efficient detecting aggregates even at low concentrations. Among LS detectors, multi-angle light scattering (MALS) detectors

are commonly used. In addition of the absolute molecular weight, MALS detectors allow the determination of the radius of gyration from the angular dependence of the scattered light. When a polydisperse sample is analyzed, the chromatogram is divided in slices eluting at different elution volumes and the different eluted fractions are considered monodisperse. The SEC-MALS measurement yields for each slice of elution volume V_i the molar mass M_i and the mean square radius R_i^2.

From the molecular weight values of each slice, it is possible to calculate the number-average molar mass (M_n) and weight-average molar mass (M_w) defined as:

$$M_n = \frac{\sum n_i M_i}{\sum n_i} \qquad \text{Eq. 5}$$

$$M_w = \frac{\sum n_i M_i^2}{\sum n_i M_i} \qquad \text{Eq. 6}$$

M_i is the molecular weight of the ith slice and n_i is the number of chains of that molecular weight calculated from concentration-sensitive detector data. The polydispersity index, defined as Đ = M_w/M_n, gives information about the heterogeneity in molecular weight among all the chains present in a polymer sample.[96,97]

SEC is a technique particularly useful for the characterization of cyclic polymers. Because of the reduction in hydrodynamic volume observed upon cyclization, ring

polymers exhibit longer retention times than their linear analogues,[98] while having identical molecular weights. Therefore, SEC-MALS analysis allows the determination of the absolute molecular weight for both linear and cyclic polymers and can be used to confirm cyclization by comparing the retention times. Another consequence of the lower hydrodynamic volume of cyclic polymers is their lower intrinsic viscosity compared to their linear analogues. This reduction of intrinsic viscosity after cyclization can be readily measured by a VIS detector. Therefore, the association of RI-MALS-VIS detectors is particularly suited for the analysis of cyclic polymers.

5.2. Matrix Assisted Laser Desorption Ionization - Time of Flight Mass Spectrometry

This mass spectrometry technique was first developed for the analysis of biomacromolecules.[99,100] However, it has been also suited for the characterization of synthetic macromolecules thanks to the minimal fragmentation induced during ionization of the analyte. In a typical experiment, the analyte is mixed with a matrix and a salt (e.g. a cationizing agent) in a dilute solution. The matrix adsorbs the energy from laser pulse and transfer it to the sample. The high energy density obtained in the matrix causes instantaneous vaporization of a microvolume and desorption of the analyte molecules. The cationized matrix and analyte molecules are then accelerated toward a detector by an electric field. The mass to charge ratio

(m/z) is obtained based on the time of flight of each analyte molecule allowing the determination of the absolute molecular weight of each individual n-mer represented within the polymer distribution.

Thanks to the high resolving power achievable nowadays, MALDI-ToF MS is particularly suited for the analysis of polymer end groups. Indeed, the most significant drawback when characterizing end groups by other methods such as NMR or FTIR spectroscopy is the low relative concentration of end groups with respect to the polymer backbone in chains with molecular weights above a few kilodaltons. One unique advantage of MALDI-ToF MS is that all signals observed contain information about end group masses. Consequently, end-group analysis is possible even for high molecular weight samples. The following equation can be used to provide a general solution for the end-group analysis of any homopolymer by MALDI-ToF MS:

$$M_{obs} = n \times M_{RU} + M_{cat} + M_{end-group} \qquad \text{Eq. 7}$$

where M_{obs} is the observed mass of the peaks, corresponding to the n-mers within the polymer distribution, M_{RU} is the mass of the repeat unit of the homopolymer, n is the corresponding number of repeat unit of each n-mer, M_{cat} is the mass of the cation added during sample preparation and $M_{end-group}$ is the summed mass of both end-groups.

During MALDI-ToF MS characterization, polymers are typically ionized by complexation with a cation. However, some polymers can undergo elimination or

fractionation and form stable ionized species. In such cases, accurate assignation of signals can be challenging, and the ionization mode must be clarified. Investigation of mass spectra obtained with different cation sources, typically, sodium, potassium, silver and lithium can help determining the ionization mode and clarify peak assignment.

Typically, the ionization efficiency differs among analytes.[101] Therefore, the intensity of a signal in MALDI-ToF MS is not proportional to the quantity of a species. To obtain quantitative characterization, the combination with other characterization techniques is usually required. Nevertheless, MALDI-ToF MS remains a powerful tool for polymer characterization since it can provide critical evidence for confirming the structure of polymers. For example, the generation of cyclic polymers has been clearly identified by revealing the absence of end-group in polyesters.[102] Also, the comparison of the mass spectra of the linear precursors and the cyclic products has confirmed, in part, the cyclization of poly(ε-caprolactone) after click coupling[103] and poly(methyl acrylate) after olefin metathesis.[83]

5.3.   **Broadband Dielectric Spectroscopy**

Molecular fluctuations of dipoles in an electric field result in relaxation phenomena, whereas motion of mobile charge carriers (i.e. electrons, ions) causes conductive contributions to the dielectric response of a material. In a typical broadband dielectric spectroscopy (BDS) experiment, a uniform periodic electric field

$E(t) = E_0 \exp(-i\omega t)$, where ω is the angular frequency, is applied to a sheet of material forming part of a parallel plate capacitor. In these experiments, the frequency dependent capacitance is determined. The dielectric constant of the material is proportional to the capacitance. The response of a material to the electric field is determined by the spontaneous fluctuations of dipole entities within the material. At frequencies much higher than the dipole fluctuation rate, the dipoles do not contribute to the polarization and the dielectric constant and capacitance are low. On the contrary, at frequencies much lower than the dipole fluctuation rate, the dipoles do contribute to the polarization that follows the electric field variations and the dielectric constant and capacitance are high. In the intermediate range, dipoles produce a partial material polarization, whose dependence on time is delayed respect to that of the electric field. This phenomenology can be conveniently described in terms of the complex permittivity defined by:

$$\varepsilon^*(\omega) = \varepsilon'(\omega) - i\varepsilon''(\omega) \qquad \text{Eq. 8}$$

where $\varepsilon'(\omega)$ is the real part and $\varepsilon''(\omega)$ the imaginary part of the complex permittivity $\varepsilon^*(\omega)$.

One of the most important applications of dielectric spectroscopy is the investigation of relaxation processes that are due to rotational fluctuations of molecular dipoles. As they are related to characteristic parts of a molecule (e.g. functional groups) or to the molecule as a whole, information about the dynamics of a molecular ensemble can be obtained by analyzing the dielectric function.[24] In BDS data, the relaxation processes are characterized by step-like decrease with increasing frequency (or decreasing

temperature) in the real part ε' and by a peak in the imaginary part ε'' of the complex permittivity. The frequency of the peak maximum f_{max} ($f_{max} = \omega_{max}/2\pi$) is related to the relaxation time (τ_{max}) of the process as:

$$\tau_{max} = {}^1\!/\omega_{max} \qquad\qquad\qquad \text{Eq. 9}$$

In most cases, the relaxation phenomena are characterized by f_{max} or τ_{max}. Those parameters are characteristic of the molecular dynamics of a material and can be extracted quite directly from the experimental data.[104]

5.3.1. Dielectric relaxations and polymer dynamics

Most of the synthesized macromolecules present fix dipole moment perpendicular to the main chain backbone. The fluctuations of the dipole moment, in this case are due to the conformational transitions related to the segmental dynamics, and therefore to the glass transition, giving rise to the so-called α-relaxation.

In linear regio-regular polymers presenting a fix dipole moment of the monomer unit as depicted in Figure 1a and 1b, the fluctuations of the end-to-end vector result in a dielectric relaxation usually referred to as normal mode (NM) relaxation. Because the dipole orientation along the chain contour differs between the two dipolar microstructures (Figure 1a and 1b), different dielectric responses will be obtained. Notably, for similar molecular weights, the NM relaxation will be faster for a

l-2a-polymer compared to a *l*-1a-polymer (i.e. the peak maximum shifts toward higher frequency) because the fluctuations of dipoles associated to the two subchains can occur without changes of the whole end-to-end vector.[105]

Upon cyclization, the dipolar microstructures depicted in Figure 1c and 1d are respectively obtained. Since cyclic polymers exhibit higher glass transition temperatures compared to their linear analogues, the α-relaxation is slower in the case of cyclic chains, i.e. the peak maximum shifts toward lower frequency. Additionally, for a *c*-1a-polymer, the cancellation of $\overrightarrow{P_A}$ will result in the disappearance of the NM relaxation peak. On the other hand, *c*-2a-polymers display a NM relaxation. Due to the extra constrains imposed by the cyclic topology, a slower relaxation is expected for the cyclic polymers compared to that of *l*-2a-polymers with similar molecular weights.

Summarizing, the analysis of the dielectric relaxation of synthesized polymers allows the determination of the dipolar microstructure of the chain. In the case of regio-regular chains, the dipolar microstructure can be associated to the architecture of the polymer chain, making BDS a particularly useful technique for the characterization of such systems.

6. <u>Objectives</u>

The main goal of this thesis is to synthesize cyclic polymers having specific dipolar microstructures. The study of dielectric relaxations of such polymers by BDS is expected to help understand the dynamic properties of ring polymers. To that end, poly(glycidyl phenyl ether) (PGPE) has been chosen as a reference material given the high dielectric signal intensity of this polymer. This investigation requires polymers with high topological purity and controlled regiochemistry. To meet these requirements, this work aims at finding the optimal conditions for generating 1) "clickable" linear precursors by AROP and 2) the corresponding cyclic structures by the ring closure approach.

The above-mentioned strategies would ultimately allow the preparation of predesigned dipolar microstructures which could be readily identified by BDS analysis.

7. <u>Outline of the thesis</u>

In **Chapter II**, linear polyethers characterized by a resultant dipole moment proportional to the end-to-end vector are prepared (Figure 1a). Tetrabutylamonium azide is used as AROP initiator of glycidyl phenyl ether monomer. The monomer activator, triisobutylaluminium, was found to be essential to guaranty control over the

macromolecular characteristics. Cyclic polymers exhibiting the cancelation of dipole moment along the chain contour (Figure 1c) are prepared with high purity by ring closure via CuAAC "click" reaction. Cyclization is demonstrated by conventional characterization techniques, ^{1}H NMR, SEC and MALDI-ToF MS. BDS, although not conventional for such a purpose, is shown to be very convenient to ensure cyclic purity in the case of regio-regular polymers.

In **Chapter III**, ethylene glycol and the phosphazene base *t*-BuP$_4$ are used to synthesize linear polyethers composed of two symmetric arms (Figure 1b). The combination of MALDI-ToF MS and BDS allowed the verification of the microstructure of obtained polymers and, in particular, the symmetry of the two sub-chains. Interestingly, it was found that only in the absence of the monomer activator, triisobutylaluminum, symmetric arms were formed.

In **Chapter IV**, the cyclization of linear polyethers composed of two symmetric arms is achieved (Figure 1d). First, it was found that using water and the phosphazene base *t*-BuP$_4$ as initiation system allowed better control of the linear precursor structure than the combination of ethylene glycol and *t*-BuP$_4$. Then, the ring closure reaction performed via Glaser coupling was optimized to produce the corresponding cyclic polymer displaying a normal mode relaxation. BDS analysis of the synthesized cyclic samples provided general results on the ring dynamics.

In **Chapter V**, the most significant conclusions of this work are presented.

8. <u>References</u>

(1)   Craik, D. J. Circling the Enemy : Cyclic Proteins in Plant Defence. *Trends Plant Sci.* **2009**, *14* (6), 328–335.

(2)   Saska, I.; Colgrave, M. L.; Jones, A.; Anderson, M. A.; Craik, D. J. Quantitative Analysis of Backbone-Cyclised Peptides in Plants. *J. Chromatogr. B* **2008**, *872*, 107–114.

(3)   Dulbecco, R.; Vogt, M. Evidence for a Ring Structure of Polyoma Virus DNA. *Proc. Natl. Acad. Sci.* **1963**, *50*, 236–243.

(4)   Kramers, H. A. The Behavior of Macromolecules in Inhomogeneous Flow. *J. Chem. Phys.* **1946**, *14* (7), 415–424.

(5)   Zimm, B. H.; Stockmayer, W. H. The Dimensions of Chain Molecules Containing Branches and Rings. *J. Chem. Phys.* **1949**, *17* (12), 1301–1314.

(6)   Hossain, M. D.; Reid, J. C.; Lu, D.; Jia, Z.; Searles, D. J.; Monteiro, M. J. Influence of Constraints within a Cyclic Polymer on Solution Properties. *Biomacromolecules* **2018**, *19* (2), 616–625.

(7)   McKenna, G. B.; Hadziioannou, G.; Lutz, P.; Hild, G.; Strazielle, C.; Straupe, C.; Rempp, P.; Kovacs, A. J. Dilute Solution Characterization of Cyclic Polystyrene Molecules and Their Zero-Shear Viscosity in the Melt. *Macromolecules* **1987**, *20* (3), 498–512.

(8)   Roovers, J. Viscoelastic Properties of Polybutadiene Rings. *Macromolecules* **1988**, *21* (5), 1517–1521.

(9)   Pasquino, R.; Vasilakopoulos, T. C.; Jeong, Y. C.; Lee, H.; Rogers, S.; Sakellariou, G.; Allgaier, J.; Takano, A.; Brás, A. R.; Chang, T.; et al. Viscosity of Ring Polymer Melts. *ACS Macro Lett.* **2013**, *2* (10), 874–878.

(10)   Kammiyada, H.; Ouchi, M.; Sawamoto, M. A Study on Physical Properties of Cyclic Poly(Vinyl Ether)s Synthesized via Ring-Expansion Cationic Polymerization. *Macromolecules* **2017**, *50* (3), 841–848.

(11)   Xu, X.; Zhou, N.; Zhu, J.; Tu, Y.; Zhang, Z.; Cheng, Z.; Zhu, X. The First Example of Main-Chain Cyclic Azobenzene Polymers. *Macromol. Rapid Commun.* **2010**, *31* (20), 1791–1797.

(12)   Córdova, M. E.; Lorenzo, A. T.; Müller, A. J.; Hoskins, J. N.; Grayson, S. M. A Comparative Study on the Crystallization Behavior of Analogous Linear and Cyclic Poly(ε-Caprolactones). *Macromolecules* **2011**, *44* (7), 1742–1746.

(13)   Wang, J.; Li, Z.; Pérez, R. A.; Müller, A. J.; Zhang, B.; Grayson, S. M.; Hu, W. Comparing Crystallization Rates between Linear and Cyclic Poly(Epsilon-Caprolactones) via Fast-Scan Chip-Calorimeter Measurements. *Polymer.* **2015**, *63*, 34–40.

(14)   Bielawski, C. W.; Benitez, D.; Grubbs, R. H. An " Endless " Route to Cyclic Polymers. *Science.* **2002**, *297*, 2041–2045.

(15)   Tezuka, Y.; Ohtsuka, T.; Adachi, K.; Komiya, R.; Ohno, N.; Okui, N. A Defect-Free Ring Polymer : Size-Controlled Cyclic Poly(Tetrahydrofuran) Consisting Exclusively of the Monomer Unit. *Macromol. Rapid Commun.* **2008**, *29*, 1237–1241.

(16)   Takeshita, H.; Poovarodom, M.; Kiya, T.; Arai, F.; Takenaka, K.; Miya, M.; Shiomi, T. Crystallization Behavior and Chain Folding Manner of Cyclic, Star and Linear Poly(Tetrahydrofuran)S. *Polymer.* **2012**, *53* (23), 5375–5384.

(17)   Gao, L.; Oh, J.; Tu, Y.; Chang, T.; Li, C. Y. Glass Transition Temperature of Cyclic Polystyrene and the Linear Counterpart Contamination Effect. *Polymer.* **2019**, *170*, 198–203.

(18)   Clarson, S. J.; Dodgson, K.; Semlyen, J. A. Studies of Cyclic and Linear Poly(Dimethylsiloxanes): 19. Glass Transition Temperatures and Crystallization Behaviour. *Polymer.* **1985**, *26* (6), 930–934.

(19) Di Marzio, E. A. The Glass Temperature of Polymer Blends. *Polymer.* **1990**, *31* (12), 2294–2298.

(20) Roovers, J.; Toporowski, P. M. Synthesis of High Molecular Weight Ring Polystyrenes. *Macromolecules* **1983**, *16*, 843–849.

(21) Brochard, F.; Gennes, P. G. d. Dynamical Scaling for Polymers in Theta Solvents. *Macromolecules* **1977**, *10* (5), 1157–1161.

(22) Ohta, Y.; Kushida, Y.; Kawaguchi, D.; Matsushita, Y.; Takano, A. Preparation, Characterization, and Nanophase-Separated Structure of Catenated Polystyrene-Polyisoprene. *Macromolecules* **2008**, *41* (11), 3957–3961.

(23) Stockmayer, W. H. Dielectric Dispersion in Solutions of Flexible Polymers. *Pure Appl. Chem.* **1967**, *15* (3–4), 539–554.

(24) Kremer, F.; Schönhals, A. *Broadband Dielectric Spectroscopy*, Springer-V.; Berlin, Heidelberg, New York, 2003.

(25) Gambino, T.; Martínez De Ilarduya, A.; Alegría, A.; Barroso-Bujans, F. Dielectric Relaxations in Poly(Glycidyl Phenyl Ether): Effects of Microstructure and Cyclic Topology. *Macromolecules* **2016**, *49* (3), 1060–1069.

(26) Dubois, P.; Coulembier, O.; Raques, J. M. *Handbook of Ring-Opening Polymerization*, WILEY-VCH.; Dubois, P., Coulembier, O., Raquez, J. M., Eds.; Weinheim, 2009.

(27) Brunelle, D. J. Introduction. In *Ring-Opening Polymerization*; Hanser publishers: Munich, 1993; pp 2–4.

(28) Duda, A.; Kowalski, A. Thermodynamics and Kinetics of Ring - Opening Polymerization. In *HandbookHandbook of Ring-Opening Polymerization*; Dubois, P., Coulembier, O., Raquez, J. M., Eds.; Weinheim, 2009; pp 1–45.

(29) Kubisa, P. Thermodynamics and Kinetics of Ring Opening Polymerisation. In *Cationic polymerizations : mechanisms, synthesis, and applications*; Matyjaszewski, K., Ed.; New York : Marcel Dekker, 1996; pp 437–553.

(30)   Erden, I. Oxiranes and Oxirenes: Monocyclic. In *Comprehensive Heterocyclic Chemistry II*; Katrizky, A. R., Rees, C. W., Scriven, E. F. V., Eds.; 1996; pp 97–144.

(31)   Childers, M. I.; Longo, J. M.; Van Zee, N. J.; Lapointe, A. M.; Coates, G. W. Stereoselective Epoxide Polymerization and Copolymerization. *Chem. Rev.* **2014**, *114* (16), 8129–8152.

(32)   Oguni, N.; Lee, K.; Tani, H. Microstructure Analysis of Poly(Propylene Oxide) by 13C Nuclear Magnetic Resonance Spectroscopy. *Macromolecules* **1972**, *5* (6), 819–820.

(33)   Deffieux, A.; Carlotti, S.; Barrère, A. Anionic Ring-Opening Polymerization of Epoxides and Related Nucleophilic Polymerization Processes. In *Polymer Science: A Comprehensive Reference, Volume 4*; Matyjaszewski, K., Möller, M., Eds.; Elsevier B.V., 2012; Vol. 4, pp 117–140.

(34)   Figueruelo, J. E.; Worsfold, D. J. The Anionic Polymerization of Ethylene Oxide in Hexamethyl Phosphoramide. *Eur. Polym. J.* **1968**, *4* (4), 439–444.

(35)   Duda, A.; Penezek, S. Thermodynamics of L-Lactide Polymerization. Equilibrium Monomer Concentration. *Macromolecules* **1990**, *23* (6), 1636–1639.

(36)   Witek, G.; Brandstätter, M.; Knauss, R.; Wiesenegger, L.; Siebenhofer, M.; Uhlig, F. Kinetics and Thermodynamics of the Ring Opening Reaction of Hexamethylcyclotrisiloxane. *AIChE Annu. Meet. Conf. Proc.* **2008**, No. November.

(37)   Boileau, S. The Synthesis, Characterization, Reactions & Applications of Polymers - Chain Polymerization Part I. In *Comprehensive Polymer Science*; Allen, G., Sigwalt, P., Eds.; Pergamon Press: Oxford, UK, 1989.

(38)   Brocas, A. L.; Mantzaridis, C.; Tunc, D.; Carlotti, S. Polyether Synthesis: From Activated or Metal-Free Anionic Ring-Opening Polymerization of Epoxides to Functionalization. *Prog. Polym. Sci.* **2013**, *38* (6), 845–873.

(39)   Kazanskii, K. S.; Solov'yanov, A. A.; Entelis, S. G. Polymerization of Ethylene Oxide by Alkali Metal- Naphtalene Complexes in Tetrahydrofuran. *Eur. Polym. J.* **1971**, *7*, 1421–1433.

(40) Solov'yanov, A. A.; Kazanskii, K. S. The Kinetics and Mechanism of Anionic Polymerization of Ethylene Oxide in Ether Solvents. *Polym. Sci. U.S.S.R.* **1972**, *14* (5), 1186–1195.

(41) Ding, J.; Heatley, F.; Price, C.; Booth, C. Use of Crown Ether in the Anionic Polymerization of Propylene Oxide - 2. Molecular Weight and Molecular Weight Distribution. *Eur. Polym. J.* **1991**, *27* (9), 895–899.

(42) Aida, T.; Inoue, S. Living Polymerization of Epoxides with Metalloporphyrin and Synthesis of Block Copolymers with Controlled Chain Lengths. *Macromolecules* **1981**, *14*, 1162–1166.

(43) Raynaud, J.; Absalon, C.; Gnanou, Y.; Taton, D. N-Heterocyclic Carbene-Induced Zwitterionic Ring-Opening Polymerization of Ethylene Oxide and Direct Synthesis of α,ω-Difunctionalized Poly(Ethylene Oxide)s and Poly(Ethylene Oxide)-b-Poly(ε-Caprolactone) Block Copolymers. *J. Am. Chem. Soc.* **2009**, *131*, 3201–3209.

(44) Maitre, C.; Ferreira, O.; Lutz, J.-F.; Paintoux, Y.; Hémery, P. Anionic Polymerization of Phenyl Glycidyl Ether in Miniemulsion. *Macromolecules* **2000**, *33*, 7730–7736.

(45) Schwesinger, R.; Schlemper, H. Peralkylated Polyaminophosphazenes—Extremely Strong, Neutral Nitrogen Bases. *Angew. Chemie Int. Ed. English* **1987**, *26* (11), 1167–1169.

(46) Schwesinger, R.; Hasenfratz, C.; Schlemper, H.; Walz, L.; Peters, E. -M; Peters, K.; von Schnering, H. G. How Strong and How Hindered Can Uncharged Phosphazene Bases Be? *Angew. Chemie Int. Ed. English* **1993**, *32* (9), 1361–1363.

(47) Eßwein, B.; Steidl, N. M.; Möller, M. Anionic Polymerization of Oxirane in the Presence of the Polyiminophosphazene Base t-BuP$_4$. *Macromol. Rapid Commun.* **1996**, *17* (2), 143–148.

(48) Dentzer, L.; Bray, C.; Noinville, S.; Illy, N.; Guéguan, P. Phosphazene-Promoted Metal-Free Ring-Opening Polymerization of 1,2-Epoxybutane Initiated by Secondary Amides. *Macromolecules* **2015**, *48* (21), 7755–7764.

(49)   Zhao, J.; Pahovnik, D.; Gnanou, Y.; Hadjichristidis, N. Phosphazene-Promoted Metal-Free Ring-Opening Polymerization of Ethylene Oxide Initiated by Carboxylic Acid. *Macromolecules* **2014**, *47* (5), 1693–1698.

(50)   Grzelka, A.; Chojnowski, J.; Fortuniak, W.; Taylor, R. G.; Hupfield, P. C. Kinetics of the Anionic Ring Opening Polymerization of Cyclosiloxanes Initiated with a Superbase. *J. Inorg. Organomet. Polym. Mater.* **2004**, *14* (2), 85–99.

(51)   Rexin, O.; Mülhaupt, R. Anionic Ring-Opening Polymerization of Propylene Oxide in the Presence of Phosphonium Catalysts. *J. Polym. Sci. Part A Polym. Chem.* **2002**, *40* (7), 864–873.

(52)   Pietzonka, B. T.; Seebach, D. The P4-Phosphazene Base as Part of a New Metal-Free Initiator System for the Anionic Polymerization of Methyl Methacrylate. *Angew. Chemie Int. Ed. English* **1993**, *32* (5), 716–717.

(53)   Isono, T.; Kamoshida, K.; Satoh, Y.; Takaoka, T.; Sato, S. I.; Satoh, T.; Kakuchi, T. Synthesis of Star- and Figure-Eight-Shaped Polyethers by t-Bu-P$_4$-Catalyzed Ring-Opening Polymerization of Butylene Oxide. *Macromolecules* **2013**, *46* (10), 3841–3849.

(54)   Misaka, H.; Tamura, E.; Makiguchi, K.; Kamoshida, K.; Sakai, R.; Satoh, T.; Kakuchi, T. Synthesis of End-Functionalized Polyethers by Phosphazene Base-Catalyzed Ring-Opening Polymerization of 1,2-Butylene Oxide and Glycidyl Ether. *J. Polym. Sci. Part A Polym. Chem.* **2012**, *50* (10), 1941–1952.

(55)   Satoh, Y.; Miyachi, K.; Matsuno, H.; Isono, T.; Tajima, K.; Kakuchi, T.; Satoh, T. Synthesis of Well-Defined Amphiphilic Star-Block and Miktoarm Star Copolyethers via t-Bu-P$_4$-Catalyzed Ring-Opening Polymerization of Glycidyl Ethers. *Macromolecules* **2016**, *49* (2), 499–509.

(56)   Boileau, S.; Illy, N. Activation in Anionic Polymerization: Why Phosphazene Bases Are Very Exciting Promoters. *Prog. Polym. Sci.* **2011**, *36* (9), 1132–1151.

(57)   Chen, Y.; Shen, J.; Liu, S.; Zhao, J.; Wang, Y.; Zhang, G. High Efficiency Organic Lewis Pair Catalyst for Ring-Opening Polymerization of Epoxides with Chemoselectivity. *Macromolecules* **2018**, *51*, 8286–8297.

(58) Satoh, Y.; Matsuno, H.; Yamamoto, T.; Tajima, K.; Isono, T.; Satoh, T. Synthesis of Well-Defined Three- and Four-Armed Cage-Shaped Polymers via "Topological Conversion" from Trefoil- and Quatrefoil-Shaped Polymers. *Macromolecules* **2017**, *50* (1), 97–106.

(59) Kruschwitz, J. *Encyclopedia of Polymer Science and Engineering, 2nd Ed*, Wiley Inte.; Kruschwitz, J., Ed.; Wiley Interscience: New, 1985; Vol. 6.

(60) Billouard, C.; Carlotti, S.; Desbois, P.; Deffieux, A. "Controlled" High-Speed Anionic Polymerization of Propylene Oxide Initiated by Alkali Metal Alkoxide/Trialkylaluminum Systems. *Macromolecules* **2004**, *37* (11), 4038–4043.

(61) Labbé, A.; Carlotti, S.; Billouard, C.; Desbois, P.; Deffieux, A. Controlled High-Speed Anionic Polymerization of Propylene Oxide Initiated by Onium Salts in the Presence of Triisobutylaluminum. *Macromolecules* **2007**, *40* (22), 7842–7847.

(62) Rejsek, V.; Sauvanier, D.; Billouard, C.; Desbois, P.; Deffieux, A.; Carlotti, S. Controlled Anionic Homo- and Copolymerization of Ethylene Oxide and Propylene Oxide by Monomer Activation. *Macromolecules* **2007**, *40* (18), 6510–6514.

(63) Stolarzewicz, A. A New Chain Transfer Reaction in the Anionic Polymerization of 2,3-epoxypropyl Phenyl Ether and Other Oxiranes. *Die Makromol. Chemie* **1986**, *187* (4), 745–752.

(64) Dodgson, K.; Semlyen, J. A. Studies of Cyclic and Linear Poly (Dimethyl Siloxanes): 1 . Limiting Viscosity Number- Molecular Weight Relationships. *Polymer.* **1977**, *18*, 1265–1268.

(65) Josse, T.; Winter, J. De; Gerbaux, P.; Coulembier, O. Cyclic Polymers by Ring-Closure Strategies. *Angew. Chemie Int. Ed.* **2016**, *55*, 13944–13958.

(66) Laurent, B. A.; Grayson, S. M. Synthetic Approaches for the Preparation of Cyclic Polymers. *Chem. Soc. Rev.* **2009**, *38* (8), 2202–2213.

(67) Kricheldorf, H. R. Cyclic Polymers: Synthetic Strategies and Physical Properties. *J. Polym. Sci. Part A Polym. Chem.* **2010**, *48*, 251–284.

(68)   Chang, Y. A.; Waymouth, R. M. Recent Progress on the Synthesis of Cyclic Polymers via Ring-Expansion Strategies. *J. Polym. Sci. Part A Polym. Chem.* **2017**, *55* (18), 2892–2902.

(69)   Ruggli, P. Über Einen Ring Mit Dreifacher Bindung. *Liebigs Ann. der Chemie* **1912**, *392*, 92.

(70)   Ziegler, K.; Eberle, H.; Ohlinger, H. Über Vielgliedrige Ringsysteme. I. Die Präparativ Ergiebige Synthese Der Polyniethylenketone Mit Mehr Als 6 Ringgliedern. *Liebigs Ann. der Chemie* **1933**, *504* (1), 94.

(71)   Jacobson, H.; Stockmayer, W. H. Intramolecular Reaction in Polycondensations. I. The Theory of Linear Systems. *J. Chem. Phys.* **1950**, *18*, 1600–1606.

(72)   Laurent, B. A.; Grayson, S. M. An Efficient Route to Well-Defined Macrocyclic Polymers via "Click" Cyclization. *J. Am. Chem. Soc.* **2006**, *128* (13), 4238–4239.

(73)   Lonsdale, D. E.; Bell, C. A.; Monteiro, M. J. Strategy for Rapid and High-Purity Monocyclic Polymers by CuAAC " Click " Reactions. *Macromolecules* **2010**, *43*, 3331–3339.

(74)   Zhang, B.; Grayson, S. M. The Ring-Closure Approach for Synthesizing Cyclic Polymers. In *Topological Polymer Chemistry: Progress of Cyclic Polymers in Syntheses, Properties, and Functions*; Tezuka, Y., Ed.; World Scientific Singapor, 2013; pp 157–197.

(75)   Glaser, C. Beitriige Zur Kenntnifs Des Acetenylbenzols. *Berichte der Dtsch. Chem. Gesellschaft* **1869**, *2*, 422–424.

(76)   Hay, A. S. Oxidative Coupling of Acetylenes. *J. Org. Chem.* **1960**, *25*, 1275–1277.

(77)   Leophairatana, P.; Samanta, S.; De Silva, C. C.; Koberstein, J. T. Preventing Alkyne-Alkyne (i.e., Glaser) Coupling Associated with the ATRP Synthesis of Alkyne-Functional Polymers/Macromonomers and for Alkynes under Click (i.e., CuAAC) Reaction Conditions. *J. Am. Chem. Soc.* **2017**, *139* (10), 3756–3766.

(78)   Jover, J.; Spuhler, P.; Zhao, L.; McArdle, C.; Maseras, F. Toward a Mechanistic

Understanding of Oxidative Homocoupling: The Glaser-Hay Reaction. *Catal. Sci. Technol.* **2014**, *4* (12), 4200–4209.

(79) Zhang, Y.; Wang, G.; Huang, J. Synthesis of Macrocyclic Poly (Ethylene Oxide) and Polystyrene via Glaser Coupling Reaction. *Macromolecules* **2010**, *43*, 10343–10347.

(80) Whittaker, M. R.; Goh, Y. K.; Gemici, H.; Legge, T. M.; Perrier, S.; Monteiro, M. J. Synthesis of Monocyclic and Linear Polystyrene Using the Reversible Coupling/Cleavage of Thiol/Disulfide Groups. *Macromolecules* **2006**, *39* (26), 9028–9034.

(81) Chen, C. W.; Cheng, C. C.; Dai, S. A. Reactive Macrocyclic Ether - Urethane Carbodiimide (MC - CDI): Synthesis, Reaction, and Ring-Opening Polymerization (ROP). *Macromolecules* **2007**, *40* (23), 8139–8141.

(82) Ji, Z.; Li, Y.; Ding, Y.; Chen, G.; Jiang, M. A Fixable Supramolecular Cyclic Polymer Based on the Cucurbit[8]Uril-Stabilized π-π Interaction. *Polym. Chem.* **2015**, *6* (38), 6880–6884.

(83) Hayashi, S.; Adachi, K.; Tezuka, Y. An Efficient Route to Cyclic Polymers by ATRP-RCM Process. *Chem. Lett.* **2007**, *36* (8), 982–983.

(84) Kolb, H. C.; Finn, M. G.; Sharpless, K. B. Click Chemistry: Diverse Chemical Function from a Few Good Reactions. *Angew. Chemie - Int. Ed.* **2001**, *40* (11), 2004–2021.

(85) Huisgen, R. 1,3-Dipolar Cycloadditions. Past and Future. *Angew. Chemie Int. Ed. English* **1963**, *2* (10), 565–598.

(86) Huisgen, R. 1,3-Dipolar Cycloaddition Chemistry. In *1,3-dipolar Cycloaddition Chemistry*; Padwa, A., Ed.; Wiley: New York, 1984.

(87) Rostovtsev, V. V; Green, L. G.; Fokin, V. V; Sharpless, K. B. A Stepwise Huisgen Cycloaddition Process : Copper(I) -Catalyzed Regioselective "Ligation" of Azides and Terminal Alkynes. *Angew. Chemie Int. Ed.* **2002**, *41* (14), 2596–2599.

(88) Tornøe, C. W.; Christensen, C.; Meldal, M. Peptidotriazoles on Solid Phase : [1 , 2 , 3] -Triazoles by Regiospecific Copper (I) -Catalyzed 1 , 3-Dipolar Cycloadditions of Terminal Alkynes to Azides. *J. Org. Chem.* **2002**, *67*, 3057–3064.

(89) Malkoch, M.; Schleicher, K.; Drockenmuller, E.; Hawker, C. J.; Russell, T. P.; Wu, P.; Fokin, V. V. Structurally Diverse Dendritic Libraries: A Highly Efficient Functionalization Approach Using Click Chemistry. *Macromolecules* **2005**, *38* (9), 3663–3678.

(90) Joralemon, M. J.; O'Reilly, R. K.; Matson, J. B.; Nugent, A. K.; Hawker, C. J.; Wooley, K. L. Dendrimers Clicked Together Divergently. *Macromolecules* **2005**, *38* (13), 5436–5443.

(91) Xu, J.; Ye, J.; Liu, S. Synthesis of Well-Defined Cyclic Poly(N-Isopropylacrylamide) via Click Chemistry and Its Unique Thermal Phase Transition Behavior. *Macromolecules* **2007**, *40* (25), 9103–9110.

(92) Chen, F.; Liu, G.; Zhang, G. Synthesis of Cyclic Polyelectrolyte via Direct Copper(I)-Catalyzed Click Cyclization. *J. Polym. Sci. Part A Polym. Chem.* **2012**, *50* (5), 831–835.

(93) Zhu, X.; Zhu, X.; Zhou, N.; Zhang, Z.; Sun, B.; Yang, Y.; Zhu, J. Cyclic Polymers with Pendent Carbazole Units: Enhanced Fluorescence and Redox Behavior. *Angew. Chemie - Int. Ed.* **2011**, *50* (29), 6615–6618.

(94) Porath, J.; Flodin, P. Gel Filtration: A Method for Desalting and Group Separation. *Nature* **1959**, *183*, 1657–1659.

(95) Moore, J. C. Gel Permeation Chromatography. I. A New Method for Molecular Weight Distribution of High Polymers. *J. Polym. Sci. Part A Gen. Pap.* **1964**, *2* (2), 835–843.

(96) Podzimek, S. Combination of SEC and Light Scattering. In *Light Scattering, Size Exclusion Chromatography and Asymmetric Flow Field Flow Fractionation*; 2011; pp 207–258.

(97) Tarazona, M. P.; Saiz, E. Combination of SEC/MALS Experimental Procedures and

Theoretical Analysis for Studying the Solution Properties of Macromolecules. *J. Biochem. Biophys. Methods* **2003**, *56*, 95–116.

(98)   Semlyen, J. A. *Cyclic Polymers*, Kluwer Aca.; Semlyen, J. A., Ed.; New York, Boston, Dordrecht, London, Moscow, 2002.

(99)   Tanaka, K.; Waki, H.; Ido, Y.; Akita, S.; Yoshida, Y.; Yoshida, T.; Matsuo, T. Protein and Polymer Analyses up to m/z 100 000 by Laser Ionization Time-of-flight Mass Spectrometry. *Rapid Commun. Mass Spectrom.* **1988**, *2* (8), 151–153.

(100) Karas, M.; Hillenkamp, F. Laser Desorption Ionization of Proteins with Molecular Masses Exceeding 10 000 Daltons. *Anal. Chem.* **1988**, *60* (20), 2299–2301.

(101) *Mass Spectrometry of Polymers*, CRC Press.; Lattimer, R., Montaudo, G., Eds.; Boca Raton, 2003; Vol. 93.

(102) Williams, J. B.; Gueev, A. L.; Hercules, D. M. Characterization of Polyesters by Matrix-Assisted Laser Desorption Ionization Mass Spectrometry. *Macromolecules* **1997**, *30* (13), 3781–3787.

(103) Hoskins, J. N.; Grayson, S. M. Synthesis and Degradation Behavior of Cyclic Poly(ε-Caprolactone). *Macromolecules* **2009**, *42* (17), 6406–6413.

(104) Schönhals, A.; Kremer, F. Analysis of Dielectric Spectra. In *Broadband Dielectric Spectroscopy*; Berlin, Heidelberg, New York, 2003; pp 59–98.

(105) Yosbida, H.; Watanabe, H.; Adachi, K.; Kotaka, T. Dielectric Normal Mode Process of Bifurcated Linear Cis-Polyisoprene. *Macromolecules* **1991**, *24* (10), 2981–2985.

Chapter II

Cyclic poly(glycidyl phenyl ether) with aligned

dipole moment along the chain contour

Table of content

As mentioned in chapter I, the synthesis of cyclic polymers via ring closure approaches is suitable for synthesizing a large variety of polymer backbones. Moreover, since this strategy relies on the ring closure of a previously synthesized linear precursor, it is possible to control the molecular characteristics of the chain.

In this chapter, the synthesis of cyclic poly(glycidyl phenyl ether) is performed by the ring closure of synthesized linear precursors via copper(I)-catalyzed alkyne-azide cycloaddition (CuAAC) "click" reaction. Linear precursors are prepared by anionic ring opening polymerization (AROP) initiated by tetrabutylammonium azide (N_3NBu_4) in the absence and presence of triisobutylaluminum (iBu_3Al). A deep investigation on the molecular characteristics of all the generated structures is performed.

1. <u>Introduction</u>

Click-chemistry has played an important role in the synthesis of complex architectures due to its ability to link molecular species with a rapid kinetics under mild conditions, high reaction yields and high functional group and solvent tolerance. In particular, CuAAC "click" reaction has allowed access to a variety of exquisite architectures including monocyclic[1] and multicyclic polymer structures,[2,3] single-chain polymer nanoparticles,[4] sequence-controlled polymers,[5] dendrimers,[6] stars,[7] and graft-polymers.[8]

Terminal azides are generally incorporated by nucleophilic substitution of terminal halogen atoms with NaN_3 in preformed linear polymers. A convenient choice to

incorporate azide end groups into the polymer chain is by direct initiation with azides. Gervais et al.[9] demonstrated that the monomer-activated AROP of epoxides mediated by N_3NBu_4 and iBu_3Al directly generated α-azido-ω-hydroxypolyethers with controlled molar masses up to 30 kDa in a few hours. They successfully polymerized a variety of monomers including ethylene oxide, propylene oxide, ethoxyethyl glycidyl ether, and epichlorohydrin. Kim et al.[10] recently demonstrated that initiation of ethylene oxide with NaN_3 can be used to generate azide-terminated poly(ethylene oxide) through an AROP mechanism. Kakuchi et al.[11] also reported a convenient way to synthesize azido-terminated polyethers by using hydroxyazides as initiator and a phosphazene base as a catalyst. They produced monocyclic structures of poly(1,2 butylene oxide) and poly(benzyl glycidyl ether) by means of CuAAC "click" reaction. The advantages of using this initiation system rely on the complex architectures that can be obtained when the initiator molecule contains multifunctional azide and hydroxyl moieties.[12,13] Although N_3NBu_4 allows the formation of only single azide-terminated polymers, this method is cheaper and simpler compared to previous techniques.

In general, AROP is prone to chain transfer reactions which compromise the end-group functionality and their utility for the synthesis of well-defined architectures by CuAAC "click" reactions. The combination of alkali metal alkoxides and trialkylaluminum has been efficiently proved to control the polymerization and to preserve a high end group fidelity.[14] Considering this, and in order to make some progress in the generation of cyclic structures with high purity, the polymerization of glycidyl phenyl ether (GPE) with N_3NBu_4 in the presence and absence of iBu_3Al is investigated.

Matrix-assisted laser desorption/ionization–time-of-flight mass spectrometry (MALDI-ToF MS), nuclear magnetic resonance (NMR), and gel permeation chromatography (GPC) are the techniques most routinely used to verify cyclization. However, the evaluation of cyclic purity is not always straightforward, as for example the appearance of high molecular weight shoulders in GPC chromatograms cannot be attributed solely to the formation of linear dimers by intermolecular coupling. Cyclic dimers can also be formed, and their identification requires the use of combined techniques.[15]

Dielectric spectroscopy is a nonconventional technique to evaluate the cyclic purity. It is very sensitive to changes in the molecular weight and the topology of the polymer chain,[16] specially in the case of regio-regular polymers. Fluctuations of the end-to-end vector in linear polymer chains are measured as a dielectric relaxation called normal mode (NM). Upon cyclization, the end-to-end vector vanishes as a consequence of the cancellation of dipole moment vectors parallel to the chain contour, resulting in the disappearance of such NM relaxation. Moreover, linear n-mers (dimers, trimers, etc.) obtained by intermolecular coupling can be detected by exhibiting much slower end-to-end vector fluctuations. The usefulness of dielectric spectroscopy to confirm the cyclic purity has been reported in a series of regio-irregular poly(glycidyl phenyl ether) (PGPE) samples obtained by zwitterionic ring expansion polymerization[17,18] after being subjected to a purification protocol by "click" scavenging of topological impurities (tadpoles and linear chains).[19] However, owing the regio-irregular nature of those samples, that study was not centered on the NM analysis but on end-group-sensitive β-relaxations, which have a limited accuracy with increasing molecular weight.

In light of these findings, the present study aims at two goals: (1) evaluating the use of N$_3$NBu$_4$ as an AROP initiator to synthesize α-azido-ω-hydroxy poly(glycidyl phenyl ether)

(N$_3$-PGPE-OH) for the generation of pure cyclic structures and (2) using dielectric spectroscopy as an additional tool to evaluate the cyclic purity in regio-regular polymers. With those purposes, the study of the polymerization of glycidyl phenyl ether (GPE) with N$_3$NBu$_4$ in the absence and presence of iBu$_3$Al is presented, as well as the evaluation of the end-group fidelity by using MALDI-ToF MS and NMR. After modification of terminal hydroxyl groups to alkyne with propargyl bromide, the efficiency of copper(I)-mediated ring-closure of α-azido-ω-alkyne poly(glycidyl phenyl ether) (N$_3$-PGPE-ALK) for the generation of pure cyclic PGPE (c-PGPE) is investigated. The cyclic purity is evaluated by means of dielectric spectroscopy, which in agreement with triple detection GPC data reveals the formation of pure cyclic structures in samples of Mn < 20 kDa generated with N$_3$NBu$_4$ and iBu$_3$Al.

2. <u>Experimental Section</u>

2.1. <u>Materials</u>

GPE, toluene and dichloromethane (Sigma-Aldrich) were distilled from CaH$_2$ under reduced pressure. N$_3$NBu$_4$, iBu$_3$Al (1.1 mol/L in toluene) and NaH (Sigma-Aldrich) were stored in the glovebox under a nitrogen atmosphere and used as received. Propargyl bromide, propargyl alcohol, (+) sodium L-ascorbate, N,N,N',N'',N''-

pentamethyldiethylenetriamine (PMDETA), methanol and tetrahydrofuran (Sigma-Aldrich) were used as received.

Cu(I)Br was purified following the Keller and Wycoff method.[20] Briefly, 1 g of Cu(I)Br was washed five times with 20 mL of glacial acetic acid, then three times with 30 mL of absolute ethanol and finally six times with 15 mL of anhydrous ether. During washing, the suction was adjusted so the liquid passed slowly over the powder. The clean Cu(I)Br was dried at 80 °C for 30 min and then kept in an airtight bottle storred in a glovebox.

2.2.   Synthesis of α-azido, ω-hydroxy poly(glycidyl phenyl ether) initiated by N_3NBu_4

In a typical experiment performed in bulk, N_3NBu_4 (200 mg; 7.03×10^{-4} mol) was transferred to a round bottom flask equipped with a magnetic stirrer in a glovebox. Then, GPE (2 mL; 1.47×10^{-2} mol) was added, the flask sealed with a stopcock and the reaction stirred at room temperature for 45 min. A high increase of the viscosity was observed. The polymer was dissolved in THF and the reaction was terminated by addition of HCl (60 μL in 0.5 mL of methanol). The polymer was purified by precipitation in cold methanol twice and dried under vacuum. Polymers with different molecular weight were prepared following the same procedure and adjusting the monomer to initiator ratio.

In a typical experiment performed in solution, N_3NBu_4 (200 mg; 7.03×10^{-4} mol) was transferred to a round bottom flask equipped with a magnetic stirrer in a glovebox and dissolved in 1 mL of toluene. Then, GPE (2 mL; 1.47×10^{-2} mol) was added, the flask sealed with a stopcock and the reaction stirred at room temperature for 20 h. The reaction was stopped by addition of HCl (60 µL in 0.5 mL of methanol). The solvent was evaporated under reduced pressure, the product redissolved in THF and purified by two precipitations in cold methanol.

2.3. Synthesis of α-azido, ω-hydroxy poly(glycidyl phenyl ether) initiated by N₃NBu₄ / iBu₃Al

In a typical experiment, GPE (2 mL; 1.47×10^{-2} mol) was transferred to a round bottom flask containing 7 mL of toluene and equipped with a magnetic stirrer in a glovebox. Then, 0.96 mL of iBuAl₃ solution (1.1 mol/L in toluene) was added to the reaction flask. Finally, N_3NBu_4 (200 mg; 7.03×10^{-4} mol) was dissolved in 2 mL of toluene and added to the reaction flask. The flask was sealed and cooled down to −30 °C during the first 15 min to reduce the initial polymerization rate. After this, the reaction was stirred for 4 h at room temperature. The reaction was stopped with 1 mL of ethanol. The solvent was evaporated under reduced pressure and the polymer was redissolved in THF and precipitated in cold methanol twice and dried under vacuum. Polymers with different molecular weights were prepared following the same procedure and adjusting the monomer to initiator ratio, keeping the iBuAl₃/ N₃NBu₄ ratio in 1.5.

2.4. End-group modification: formation of α-azido, ω-alkyne poly(glycidyl phenyl ether)

A solution of N_3-PGPE-OH (375 mg; 4.69×10^{-5} mol) and NaH (33 mg; 1.38×10^{-3} mol) was stirred at 40 °C for 1 h in THF (2.5 mL) under argon atmosphere. Then, propargyl bromide (200 mg; 1.68×10^{-3} mol) was added. The reaction was stirred for 72 h at room temperature.

In order to verify the presence of terminal azide groups, a reaction with propargyl alcohol was performed. Cu(I)Br (78 mg; 5.5×10^{-4} mol) was introduced in a round bottom flask equipped with a magnetic stirrer. Oxygen was removed by purging with argon. In a second flask, N_3-PGPE-OH (50 mg; 1.1×10^{-5} mol) was dissolved in 3 mL of toluene and purged with argon for 15 min. This solution was added under argon to the first flask. Immediately after, PMDETA (0.11 mL; 5.5×10^{-4} mol) and propargyl alcohol (0.01 mL; 1.7×10^{-4} mol) were added. The reaction was stirred at room temperature for 24 h.

2.5. Cyclization of α-azido, ω-alkyne poly(glycidyl phenyl ether)

A typical procedure for the cyclization of α-azido,ω-alkyne PGPE is as follows: in a round bottom flask, Cu(I)Br (30 mg; 2×10^{-4} mol), (+) sodium L-ascorbate (41 mg; 2×10^{-4} mol) and PMDETA (0.04 mL; 2×10^{-4} mol) were added. The flask was purged with argon for 15 min and 1 mL of dichloromethane was added under argon atmosphere. In a second flask, α-azido,ω-alkyne PGPE (35 mg; 4×10^{-6} mol) was introduced and the flask was purged for 15 min. Then, 1 mL of dichloromethane was added under argon. The polymer solution was transferred to a syringe under argon and added slowly (7.44 mL/h) to the Cu(I)Br solution. After all the polymer solution was added (about 8 min), the reaction was stirred at room temperature for 3 h. The copper catalyst and the amine were removed by extraction with a saturated ammonium chloride solution. The organic phase was dried with magnesium sulfate. After evaporation of the solvent under reduced pressure, the polymer was redissolved in THF and precipitated in cold methanol and dried under vacuum.

2.6. Characterization

The molecular weight, molecular weight distribution and intrinsic viscosity data were determined by GPC on an Agilent G-1310A HPLC pump connected to miniDAWN MALS, Optilab rEX dRI and ViscoStar II detectors from Wyatt. All the detectors were at 25 °C.

PLgel 5µm 500Å and PLgel 5µm Mixed-C columns were used for separation, both kept in a column heater at 30 °C. THF (1.0 mL/min) was used as an eluent. ASTRA software (Wyatt, version 6.1.2.84) was used for data collection and processing. A differential refractive index (dn/dc) value for PGPE of 0.137 mL/g was used, as previously determined.[18]

MALDI-ToF MS measurements were performed on a Bruker Autoflex Speed system (Bruker, Germany) equipped with a 355 nm NdYAG laser. Spectra were acquired in both positive reflector mode and linear mode. *Trans*-2-[3-(4-*tert*-Butylphenyl)-2-methyl-2-propenylidene]malononitrile (DCTB, Fluka) was used as a matrix. Potassium trifluoroacetate (KTFA, Aldrich) or Sodium trifluoroacetate (NaTFA, Aldrich) were added as the cationic ionization agent (~10 mg/ml dissolved in THF). The matrix was also dissolved in THF at a concentration of 20 mg/ml. Polymer samples were dissolved in THF at a concentration of ~10 mg/ml. In a typical MALDI experiment, the matrix, salt and polymer solutions were premixed at a 20:1:3 ratio. Approximately 0.5 µL of the obtained mixture were hand spotted on the ground steel target plate. For each spectrum 10000 laser shots were accumulated. The spectra were externally calibrated using a mixture of different poly(ethylene glycol) standards (PEG, Varian).

^{1}H and ^{13}C NMR data were recorded on a Bruker Avance spectrometer at 400 MHz. CDCl$_3$ or (CD$_3$)$_2$CO at 25 °C were used as a solvent.

Fourier transform infrared spectroscopy (FTIR) measurements were performed at 25 °C in a Jasco 6300 FTIR. Spectra were registered in transmission mode under nitrogen atmosphere. The polymer samples were spread on ZnSe windows with a spatula to form films of about 0.2 mm. Baselines of FTIR spectra were not corrected.

A broadband and high-resolution dielectric spectrometer, Novocontrol Alpha, was used to measure the complex dielectric function, $\varepsilon^*(\omega) = \varepsilon'(\omega) - i\varepsilon''(\omega)$, $\omega = 2\pi f$, in the frequency (f) range from $f = 10^{-2}$ Hz to $f = 10^{6}$ Hz. Samples were placed between parallel gold-plated electrodes with 20 mm diameter and 0.1 mm thick, by using finely cut 0.1 mm thick cross-shaped Teflon as spacer. To remove the water traces, the samples were heated within the cell at 420 K for 15 min until constant conductivity. The data were collected isothermally during cooling from 420 to 130 K. The temperature was controlled within ±0.1 K using a Novocontrol Quatro cryostat that uses a continuous nitrogen-jet flow.

Differential scanning calorimetry (DSC) measurements were carried out on ~5 mg specimens using a Q2000 TA Instruments. All samples were measured by placing the samples in sealed aluminum pans, cooling to −100 °C at 20 °C/min, and heating to 150 °C at 20 °C/min (first run). Then, samples were cooled back to −100 °C at 20 °C/min (second run) and finally heated to 150 °C at 20 °C/min (third run). A helium flow rate of 25 mL/ min was used throughout. The glass transition temperatures (T_g) were evaluated in the third run.

3. <u>Results and discussion</u>

3.1. <u>Synthesis of α-azido, ω-hydroxy poly(glycidyl phenyl ether)</u>

Polymerization of GPE was performed with N_3NBu_4 in the absence and presence of iBu_3Al. In the absence of iBu_3Al, N_3NBu_4 was found to initiate the polymerization of GPE by generating polymer chains with very low polydispersity (Tables 1 and 2). The reaction occurred very rapidly in bulk, obtaining a yield of 90 wt% in 1 h. In solution, the reaction occurred more slowly, it being necessary to increase the reaction time to 24 h. The experimental number average molecular weights, M_n, were in agreement with the theoretical ones at low monomer to initiator ratios ($[M_0]/[I_0]$) in both reaction conditions, bulk and solution. However, $[M_0]/[I_0] \geq 100$, the experimental M_n obtained in bulk deviated considerably from the theoretical one likely because this polymerization system is dominated by transfer, whose effect is much higher at low initiator concentration.[21]

Table 1. Polymerization of GPE initiated by N_3NBu_4 in bulk at room temperature.

Entry	$[M_0]/[I_0]$	Time (h)	$M_{n\,(theo)}$ (kDa)	$M_{n\,(obs)}$ (kDa)	Đ	Yield (wt%)
1	21	1	3.0	4.6	1.02	95
2	42	1	5.8	7.6	1.04	93
3	100	24	13.8	9.5	1.07	92
4	214	24	22.5	8.7	1.11	70

Table 2. Polymerization of GPE initiated by N_3NBu_4 in toluene at room temperature. $[M_0]$ = 15 mol/L.

Entry	$[M_0]/[I_0]$	Time (h)	$M_{n\,(theo)}$ (kDa)	$M_{n\,(obs)}$ (kDa)	Đ	Yield (wt%)
5	21	24	2.7	5.5	1.05	85
6	42	24	5.4	6.2	1.11	85

Polymerization of GPE with N_3NBu_4 in the presence of iBu_3Al was performed in solution by keeping a $[iBu_3Al]/[N_3NBu_4]$ ratio higher than 1 to ensure the activating effect of free iBu_3Al species according to a monomer-activated mechanism[9] (Table 3). A verification experiment with $[iBu_3Al]/[N_3NBu_4]$ < 1 conducted to the expected nonpolymerization reaction.[9] Experimental M_n values were found to also deviate from the theoretical ones (Table 3), although higher molecular weights than by using N_3NBu_4 alone could be reached.

Table 3. Polymerization of GPE initiated by N_3NBu_4 / iBu_3Al in toluene. $[M_0] = 1.5$ mol/L.

Entry	$[M_0]/[N_3NBu_4]$	$[iBu_3Al]/[N_3NBu_4]$	Time (h)	M_n (theo) (kDa)	M_n (obs) (kDa)	Đ	Yield (wt%)
7	21	1.5	4	2.9	6.7	1.27	90
8	42	1.5	4	5.7	13.6	1.27	90
9	100	1.5	4	13.5	24.5	1.05	90
10	214	1.5	4	28.9	20.8	1.11	90

3.1.1. End group fidelity

^{1}H NMR data of a representative PGPE sample synthesized with N_3NBu_4 alone is shown in Figure 1a. Main peaks were assigned to the backbone of the polymer chain and confirmed the formation of the targeted polymer. However, the spectral data in the region between 4.3 and 6.5 ppm showed the formation of alkene groups, which are likely formed by proton abstraction from the methyleneoxy group of GPE through a transfer to monomer reaction (Figure 2). Cis and trans alkene groups were identified and assigned as h, i and h', i', respectively. Integration of the alkene ^{1}H NMR signals yielded amounts as high as 17 % of X-PGPE chains in the sample. To confirm the presence of alkene groups, a reaction with HCl was performed and the obtained product characterized by ^{1}H NMR (Figure 1b). All the peaks assigned to alkene groups

in the region between 4.8 and 6.6 ppm disappeared as a consequence of the addition of HCl to the double bond, thus confirming proton assignment. The formation of alkene groups by side reactions during AROP typically occurs by initiation with alkali metal alkoxides and hydroxides due to the high basicity of the propagating species.[22,23] As a consequence, the molar mass of the obtained polyethers is reduced. In the polymerization of propylene oxide with conventional alkali metal initiators the molar mass was found to be limited to values up to 6 kDa.[24,25] In the case of PGPE, the M_n reached values up to 9.5 kDa.
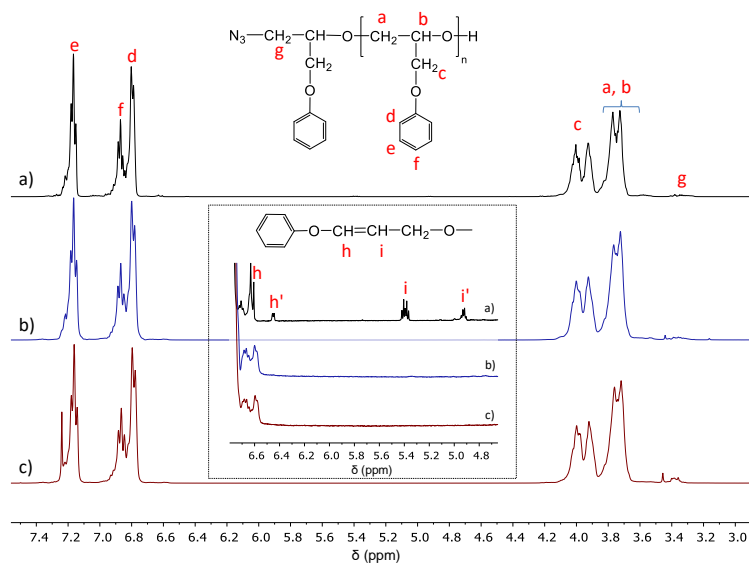
Figure 1. ^{1}H NMR data of PGPE obtained by initiation mediated by a) N_3NBu_4 (Entry 1, Table 1), b) N_3NBu_4 and further modification with HCl, and c) N_3NBu_4 / iBu_3Al (Entry 7, Table 3). Solvent: $CDCl_3$.
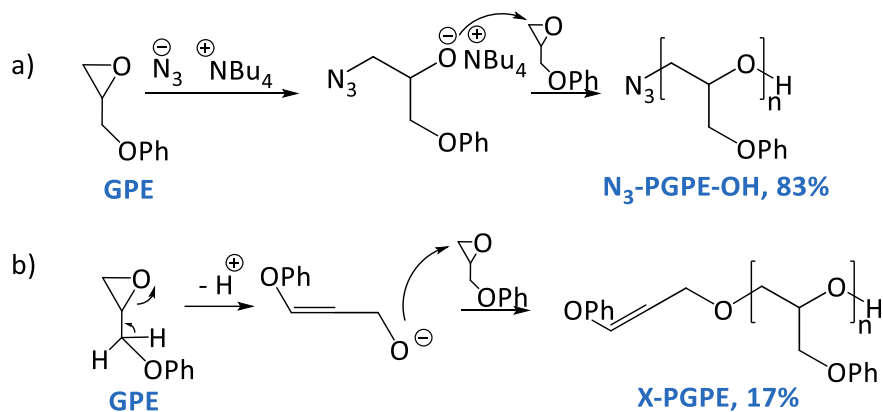
Figure 2. a) Polymerization of GPE initiated with N_3NBu_4 alone. b) Transfer to monomer with the generation of alkene functionalities.

When polymerization was performed with both N_3NBu_4 / iBu_3Al, ^{1}H NMR data revealed the total absence of alkene impurities in the region between 4.8 to 6.6 ppm (Figure 1c). The Lewis acid is believed to form an "ate" complex with the amine which can initiate the polymerization. The excess of iBu_3Al is on the other hand activating the monomer. This process speeds up the reaction and favors the nucleophile attack on the epoxy ring.[26]

The formation of carbonyl groups was not detected by FTIR analysis in none of the catalytic systems (Figure 3), which suggests that other side reactions as previously reported for the polymerization of GPE do not occur.[27] The presence of terminal azide group at the chain head (α-position) was verified by FTIR (Figure 3) and MALDI-ToF MS (Figure 4). FTIR data exhibit a strong absorption band at 2100 cm^{-1} that corresponds to the symmetric stretching of azide groups.
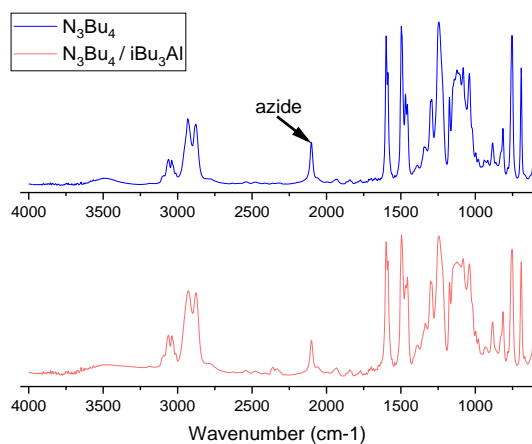
Figure 3. FTIR spectra of N_3-PGPE-OH samples obtained by initiation with N_3NBu_4 (Entry 1, Table 1) and N_3NBu_4 / iBu_3Al (Entry 7, Table 3).
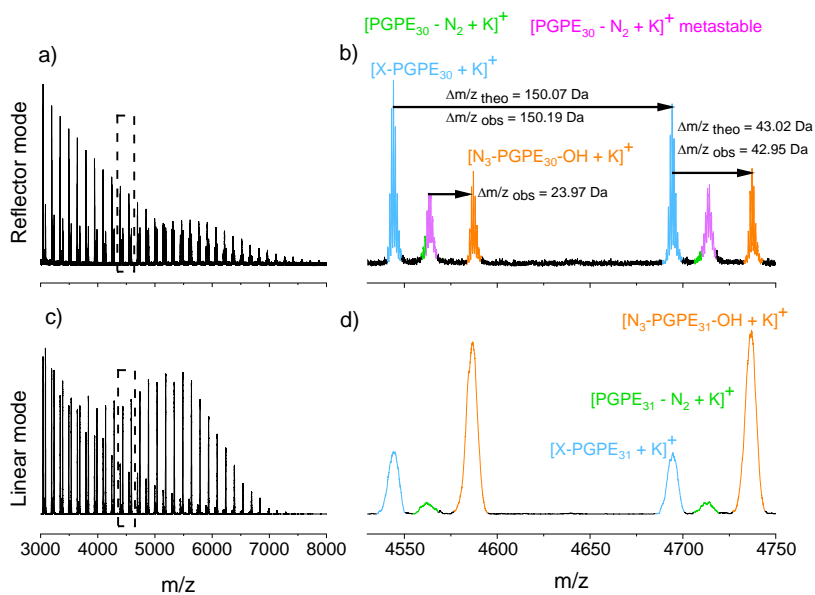
Figure 4. MALDI-ToF MS data of PGPE synthesized with N_3NBu_4 alone (Entry 1, Table 1) in a), b) reflector mode and c),d) linear mode with potassium as counter ion.

MALDI-ToF MS data of PGPE synthesized with N_3NBu_4 alone is shown in Figure 4. The data exhibited three main distribution peaks whose relative intensities changed with the analysis method, in reflector or linear mode. Orange colored signals are attributed to N_3-PGPE-OH species; polymer chains that contain an azide groups at the chain head (α-position) and a hydroxyl group at the chain tail (ω-position). Their peaks are separated by 150.19 Da, corresponding to the repeat unit mass of GPE. Signals in blue are shifted by -42.95 Da respect to those of N_3-PGPE-OH, which correspond to the mass of X-PGPE species. Signals in green and pink are assigned to fragments ions resulting from a loss of N_2 (-N_2) via both in-source and postsource metastable ion formation according to the work of Grayson et al.[28] The latter is known to be nonuniform and to be characterized by having noninteger mass offset (approximately -24.0 Da in the region shown in Figure 4b) relative to the parent ion and to disappear in linear mode detection.[28] By changing from reflector to linear mode detection,[28] a clear intensity reduction of postsource metastable PGPE(-N_2) ions is observed with a concomitant increase of the signals attributed to N_3-PGPE-OH relative to X-PGPE species. The relative intensity between both species in the data recorded in linear mode (orange to blue signal ratio) seems to exhibit a high population of X-PGPE species, in agreement with NMR data.

To confirm the presence and absence of azide end groups in PGPE chains, a CuAAC "click" reaction with propargyl alcohol was performed in the presence of Cu(I)Br as a catalyst. MALDI-ToF MS data of the obtained product are shown in Figure 5. The data exhibited a mass shift of +56.31 Da with respect to N_3-PGPE-OH indicating the addition of a propargyl alcohol moiety at the chain end by forming a triazole ring (T-PGPE

species). The data also exhibited that the signals assigned to X-PGPE remained at the same position as those of the unmodified product, thus confirming the non-reactivity of X-PGPE species toward the "click" addition of propargyl alcohol, as expected. Moreover, upon modification of azide terminal groups, the signals assigned to the fragments ions resulting from the loss of N_2 (- N_2) were no longer observed, which confirms quantitative modification of end groups terminated in azide groups.
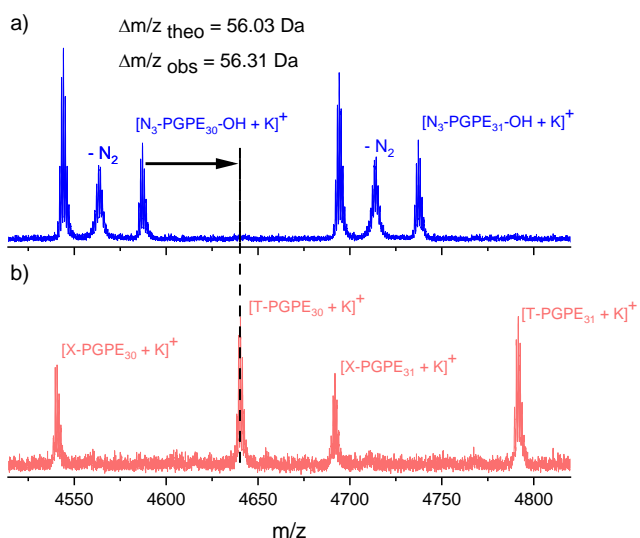
Figure 5. MALDI-ToF MS data in reflector mode of a) the crude PGPE precursor and b) the product obtained by reaction of propargyl alcohol and a PGPE sample synthesized with N_3NBu_4 alone.

MALDI-ToF MS data of PGPE synthesized with N_3NBu_4 / iBu_3Al revealed two cases. Samples with $M_n < 20$ kDa (Entries 7 and 8, Table 3) exhibited the absence of X-PGPE

species and the exclusive formation of N_3-PGPE-OH chains, assigned to the orange colored signals in Figure 6.
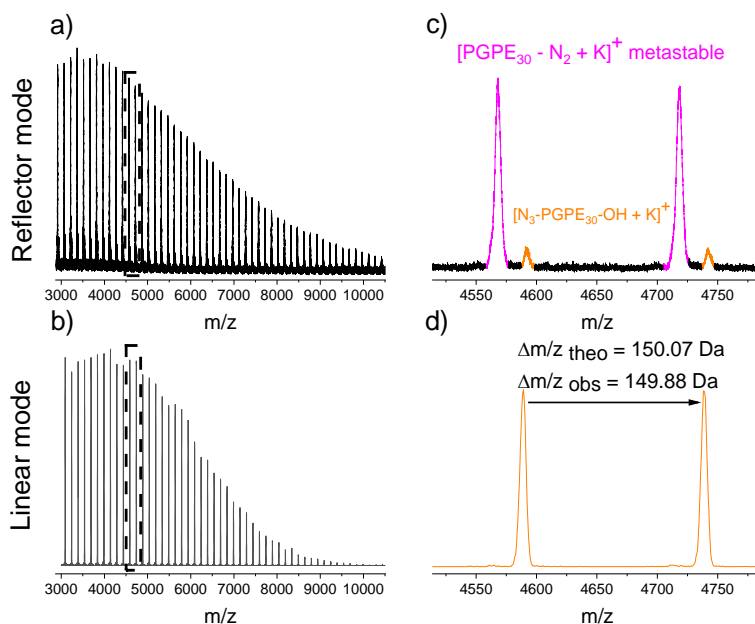
Figure 6. MALDI-ToF MS data of PGPE synthesized with N_3NBu_4 / iBu_3Al (Entry 7, Table 3) in linear and reflector mode.

Samples with M_n > 20 kDa (Entries 9 and 10, Table 3) contained macromolecular species not reactive toward propargyl alcohol (Figure 7, expected shift of +56.03 Da). Those new species can be attributed to PGPE chains obtained by initiation with hydride (H-PGPE) and with an isopropyl anion (I-PGPE) in side reactions. Table 4 lists the abbreviations and proposed structures. Previous studies on the ROP of propylene

oxide[26] and on the anionic polymerization of n-butyl acrylate[29] in the presence of iBu$_3$Al also observed the occurrence of such side reactions. The formation of alkene moieties was not detected by NMR in none of the samples synthesized with N$_3$NBu$_4$/iBu$_3$Al, indicating that transfer to monomer reactions leading to X-PGPE species were reduced by the addition of iBu$_3$Al, in agreement with previous works.[14] All of the identified species were reactive toward propargyl bromide (shift of +37.78 Da) confirming termination in OH groups.
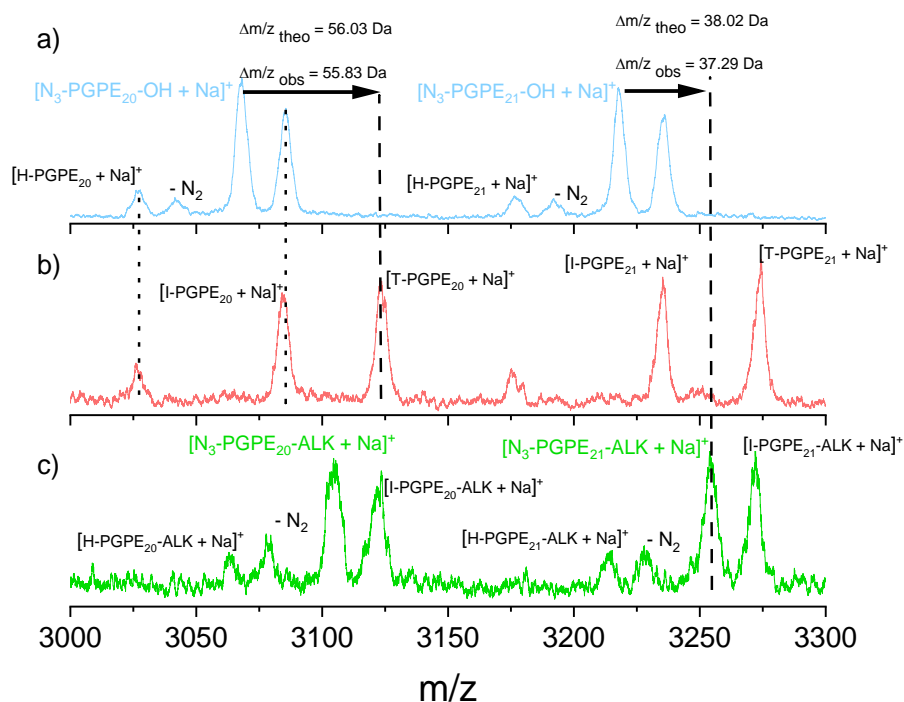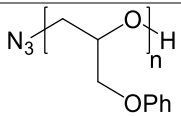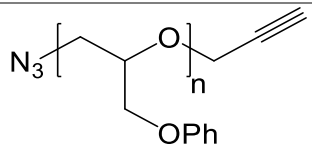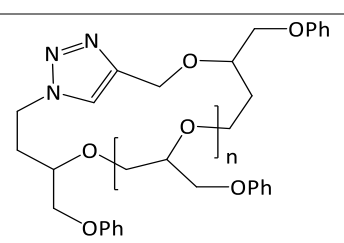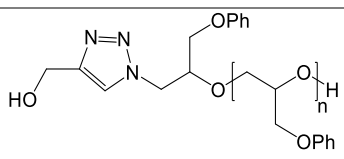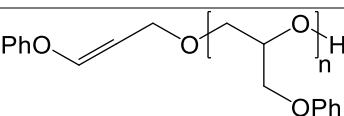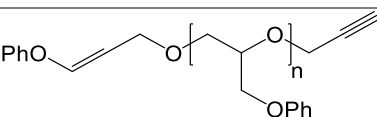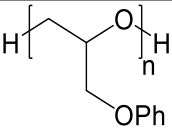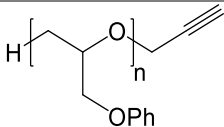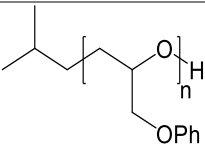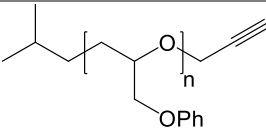
Figure 7. MALDI-ToF MS data registered in linear mode of a) N$_3$-PGPE sample obtained by initiation with N$_3$NBu$_4$/iBu$_3$Al (Entry 9, Table 3), b) the product obtained upon reaction with propargyl alcohol, and c) the product obtained upon reaction with propargyl bromide. See structures in Table 4.

Table 4. Structures assigned to MALDI−ToF MS signals.

Name	Structure	Mass
N₃-PGPE-OH		150 n + 43
N₃-PGPE-ALK		150 n + 81
c-PGPE		150 (n+2) + 81
T-PGPE		150 (n+1) + 99
X-PGPE		150 n + 150
X-PGPE-ALK		150 n + 188

Name	Structure	Mass
H-PGPE		150 n + 2
H-PGPE-ALK		150 n + 40
I-PGPE		150 n + 58
I-PGPE-ALK		150 n + 96

3.1.2. Regiochemistry

The regioregularity of PGPE samples synthesized with both initiating systems, N_3NBu_4 and N_3NBu_4/iBu_3Al, was investigated by ^{13}C NMR (Figure 8). Assignment of triad regiosequences was done according to previous study.[18] The data revealed the appearance of signals that correspond to a configuration produced by only head-to tail or tail-to-head enchainment, indicating the formation of highly regio-regular polymers with both initiating systems.[18] This analysis is relevant for studying the dielectric chain relaxation as explained below.
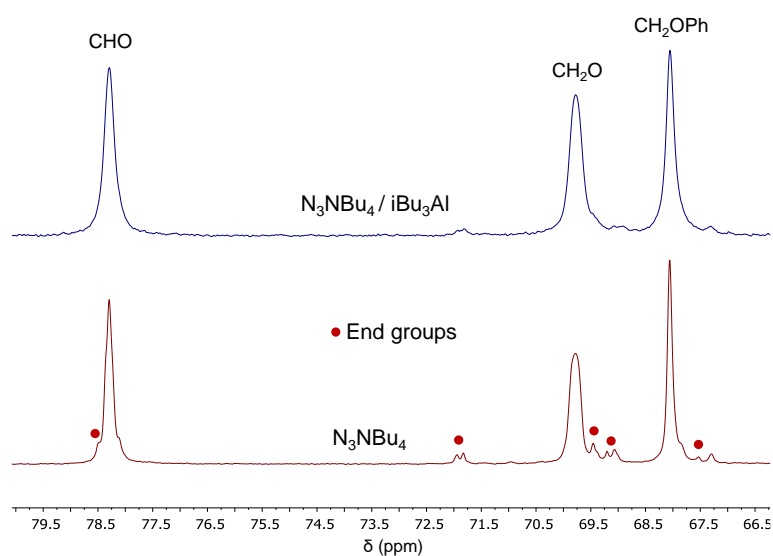
Figure 8. Methylene and methine region of ^{13}C NMR spectra of PGPE samples obtained with N_3NBu_4 and N_3NBu_4 / iBu_3Al. Spectra were recorded in $(CD_3)_2CO$ at 25 °C.

3.2. <u>Cyclization of α-azido, ω-alkyne poly(glycidyl phenyl ether)</u>

The presence of chains-end heterogeneities leads to non-quantitative cyclization. For that reason, the synthesis of PGPE with N_3NBu_4 alone is not a convenient route to generate pure cycles. On the contrary, the synthesis of PGPE with N_3NBu_4 / iBu_3Al exhibited high end-group fidelity which makes these samples suitable for generating cyclic structures with high purity. To this aim, the polymer samples were first subjected to propargylation and then to CuAAC "click" reaction according to Figure 8. The cyclization reactions of N_3-PGPE-ALK were performed at high dilution by using a continuous addition technique.[1]
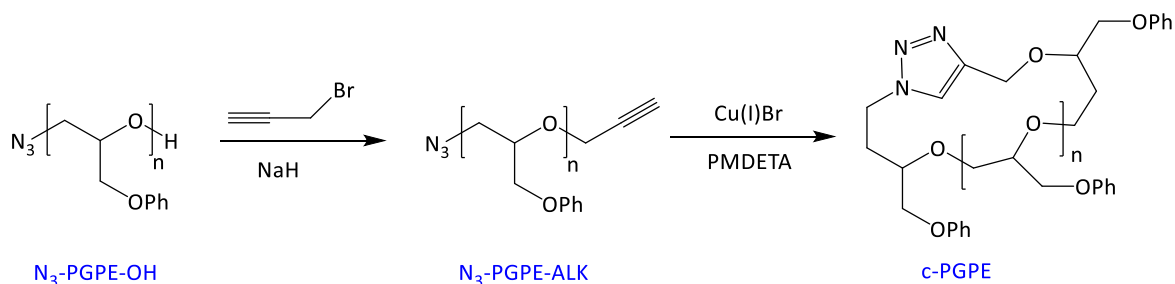
Figure 9. Scheme of end group modification and cyclization of PGPE.

3.2.1. Optimization of the cyclization reaction

During cyclization via ring closure, the competition between intermolecular coupling leading to high molecular weight linear chains and intramolecular coupling leading to cyclic chains determines the final purity of the product. In this section, different parameters were tested and their influence on cyclic purity was verified by GPC. The first parameter investigated was the temperature. For this set of experiments, the concentration of the linear precursor solution was fixed at 4.10^{-3} M (in 1 mL of toluene). In a second flask, 50 equivalents of Cu(I)Br respect to the azide function were dissolved in 1 mL of toluene. The polymer solution was added to the copper catalyst solution at 7.44 mL/h. Before addition, the polymer solution was heated at 70 °C to ensure good dissolution and to break potential polymer aggregates. During addition the copper catalyst solution was maintained at 0°C, 25 °C or 50 °C. The GPC measurements of the three obtained samples are presented in Figure 10.
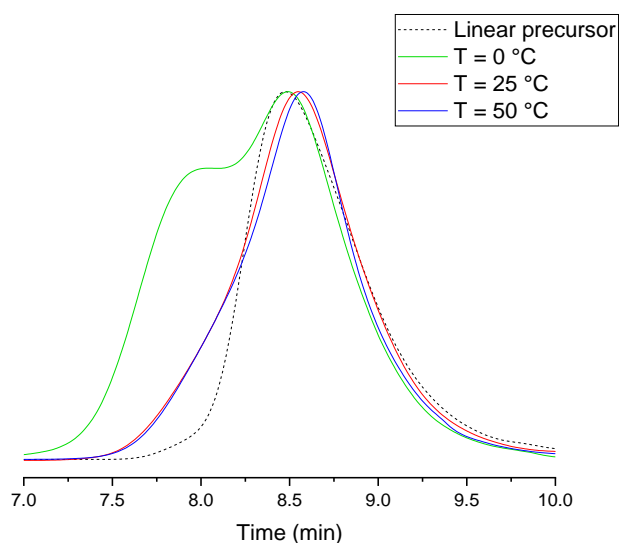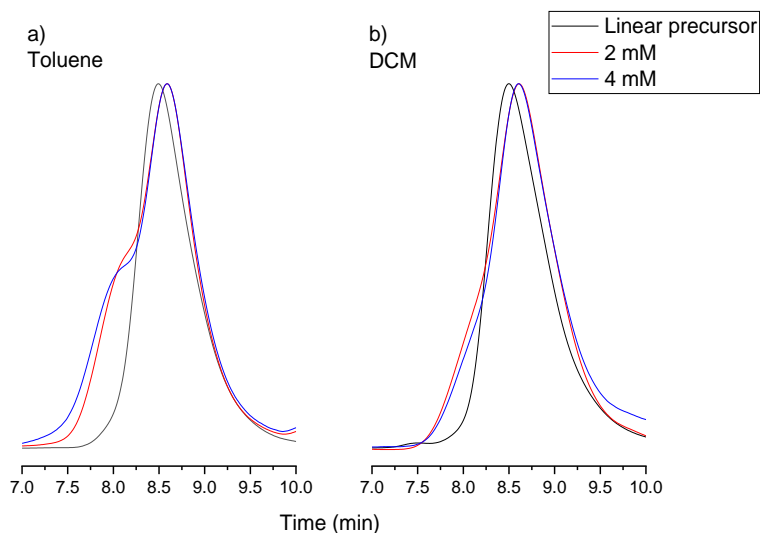
Figure 10. GPC data (RI detector) of N$_3$-PGPE-ALK linear precursor and samples generated by CuAAC "click" reaction at different temperatures to evaluate the influence of temperature on the cyclization reaction.

When the reaction was performed at 0 °C, no shift in retention time was observed, and in addition, an intense shoulder at the high molecular weight region appeared. At this low temperature, the "click" reaction between azide and alkyne is too slow favoring the intermolecular coupling of chains. As a result, a high proportion of high molecular weight linear chains were obtained. Increasing the temperature to 25 °C did helped to reduce the intermolecular coupling. However, a further increase in temperature did not show a significant improvement of the yield of cyclization.

For the second set of experiments, the influence of the concentration of the linear polymer solution in toluene and dichloromethane (DCM), was investigated. The

temperature was fixed at 25 °C and the rest of the parameters mentioned above were maintained constant. The GPC traces of the obtained cyclic samples are compared respect to that of their linear precursors (Figure 11). As observed in both solvents, the concentration did not have a significant influence over the cyclization yield. However, when the syntheses were performed in DCM, the intensity of the shoulder in the high molecular weight region was greatly reduced. This was attributed to the higher solubility of Cu(I)Br in DCM than in toluene, thus increasing its efficiency.

Figure 11. GPC data (RI detector) of N$_3$-PGPE-ALK linear precursor and samples generated by CuAAC "click" reaction at different polymer concentrations and solvents: a) toluene and b) DCM.

CuAAC proceeds via a complex multi-step mechanism during which the copper catalyst plays a key role.[30] The first step of the mechanism involves the formation of a copper (I) acetylide species able to activate the azide function by coordination. As a result, the electrophilic character of the azide and the nucleophilic character of the acetylide are enhanced allowing the formation of a first N-C bound and finally of the triazole ring.

In the third set of experiments the effect of Cu(I)Br purity was investigated. The temperature was fixed at 25 °C and the concentration of the polymer solution at 4.10^{-3} M in DCM. Cu(I)Br was either used as received or washed following the Keller and Wycoff method.[20] Finally, sodium L-ascorbate was added as reducing agent in an experiment using washed Cu(I)Br. The GPC traces of the obtained cyclic samples are presented in Figure 12.

When crude Cu(I)Br was used, a shift toward lower retention times was observed. It is known that Cu(I) is oxidized to Cu(II) by reaction with oxygen and that the CuAAC reaction is very sensitive to the presence of Cu(II), which does not catalyze the azide-alkyne reaction but promotes the coupling between two alkyne end groups leading to intermolecular coupling.[31] The purification of copper catalyst was observed to help in the reduction of intermolecular coupling. However, the maximum cyclization efficiency was only observed when the reducing agent, sodium L-ascorbate, was added to the reaction as observed by the absence of any shoulder in the GPC trace at shorter retention times. It is likely that sodium L-ascorbate prevented the oxidation of Cu(I) to Cu(II) by residual oxygen in the reaction.[32]
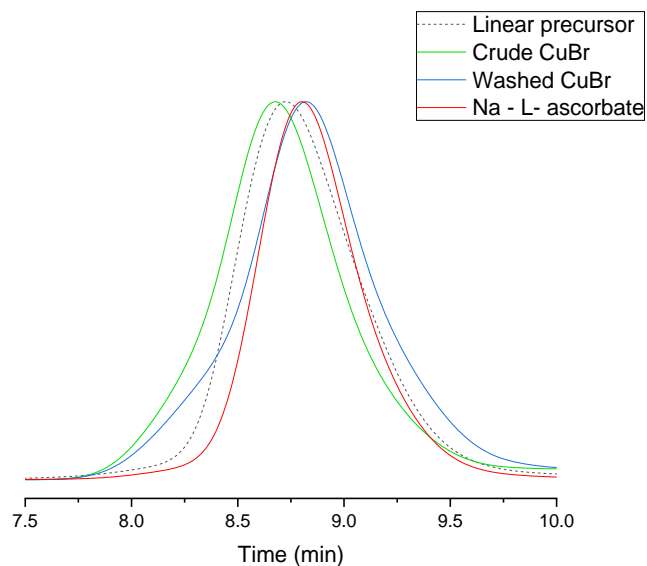
Figure 12. GPC data (RI detector) of N_3-PGPE-ALK linear precursor and samples generated by CuAAC "click" reaction with crude and pure Cu(I) catalyst, and with pure Cu(I) + sodium L-ascorbate.

As a conclusion of this section, the optimization of cyclization reaction was achieved by taking special care of the following factors: good solubility of all the reagents in the selected solvent (DCM much better than toluene), careful purification of Cu(I)Br, and addition of sodium L-ascorbate reducing agent. If one of the previous prerequisites were not fulfilled, then a shoulder at the high molar mass side of GPC chromatograms was observed indicating intermolecular coupling.

3.2.2. Evaluation of cyclic purity

MALDI-ToF MS data of end-group modified (N_3-PGPE-ALK) and cyclic PGPE (*c*-PGPE) products are shown in Figure 13 (generated from sample of Entry 7, Table 3). The data show a +38.31 Da shift with respect to N_3-PGPE-OH distribution in agreement with the addition of a terminal propargyl group in N_3-PGPE-ALK sample. Upon cyclization, these signals remain at the same position, as expected from the identical molecular mass of the linear precursor and cyclic product. The data also exhibit the presence of signals corresponding to the fragmentation of the azide functionality in N_3-PGPE-ALK via expulsion of N_2 (-N_2). These signals completely disappear after CuAAC reaction in *c*-PGPE sample. However, this behavior cannot be completely attributed to the occurrence of cyclization because intermolecular reactions between N_3-PGPE-ALK chains would also lead to the consumption of azide functionalities.
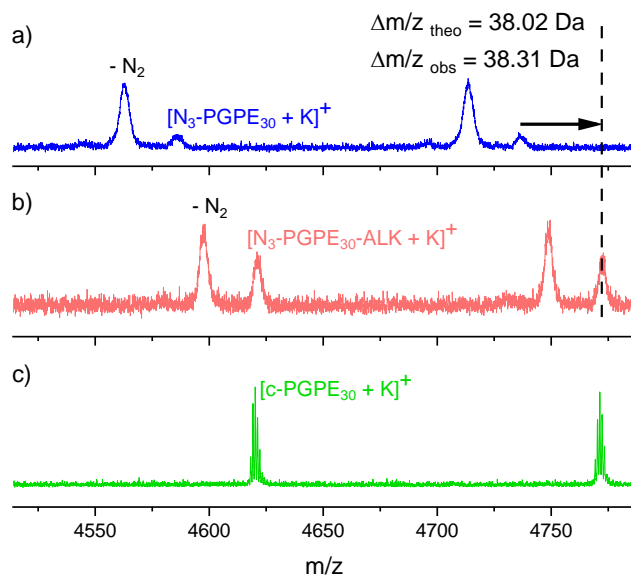
Figure 13. MALDI-ToF MS data in reflector mode of a) N_3-PGPE-OH sample synthesized with N_3NBu_4 / iBu_3Al, b) N_3-PGPE-ALK, and c) cyclic PGPE obtained by ring-closure of N_3-PGPE-ALK. $-N_2$ represents the fragments ions resulting from a loss of N_2 from their linear precursors via both in-source and postsource metastable ion formation.

In this sense, SEC-MALS-Vis provides more reliable data to verify cyclization as observed in Figure 14a. First, the peak of *c*-PGPE shifts to longer retention times with respect to that of its linear precursor, as expected from its structural compaction. Second, the data of *c*-PGPE exhibit monomodal molecular weight distribution and the lack of any shoulder at shorter retention times, indicating the absence of intermolecular coupling. Furthermore, viscosity data exhibit the expected reduction in the intrinsic viscosity ($[\eta]$) of the cyclic product in comparison with its linear precursor (Figure 14b). The $g' = [\eta]_C/[\eta]_L$ value obtained for this series of polymers in THF at 25 °C over a

molecular weight range from 5.9 to 15.8 kDa was 0.87 ± 0.01 and a Mark–Houwink exponent for both the linear and cyclic product of 0.39 ± 0.01. The K values of Mark–Houwink expression were 0.19 and 0.14 mL/g for the linear and cyclic product, respectively.
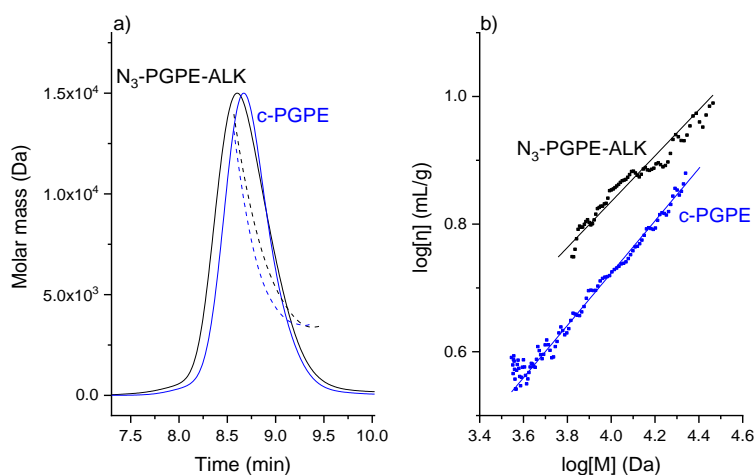

Figure 14. a) Normalized refractive index-GPC data and molar mass of N_3-PGPE-ALK and c-PGPE (synthesized from sample of Entry 7, Table 3). b) Mark–Houwink–Sakurada plot.

The g' value found for c-PGPE is higher than that reported for cyclic polystyrene, which typically varies from 0.5 to 0.7 depending on the molecular weight range, temperature, and solvent (good solvent and theta solvent).[33] The major discrepancy in the *g'* values found among those studies seems to be originated from the cyclic purity. In the case of *c*-PGPE, no reported *g'* values were found for comparison. The closest cyclic polyether structures with already reported *g'* values are the cyclic poly(butylene oxide),[12] whose

g' values (determined in THF at 25 °C) vary from 0.61 to 0.88 in going from 9 to 4 kDa of M_n.

Finally, the cyclic purity was verified by dielectric spectroscopy. In this technique the frequency dependence of the complex dielectric permittivity is measured and the relaxation processes are detected as peaks in the first derivative of the real part of the dielectric permittivity with respect to the log frequency, $d\varepsilon'/d[\log(f)]$. Figure 15 shows - $d\varepsilon'/d[\log(f)]$ as a function of frequency for the c-PGPE sample whose GPC data is shown in Figure 14 (hereafter named pure *c*-PGPE sample). To compare, the dielectric data of its linear precursor N_3-PGPE-OH and an impure *c*-PGPE sample are also exhibited. The impure *c*-PGPE sample was obtained by using washed Cu(I)Br but in the absence of sodium L-ascorbate (washed Cu(I)Br in Figure 12). This impure *c*-PGPE sample exhibits a high molecular weight tail in the GPC chromatogram. The area of this tail respect to the total GPC area is about 17 %. This tail could be attributed to the formation of higher molecular weight chains by intermolecular coupling. It is likely that in the presence of Cu(II) the reaction between two alkyne groups (Glaser coupling)[31] is also favored in addition to the reaction catalyzed by Cu(I) between alkyne and azido groups of different chains.
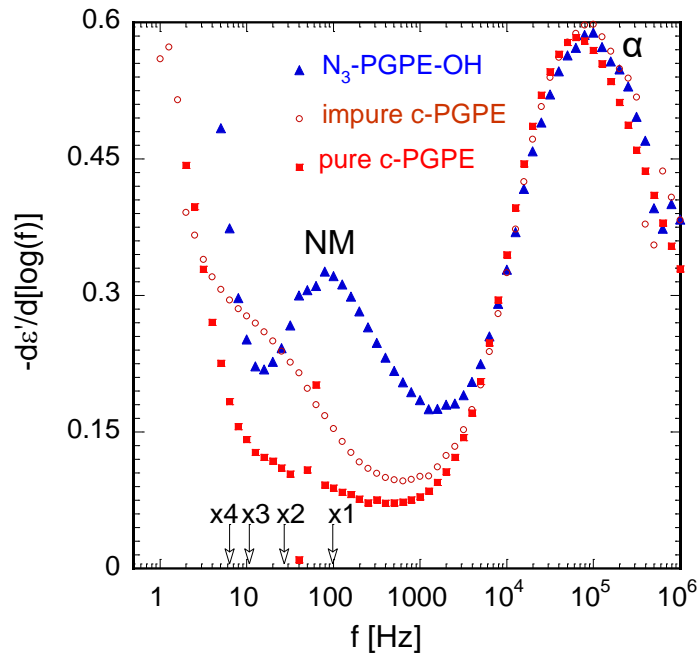
Figure 15. Dielectric spectroscopy data of pure and impure *c*-PGPE samples at 320 K and of their linear precursor (N$_3$-PGPE-OH) at 315 K. "xn" represents the position at which the NM contribution is expected from linear chain impurities with "n" times the mass of the N$_3$-PGPE-OH precursor.

The dielectric data of N$_3$-PGPE-OH in Figure 15 show two relaxation peaks, the segmental α-relaxation peak (at the high frequency side) and the normal mode (NM) peak (at the low frequency side). The lowest frequency side exhibits a signal increase which is related to interfacial polarization processes originated from ionic conductivity in the material. The peak assignment is in agreement with previous dielectric studies of PGPE samples with different microstructures and topologies.[18] The α-relaxation is related to the glass transition of the material. DSC data showed that pure *c*-PGPE has a

higher T_g value (287.3 K) than its linear precursor, N_3-PGPE-OH (281.2 K), as expected by theory and previous experiments[34] (Figure 16). Consequently, to easily compare the dielectric data and to find good superposition of the α-relaxation peaks, the data of the cyclic compounds are shown at a temperature 5 K higher than that of their linear precursor.
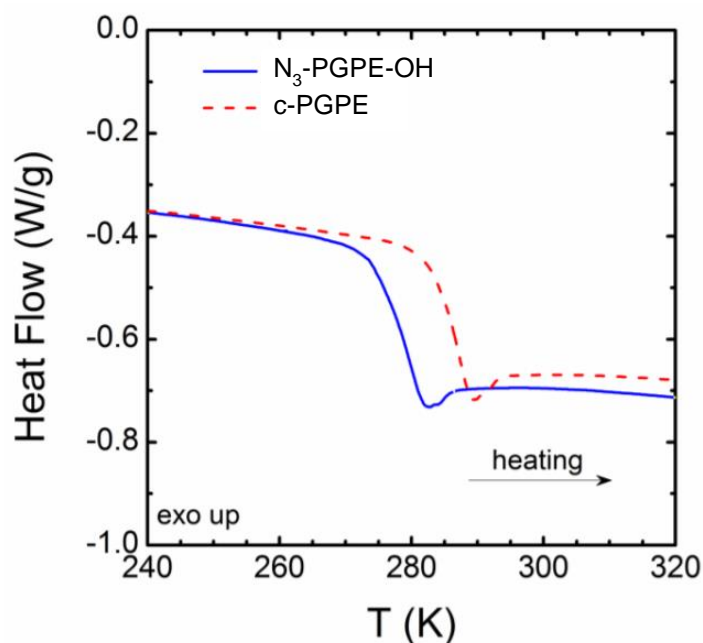

Figure 16. DSC data exhibiting the glass transition of linear and cyclic PGPE samples (2nd heating run).

The NM peak in regio-regular linear polymer chains is related to the fluctuations of end-to-end vector, as mentioned above. As observed in Figure 15, the NM peak detected in the linear precursor, N_3-PGPE-OH, drastically changes after cyclization. In the impure

c-PGPE sample a lower frequency shoulder is detected. According to the simple Rouse model,[35] the NM peak frequency depends dramatically on the molecular mass, ($f_{NM} \propto M^{-2}$). Therefore, the shoulder can be attributed to the presence of linear n-mers (n < 4) generated from intermolecular coupling (see arrows in Figure 15). Contrarily, in the pure c-PGPE sample, no clear shoulder is detected, and the remaining signal is close to the detection limit. The former result confirms the presence of linear impurities of higher molecular weights detected by GPC in the impure c-PGPE sample. Moreover, the absence of a detectable NM in pure c-PGPE indicates a high purity level of this sample in agreement with the GPC analysis.

4. <u>Conclusions</u>

Pure monocyclic structures of poly(glycidyl phenyl ether) can be generated by combining AROP and CuAAC "click" reaction but only after guaranteeing the end-group fidelity of as-generated linear polymers with N_3NBu_4 initiator and a series of reaction conditions during cyclization. In particular, initiation with N_3NBu_4 / iBu_3Al allows the formation of polymer chains with high end-group fidelity at $M_n < 20$ kDa. All the chains contain an azide group at the chain head (α-position) and a hydroxyl group at the chain tail (ω-position), which can be conveniently transformed into alkyne functionalities for a subsequent cyclization reaction. However, the polymerization initiated with N_3NBu_4 alone conducted to the formation of only 83 % of linear chains containing azide groups at the α-position due to the formation of 17 % of undesired alkene functionalities in

monomer transfer reactions. High cyclic purity was achieved after optimization of CuAAC "click" reaction conditions. The copper (I) catalyst purity was found to be of great importance in the generation of pure cyclic polymers. For that reason, Cu(I)Br was thoroughly washed before reaction and stored under inert atmosphere. With the addition of sodium L-ascorbate, oxidation of Cu(I) during reaction was avoided preventing intermolecular coupling and therefore, the formation of higher molecular weight impurities.

The cyclic purity was demonstrated by a combination of techniques including GPC with triple detection and dielectric spectroscopy. The latter have been demonstrated to be a convenient technique for verifying cyclization in polymers that present dielectric relaxations due to fluctuations of the end-to-end vector in their linear form. In the case of regio-regular polymers, it is possible to detect the presence of linear impurities in cyclic samples since BDS is highly sensitive to changes in the topology of the polymer chain.

5. <u>References</u>

(1)   Laurent, B. A.; Grayson, S. M. An Efficient Route to Well-Defined Macrocyclic Polymers via "Click" Cyclization. *J. Am. Chem. Soc.* **2006**, *128* (13), 4238–4239.

(2)   Hossain, M. D.; Lu, D.; Jia, Z.; Monteiro, M. J. Glass Transition Temperature of Cyclic Stars. *ACS Macro Lett.* **2014**, *3* (12), 1254–1257.

(3)   Tomikawa, Y.; Fukata, H.; Ko, Y. S.; Yamamoto, T.; Tezuka, Y. Construction of Double-Eight and Double-Trefoil Polymer Topologies with Core-Clickable Kyklo - Telechelic Precursors. *Macromolecules* **2014**, *47* (23), 8214–8223.

(4)   De Luzuriaga, A. R.; Ormategui, N.; Grande, H. J.; Odriozola, I.; Pomposo, J. A.; Loinaz, I. Intramolecular Click Cycloaddition: An Efficient Room-Temperature Route towards Bioconjugable Polymeric Nanoparticles. *Macromol. Rapid Commun.* **2008**, *29* (12–13), 1156–1160.

(5)   Barnes, J. C.; Ehrlich, D. J. C.; Gao, A. X.; Leibfarth, F. A.; Jiang, Y.; Zhou, E.; Jamison, T. F.; Johnson, J. A. Iterative Exponential Growth of Stereo- and Sequence-Controlled Polymers. *Nat. Chem.* **2015**, *7* (10), 810–815.

(6)   Voit, B. The Potential of Cycloaddition Reactions in the Synthesis of Dendritic Polymers. *New J. Chem.* **2007**, *31* (7), 1139–1151.

(7)   Zhu, W.; Zhong, M.; Li, W.; Dong, H.; Matyjaszewski, K. Clickable Stars by Combination of AROP and Aqueous AGET ATRP. *Macromolecules* **2011**, *44* (7), 1920–1926.

(8)   Binder, W. H.; Sachsenhofer, R. "Click" Chemistry in Polymer and Material Science: An Update. *Macromol. Rapid Commun.* **2008**, *29* (12–13), 952–981.

(9)   Gervais, M.; Deffieux, A. Direct Synthesis of α -Azido , ω -Hydroxypolyethers by Monomer-Activated Anionic Polymerization. *Macromolecules* **2009**, *3* (42), 2395–2400.

(10) Yang, S.; Kim, Y.; Kim, H. C.; Siddique, A. B.; Youn, G.; Kim, H. J.; Park, H. J.; Lee, J. Y.; Kim, S.; Kim, J. Azide-Based Heterobifunctional Poly(Ethylene Oxide)s: NaN3-Initiated "Living" Polymerization of Ethylene Oxide and Chain End Functionalizations. *Polym. Chem.* **2016**, *7* (2), 394–401.

(11) Misaka, H.; Tamura, E.; Makiguchi, K.; Kamoshida, K.; Sakai, R.; Satoh, T.; Kakuchi, T. Synthesis of End-Functionalized Polyethers by Phosphazene Oxide and Glycidyl Ether. **2012**, *50*, 1941–1952.

(12) Isono, T.; Kamoshida, K.; Satoh, Y.; Takaoka, T.; Sato, S. I.; Satoh, T.; Kakuchi, T. Synthesis of Star- and Figure-Eight-Shaped Polyethers by t-Bu-P$_4$-Catalyzed Ring-Opening Polymerization of Butylene Oxide. *Macromolecules* **2013**, *46* (10), 3841–3849.

(13) Satoh, Y.; Matsuno, H.; Yamamoto, T.; Tajima, K.; Isono, T.; Satoh, T. Synthesis of Well-Defined Three- and Four-Armed Cage-Shaped Polymers via "Topological Conversion" from Trefoil- and Quatrefoil-Shaped Polymers. *Macromolecules* **2017**, *50* (1), 97–106.

(14) Billouard, C.; Carlotti, S.; Desbois, P.; Deffieux, A. "Controlled" High-Speed Anionic Polymerization of Propylene Oxide Initiated by Alkali Metal Alkoxide/Trialkylaluminum Systems. *Macromolecules* **2004**, *37* (11), 4038–4043.

(15) Elupula, R.; Oh, J.; Haque, F. M.; Chang, T.; Grayson, S. M. Determining the Origins of Impurities during Azide – Alkyne Click Cyclization of Polystyrene. *Macromolecules* **2016**, *49*, 4369–4372.

(16) Kremer, F.; Schönhals, A. *Broadband Dielectric Spectroscopy*, Springer-V.; Berlin, Heidelberg, New York, 2003.

(17) Asenjo-Sanz, I.; Veloso, A.; Miranda, J. I.; Pomposo, J. A.; Barroso-Bujans, F. Zwitterionic Polymerization of Glycidyl Monomers to Cyclic Polyethers with B(C6F5)3. *Polym. Chem.* **2014**, *5* (24), 6905–6908.

(18) Gambino, T.; Martínez De Ilarduya, A.; Alegría, A.; Barroso-Bujans, F. Dielectric Relaxations in Poly(Glycidyl Phenyl Ether): Effects of Microstructure and Cyclic Topology. *Macromolecules* **2016**, *49* (3), 1060–1069.

(19)   Haque, F. M.; Alegria, A.; Grayson, S. M.; Barroso-bujans, F. Detection, Quanti Fi Cation, and " Click-Scavenging " of Impurities in Cyclic Poly(Glycidyl Phenyl Ether) Obtained by Zwitterionic Ring- Expansion Polymerization with B(C$_6$F$_5$)$_3$. *Macromolecules* **2017**, *50*, 1870–1881.

(20)   Keller, R. N.; Wrcoff, H. D.; Marchi, L. E. Copper(I) Chloride. In *Inorganic Syntheses*; Conard Fernelius, W., Ed.; 1946; Vol. 2, pp 1–4.

(21)   Matyjaszewski, K. Introduction to Living Polymeriz. Living and/or Controlled Polymerization. *J. Phys. Org. Chem.* **1995**, *8* (4), 197–207.

(22)   Brocas, A. L.; Mantzaridis, C.; Tunc, D.; Carlotti, S. Polyether Synthesis: From Activated or Metal-Free Anionic Ring-Opening Polymerization of Epoxides to Functionalization. *Prog. Polym. Sci.* **2013**, *38* (6), 845–873.

(23)   Herzberger, J.; Niederer, K.; Pohlit, H.; Seiwert, J.; Worm, M.; Wurm, F. R.; Frey, H. Polymerization of Ethylene Oxide, Propylene Oxide, and Other Alkylene Oxides: Synthesis, Novel Polymer Architectures, and Bioconjugation. *Chem. Rev.* **2016**, *116* (4), 2170–2243.

(24)   Price, C. C.; Carmelite, D. D. Reactions of Epoxides in Dimethyl Sulfoxide Catalyzed by Potassium T-Butoxide. *J. Am. Chem. Soc.* **1966**, *88* (17), 4039–4044.

(25)   Pierre, L. E.; Price, C. C. The Room Temperature Polymerization of Propylene Oxide. *J. Am. Chem. Soc.* **1956**, *78* (14), 3432–3436.

(26)   Labbé, A.; Carlotti, S.; Billouard, C.; Desbois, P.; Deffieux, A. Controlled High-Speed Anionic Polymerization of Propylene Oxide Initiated by Onium Salts in the Presence of Triisobutylaluminum. *Macromolecules* **2007**, *40* (22), 7842–7847.

(27)   Stolarzewicz, A. A New Chain Transfer Reaction in the Anionic Polymerization of 2,3-epoxypropyl Phenyl Ether and Other Oxiranes. *Die Makromol. Chemie* **1986**, *187* (4), 745–752.

(28)   Li, Y.; Hoskins, J. N.; Sreerama, S. G.; Grayson, S. M. MALDI-TOF Mass Spectral Characterization of Polymers Containing an Azide Group: Evidence of Metastable Ions. *Macromolecules* **2010**, *43* (14), 6225–6228.

(29)   Schmitt, B.; Stauf, W.; Müller, A. H. E. Anionic Polymerization of (Meth)Acrylates in the Presence of Cesium Halide-Trialkylaluminum Complexes in Toluene. *Macromolecules* **2001**, *34* (6), 1551–1557.

(30)   Hein, J. E.; Fokin, V. V. Copper-Catalyzed Azide–Alkyne Cycloaddition (CuAAC) and beyond: New Reactivity of Copper(i) Acetylides. *Chem. Soc. Rev.* **2010**, *39* (4), 1302–1315.

(31)   Leophairatana, P.; Samanta, S.; De Silva, C. C.; Koberstein, J. T. Preventing Alkyne-Alkyne (i.e., Glaser) Coupling Associated with the ATRP Synthesis of Alkyne-Functional Polymers/Macromonomers and for Alkynes under Click (i.e., CuAAC) Reaction Conditions. *J. Am. Chem. Soc.* **2017**, *139* (10), 3756–3766.

(32)   Rostovtsev, V. V; Green, L. G.; Fokin, V. V; Sharpless, K. B. A Stepwise Huisgen Cycloaddition Process : Copper(I) -Catalyzed Regioselective "Ligation" of Azides and Terminal Alkynes. *Angew. Chemie Int. Ed.* **2002**, *41* (14), 2596–2599.

(33)   Jeong, Y.; Jin, Y.; Chang, T.; Uhlik, F.; Roovers, J. Intrinsic Viscosity of Cyclic Polystyrene. *Macromolecules* **2017**, *50* (19), 7770–7776.

(34)   Yamamoto, T.; Tezuka, Y. Topological Polymer Chemistry: A Cyclic Approach toward Novel Polymer Properties and Functions. *Polym. Chem.* **2011**, *2* (9), 1930–1941.

(35)   Rubinstein, M.; Colby, R. H. *Polymer Physics*, Oxford Uni.; Oxford, 2003.

Linear poly(glycidyl phenyl ether) with a symmetric "two-arm" dipolar microstructure

Table of Contents

In this chapter, the combination of ethylene glycol and the phosphazene base 1-tert-Butyl-4,4,4-tris(dimethylamino)-2,2-bis[tris(dimethylamino)-phosphoranylidenamino]-2λ5,4λ5-catenadi(phosphazene) (t-BuP$_4$) is used to produce poly(glycidyl phenyl ether) (PGPE) containing a dipole inversion along the chain contour. In other words, each polymer chain is composed of two regio-regular sub-chains with its own dipole moment facing opposite direction. Broadband dielectric spectroscopy (BDS) is used to verify the bi-directional growth of arms in synthesized PGPE samples.

1. __Introduction__

Neutral phosphazene bases developed by Schwesinger et al.[1] have played an important role in the synthesis of complex structures through the utilization of functional or multifunctional initiators.[2] t-BuP$_4$, the most basic one of this phosphazene family, has been used in combination with alcohols in the anionic ring opening polymerization (AROP) of monosubstituted epoxides[3–9] and ethylene oxide.[10] t-BuP$_4$ promotes hydroxyl deprotonation generating alkoxide initiators. By playing with the functionality of the alcohol, a diversity of architectures can be produced including linear, star-shaped and multicyclic structures.[6–9,11–13]

Transfer to monomer reactions are frequently observed in t-BuP$_4$ / alcohol-initiated polymerizations of asymmetric epoxide monomers.[14] The addition of a Lewis acid such as iBu$_3$Al was proven efficient to reduce transfer reactions. The Lewis acid forms a 1:1 "ate" complex with the alkoxide species while the excess of iBu$_3$Al activates the

monomer. As a result, an increase of the polymerization rate and a decrease of the basicity of the growing chains occur.[15] However, initiation by hydride coming from an isobutyl group of iBu_3Al can still occur, as observed in the monomer-activated polymerization of propylene oxide initiated by onium salts (tetrabutylammonium chloride, tetrabutylammonium bromide and tetrabutylphosphonium chloride)[16] and that of glycidyl phenyl ether (GPE) initiated by tetrabutylammonium azide.[17] Initiation by an isobutyl anion coming from iBu_3Al has also been observed in the polymerization of methacrylates initiated by cesium halide[18] and GPE initiated by tetrabutylammonium azide.[17] Side reactions affect end-group fidelity and consequently limit the generation of macromolecular architectures with high purity.

Figure 1 exhibits different structures that can be produced in a synthetic polymer sample obtained by initiation with ethylene glycol via AROP. As indicated, in addition to the expected two-symmetric-arm polymer, other structures can be formed either by termination or initiation from impurities. Note that the three cases in Figure 1a-c are depicted with similar chain length, so they would not be differentiated by size exclusion chromatography (SEC). Structure (c) can be differentiated from structures (a) and (b) by NMR and matrix-assisted laser desorption/ionization–time-of-flight mass spectrometry (MALDI-ToF MS), but structure (b) cannot be differentiated from structure (a) by any of these methods. It has been recognized that the uniformity of arm segments in star polymers synthesized from core-first initiators cannot be unambiguously determined by SEC.[19] In order to verify the arm symmetry in star copolyethers of three and four arms synthesized via t-BuP$_4$-catalyzed AROP, Satoh et al. performed arm cleavage by hydrogenolysis with Pd/C and characterized their molecular weight by SEC.[8] By means

of this laborious method, they demonstrated not only that the arm length was homogeneous but also that each hydroxyl group of the initiator led to initiation.
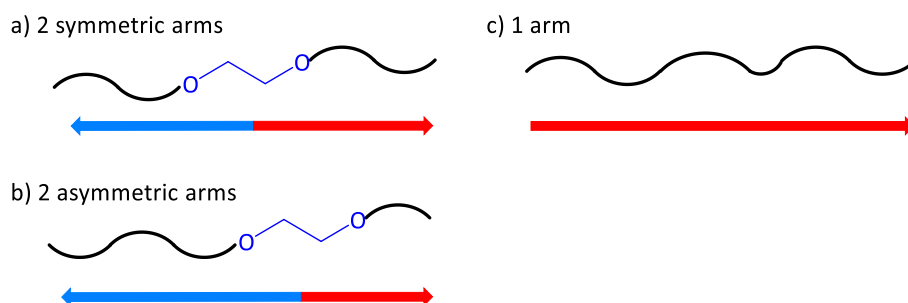

Figure 1. Expected two-symmetric-arm polymer a) and possible byproducts b, c) in AROP initiated by a diol. All of them will exhibit identical molecular weights but different dielectric responses associated to the dipolar moment along the chain contour (indicated by arrows in a simplified way).

Broadband dielectric spectroscopy (BDS) is a technique particularly useful for examining certain molecular characteristics, especially those related to the dipolar microstructure. BDS measures the fluctuations of molecular dipoles in an alternating electric field and provides useful information about the molecular mobility at different time scales including the chain, segmental, and local mobility.[20] The dielectric normal mode (NM) relaxation is associated with chain fluctuations and is affected by the dipolar moment orientation along the chain contour. Therefore it is sensitive to changes in both the regiochemistry and the chain topology.[17,21,22] The dipolar moment orientations of the linear chains depicted in Figure 1 exhibit clear differences among them. It is possible to

take advantage of these differences by analyzing the BDS results of samples that exhibit a NM relaxation. Furthermore, for unentangled polymer chains, the Rouse theory provides accurate quantitative predictions on the dielectric NM. According to this theory, a polymer chain is represented by N beads connected by springs. The chain relaxation is described by N different relaxation modes, numbered by a mode index p = 1, 2, 3, ..., N. The relaxation time of the pth mode is described as $\tau_p \approx \tau_0 \left(\frac{N}{p}\right)^2$, where τ_0 is the relaxation time of the monomer. For polymers composed by a single arm, as in Figure 1c, only odd modes contribute to the dielectric NM relaxation (p = 1, 3, 5, ...). However, the NM relaxation of polymers composed of two symmetric arms (Figure 1a) is described by even-numbered Rouse modes (p = 2, 4, 6, ...). Then, for two polymer chains of equal molecular weight (same N) but different topology, the NM relaxation time will be different because of the Rouse modes contributing to each case. The analysis of the NM relaxation using this framework allows the application of BDS to identify different polymer architectures. Moreover, BDS requires only a small mass of material, the polymer does not suffer chemical changes during the experiment, and the sample is fully recoverable after measurements.

In this chapter, the effects of initiation with t-BuP$_4$ – diol on the symmetrical growth of poly(glycidyl phenyl ether) (PGPE) in two directions in the presence and absence of iBu$_3$Al is investigated. The prepared polymers were characterized combining NMR, MALDI-ToF MS and BDS. The latter technique allows the identification of two-arm PGPE samples in a direct and easy way and the assessment of their arm symmetry without the need of using chemical cleavage of arms. To this end, the molecular weight dependence of the NM relaxation for bidirectionally grown PGPE samples (hereafter called l-2a-PGPE) obtained with a t-BuP$_4$ / diol initiating system is compared with that

of PGPE samples obtained with monofunctional initiators presented in Chapter II (hereafter called *l*-1a-PGPE). The BDS analysis showed that polymers obtained in the absence of iBu$_3$Al were formed by two symmetrical arms whereas those obtained in the presence of iBu$_3$Al were mainly formed by unidirectionally grown PGPE chains due to side reactions.

2. <u>Experimental section</u>

GPE and toluene (Sigma-Aldrich) were distilled from CaH$_2$ under reduced pressure and stored under nitrogen atmosphere. iBu$_3$Al and *t*-BuP$_4$ (Sigma-Aldrich) were stored in a glovebox and used as received. Ethylene glycol (Sigma-Aldrich) was washed three times with hexane and dried at 80 °C overnight before being stored in a glovebox.

2.1. <u>Synthesis of two-arm poly(glycidyl phenyl ether) with *t*-BuP$_4$ / ethylene glycol</u>

In a typical experiment, ethylene glycol (5 µL; 9.0×10^{-5} mol) and 180 µL of *t*-BuP$_4$ solution (0.8 mol/L in hexane) were transferred to a round bottom flask containing 0.9 mL of toluene and equipped with a magnetic stirrer in a glovebox. The obtained solution was stirred at room temperature for 30 min. GPE (1 mL; 7.0×10^{-3} mol) was added under nitrogen atmosphere. Then the flask was sealed and cooled

down to –30 °C and stirred at that temperature for 15 minutes. After this, the reaction was carried out at room temperature for 72 h. The reaction was quenched with a solution of HCl (0.5 M in methanol), The solvent was evaporated under reduced pressure, the product redissolved in THF and purified by two precipitations in cold hexane. Different molecular weight polymers were prepared by adjusting the monomer to initiator (ethylene glycol) ratio.

2.2.   Synthesis of two-arm poly(glycidyl phenyl ether) with t-BuP$_4$/ethylene glycol and iBu$_3$Al as monomer activator

In a typical experiment, ethylene glycol (5 µL; 9.0×10^{-5} mol) and 180 µL of t-BuP$_4$ solution (0.8 mol/L in hexane) were transferred to a round bottom flask containing 0.9 mL of toluene in a glovebox. The obtained solution was stirred at room temperature for 30 min. GPE (1 mL; 7.0×10^{-3} mol) and, immediately after, 255 µL of iBu$_3$Al solution (1.1 mol/L in toluene) were added under nitrogen atmosphere. Then, the flask was sealed and cooled down to – 30 °C and stirred at that temperature for 15 min. After this, the reaction was carried out at room temperature for 6 h. The reaction was quenched with a solution of HCl (0.5 M in methanol), The solvent was evaporated under reduced pressure, the product redissolved in THF and purified by two precipitations in cold hexane. Different molecular weight polymers were prepared by adjusting the monomer to initiator (ethylene glycol) ratio.

2.3. <u>Characterization</u>

MALDI-ToF MS measurements were performed on a Bruker Autoflex Speed system (Bruker, Germany) equipped with a 355 nm Nd:YAG laser. Spectra were acquired in linear and reflector mode. *Trans*-2-[3-(4-*tert*-Butylphenyl)-2-methyl-2-propenylidene] malononitrile (DCTB, Fluka) was used as a matrix. Potassium trifluoroacetate (KTFA) (Aldrich) was added as the cationic ionization agent (~10 mg/ml dissolved in THF). The matrix was dissolved in THF at a concentration of 20 mg/ml. Polymer samples were also dissolved in THF at a concentration of ~10 mg/ml. In a typical MALDI experiment, the matrix, salt, and polymer solutions were premixed at a 20:1:3 ratio. Approximately 0.5 μL of the obtained mixture were hand spotted on the ground steel target plate. The spectra were externally calibrated using a mixture of different polyethylene glycol standards (PEG, Varian).

^{1}H and ^{13}C NMR spectra were acquired at 25 °C or 50 °C on a Bruker Avance 400 in CDCl$_3$ or acetone-d_6 at 25 °C. To differentiate end-group signals from those of the backbone, a small amount (a drop) of trichloroacetyl isocyanate (TAI) derivatizing agent was added to the samples recorded in acetone-d_6.

BDS measurements were performed using an Alpha analyzer (Novocontrol) and the temperature was controlled by a nitrogen gas jet (Quatro from Novocontrol), with a temperature stability during every single frequency sweep of ±0.1 K. Starting at room temperature (*c.a.* 300 K), all samples were heated up to 420 K at a 3 K/min rate inside the cell. The temperature was maintained at 420 K for 15 min to remove water and

residual solvents. Then, a frequency sweeps was performed over a broad frequency range, $10^{-1} \leq f$ (Hz) $\leq 10^{6}$, in 5 K isothermal cooling steps from 420 K to 270 K. In order to minimize conductivity-related contributions, all the polymer samples were thoroughly purified before BDS measurements, as follows. A 1 mg/mL solution of the polymer in dichloromethane was prepared. To this solution, a mixed-bed ion-exchange resin (Dowex Monosphere MR-450 by Sulpeco) was added in a proportion of 100 mg resin per each mL of the polymer solution. The resin/solution mixture was stirred for 2 h at room conditions. Afterward, the resin was filtered out and the solution concentrated by rotary evaporation. The resulting liquid was left in a vacuum oven at 60 °C for 24 h to evaporate the residual solvent. For BDS measurements, the purified samples were sandwiched between gold electrodes by melt pressing. Briefly, the bottom electrode (20 mm diameter) was placed on a hot plate at 150 °C and the sample was deposited on top of it. This temperature was high enough for the polymer to be in its liquid state. Then, a Teflon spacer (0.1 mm in thickness) was placed on the polymer melt, and finally, the top electrode (10 mm diameter) was attached. The formed capacitor was cooled down fast by placing it on a cold plate.

3. Results and discussion

3.1. Synthesis of two-symmetric-arm (or dipole-inverted) poly(glycidyl phenyl ether)

3.1.1. End group fidelity

To synthesize α, ω–hydroxy telechelic PGPE with two symmetric arms, the polymerization of GPE was first initiated with ethylene glycol and t-BuP$_4$. If no transfer reactions occur, a two-symmetric-arm polyether should be formed with a dipole-inverted structure (Figure 2).
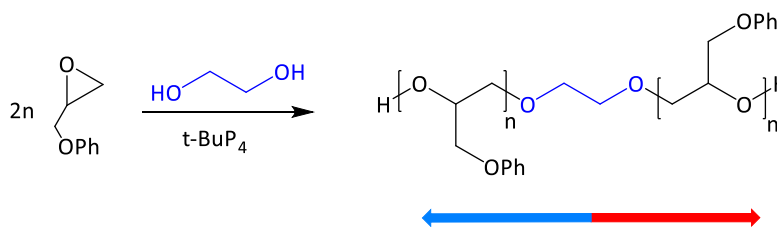

Figure 2. Polymerization of GPE leading to two-symmetric-arm (or dipole-inverted) PGPE.

In these conditions, the polymerization occurred very slowly, in 7-15 days, but PGPE samples with high end-group fidelity were generated. Then, the polymerization was performed in the presence of iBu$_3$Al with the purpose of accelerating the reaction,[11] but the results showed a detriment of the molecular characteristics of synthesized polymers. Table 1 compares the molecular characteristics of synthesized polymers and Figure 3 exhibits ^{1}H NMR data of representative PGPE samples obtained in the presence and absence of iBu$_3$Al.

Table 1. Molecular characteristics of representative PGPE samples.

Entry	[GPE]$_0$ / [OH] / [t-BuP$_4$] / [iBu$_3$Al]	Time (h)^a	M$_{n (theo)}$ (kDa)	M$_{n (SEC)}$ (kDa)	Đ	Yield (wt%)^b
1	25/1/0.1/0	20	3.8	2.6	1.04	95
2	50/1/0.2/0	200	7.5	6.1	1.11	80
3	39/1/0.8/0	72	5.9	5.4	1.09	80
4	51/1/1/0	360	7.7	7.3	1.05	85
5	86/1/1/0	300	13.0	6.5	1.14	85
6	39/1/0.2/1.5	70	5.8	7.7	1.52	75
7	19/1/0.8/1.5	6	2.9	6.0	1.50	85
8	39/1/0.8/1.5	6	5.8	5.8	1.28	90
9	49/1/1/1.5	35	7.3	6.8	1.21	100
10	87/1/1/1.5	48	13.0	10.5	1.12	99

^{a}Time at which the reaction was stopped after observing high viscosity. ^{b}Yield determined gravimetrically.

^{1}H NMR data of PGPE samples obtained in the absence and presence of iBu$_3$Al exhibit the proton signals corresponding to depicted PGPE structure (Figure 2). The spectra do not exhibit signals corresponding to alkene moieties, which indicate the absence of chain transfer to monomer in both samples (Figure 3). However, the spectra do exhibit that the signal integration of aliphatic protons differs between both samples, which have similar SEC-determined molecular weights. The results indicate that the polymer synthesized in the presence of iBu$_3$Al contains more GPE units per ethylene glycol moieties than that synthesized in the absence of iBu$_3$Al. In fact, the molecular weight that could be determined through proton integration would indicate that $M_{n(NMR)}$ of the former is overestimated, 11.8 kg/mol, whereas that of the latter is 4.8 kg/mol in agreement with $M_{n(SEC)}$. These results suggest that in the presence of iBu$_3$Al, ethylene glycol does not initiate all the chains in contrast to what happens in the absence of iBu$_3$Al. These results are further confirmed by MALDI-ToF MS.
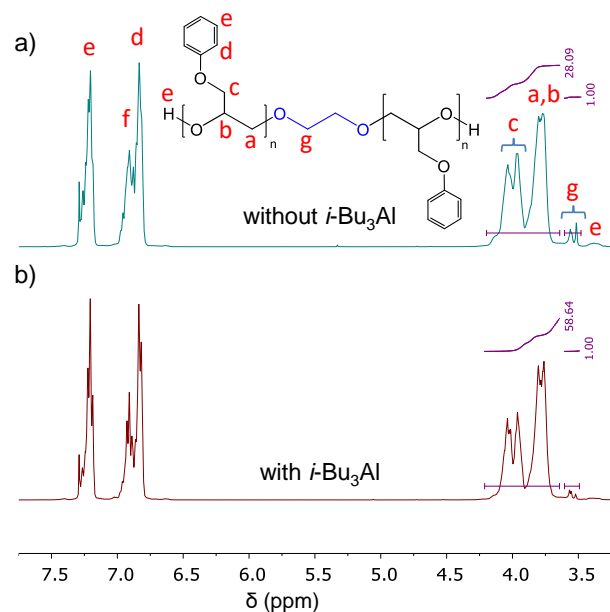
Figure 3. ^{1}H NMR (in CDCl$_3$) of PGPE samples of similar M$_{n \text{ (SEC)}}$ obtained in the (a) absence and (b) presence of iBu$_3$Al (Entries 3 and 8, respectively).

MALDI-ToF MS data of a representative PGPE sample obtained in the absence of iBu$_3$Al (Figure 4a) exhibit high-intensity signals corresponding to potassium-complexed PGPE chains obtained by initiation with deprotonated ethylene glycol [PGPE-EG$_n$+K]$^+$ and termination with two protons (one at each chain end, Figure 2). The signals are separated by 150.17 Da, which corresponds to the repeat unit mass of PGPE.
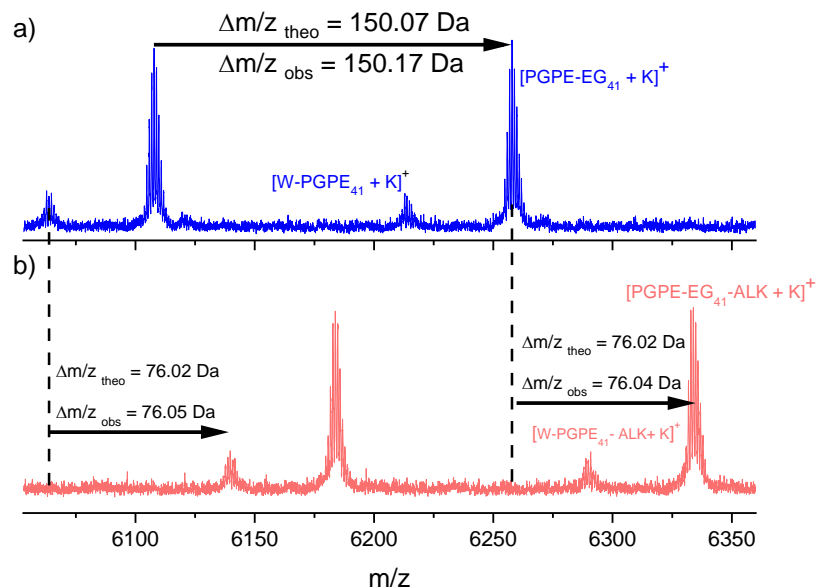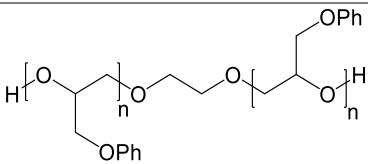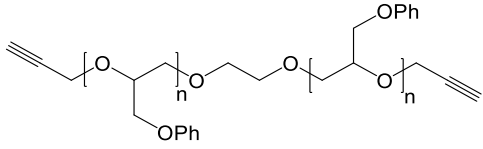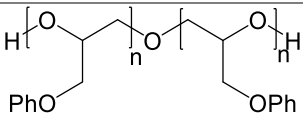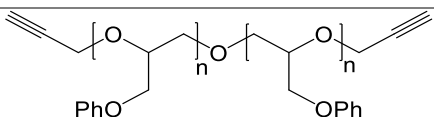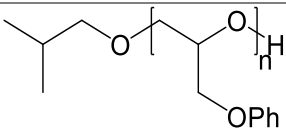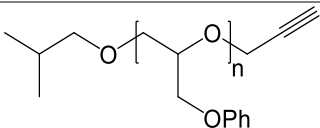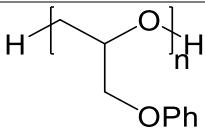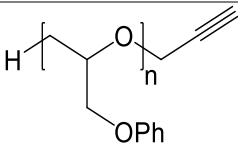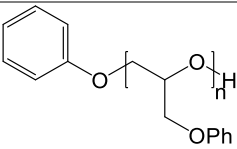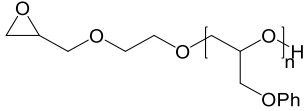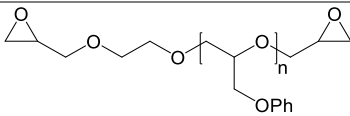
Figure 4. MALDI-ToF MS of a) crude PGPE sample synthesized in the absence of iBu$_3$Al (Entry 3) and b) its propargylated product. The spectra were taken in reflector mode.

Upon reaction with propargyl bromide in basic medium (Figure 4b), the signals shifted by +76.04 Da confirming the functionalization of two hydroxyl groups.[23] Side reactions were not observed except initiation by adventitious water. The small signals indicated by species [W-PGPE$_n$+K]$^+$ and its propargylated product that exhibit an offset of +76.05 Da point out to the presence of a second population of PGPE chains initiated by water and terminated in two hydroxyl groups. An investigation on water-initiated PGPE will be detailed in chapter IV. See Table 2 for abbreviations and proposed structures.

Table 2. Structures assigned to MALDI–ToF MS signals.

Name	Structure	Mass (Da)
PGPE-EG		$150\ n + 62$
PGPE-EG-ALK		$150\ n + 138$
W-PGPE		$150\ n + 18$
W-PGPE-ALK		$150\ n + 94$
Bu-PGPE		$150\ n + 74$
Bu-PGPE-ALK		$150\ n + 112$
H-PGPE		$150\ n + 2$
H-PGPE-ALK		$150\ n + 40$

Name	Structure	Mass (Da)
Ph-PGPE		150 n + 94
R-PGPE		150 n + 118
RR-PGPE		150 n + 174

In contrast to previous results, MALDI-ToF MS of a PGPE sample obtained in the presence of iBu_3Al revealed the formation of three distinct potassium-cationized species, one of them identified as the target PGPE initiated by deprotonated ethylene glycol $[PGPE-EG_n+K]^+$ (Figure 5a). This signal exhibited the expected shift of +76.83 Da upon reaction with propargyl bromide (Figure 5b). The other two signals exhibited a shift of only the half of the expected mass upon propargylation, which indicates that they arise from chains terminated in single hydroxyl groups. Based on their mass position, these signals were assigned to PGPE chains likely formed by initiation with isobutanol $[Bu-PGPE_n+K]^+$ and hydride $[H-PGPE_n+K]^+$. The former could be formed by reaction of iBu_3Al and water, and the latter by hydride abstraction from an isobutyl group of iBu_3Al[16–18] (see Table 2 for abbreviations and proposed structures). Upon propargylation, an additional peak that could not be attributed to any species was also observed (signal "Unknown") which suggests the existence of other byproducts in this sample. In fact, by analyzing a PGPE sample synthesized with a larger $[GPE]_0$ to $[iBu_3Al]$

ratio (32 compared to 25 in previous sample) the formation of a series of other byproducts was detected (Figure 6), whose origin seems to be related to the activation of the glycidyl ether with iBu$_3$Al, followed by the attack of active oxygen species (from ethylene glycol or the growing chain) to the methylene carbon next to glycidyl ether oxygen and the formation of phenol (Table 2).
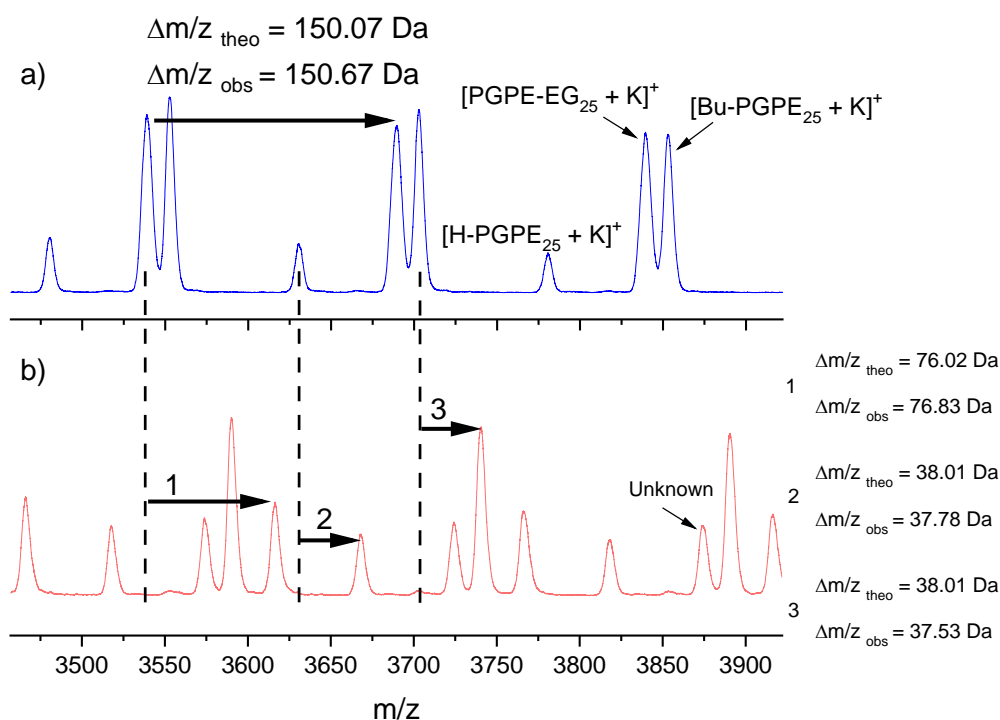

Figure 5. MALDI-ToF MS of a) crude PGPE sample synthesized in the presence of iBu$_3$Al (Entry 6) and b) its propargylated product. The spectra were taken in linear mode. A potassium salt was used as a cationizing agent.
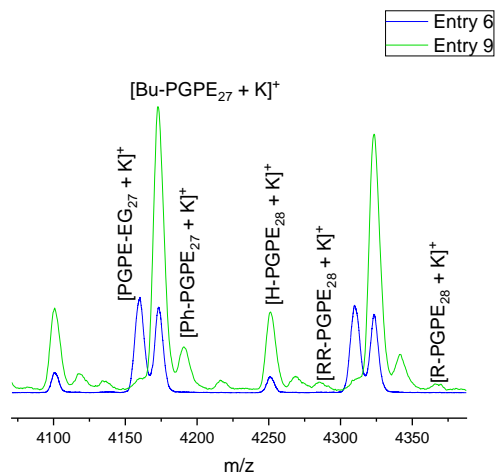
Figure 6. MALDI-ToF MS of PGPE samples synthesized in the presence of iBu$_3$Al. The spectra were taken in linear mode. A potassium salt was used as a cationizing agent. See proposed structures in Table 2.

In general, in the absence of iBu$_3$Al, the M$_{n(SEC)}$ values were similar as those theoretically expected at M$_{n(theo)}$ < 7 kDa (Figure 7a). The variation of M$_{n(SEC)}$ as a function of M$_{n(theo)}$ exhibited a plateau at about 6 kDa for M$_{n(theo)}$ > 7 kDa, independently of the [t-BuP$_4$] / [OH] ratios used in the reaction. The polydispersity index (Đ) remained the same and low in all the synthesized polymers. In the presence of iBu$_3$Al, M$_{n(SEC)}$ were about 1.5 times larger than those expected (Figure 7b), which implies that only two-thirds of alkoxides were active in the polymerization, in agreement with the MALDI-ToF MS data discussed above. The Đ values were not as uniform as those obtained in the absence of iBu$_3$Al exhibiting variations from 1.1 to 1.6. No clear effect of the [t-BuP$_4$] / [OH] ratio on the end-group nature was detected, although an increase of the reaction rate was indeed observed at higher [t-BuP$_4$] / [OH] values.
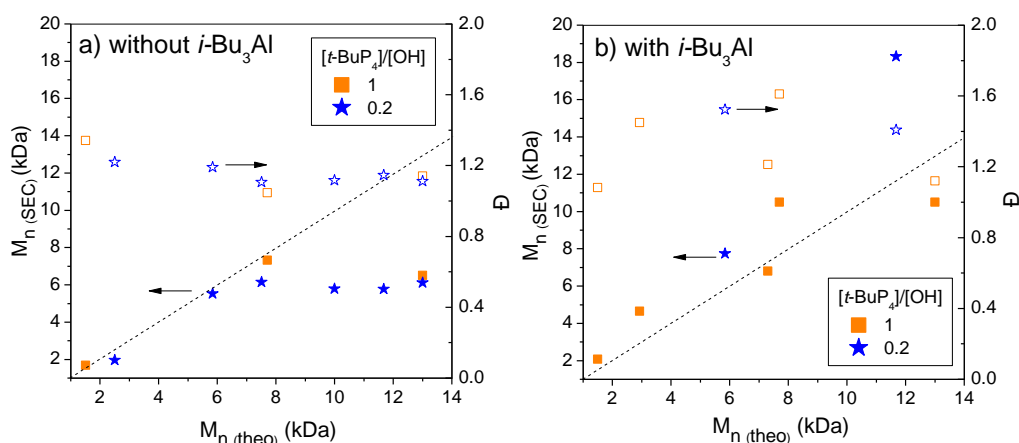
Figure 7. Solid symbols: M_n values measured by SEC as a function of theoretical M_n for PGPE samples obtained in the a) absence and b) presence of iBu₃Al. Open symbols: Polydispersity index. The dashed line represents the expected M_n.

3.1.2. Regiochemistry

The analysis of regiosequences in synthesized PGPE samples is relevant in the evaluation of the dielectric NM since the fluctuations of the chain dipole moment are proportional to the end-to-end vector only in regio-regular linear chains. ^{13}C NMR analysis confirmed that samples generated either by initiation with ethylene glycol/ *t*-BuP₄ or ethylene glycol/*t*-BuP₄/iBu₃Al are regio-regular (Figure 8). The data revealed the appearance of signals that correspond to a configuration produced by only head-to tail or tail-to-head enchainment as observed by the appearance of sharp methylene (CH₂O) and methine (CHO) peaks of GPE repeated units in the main chain. Assignment

of triad regiosequences was done according to previous studies.[21,24] Assignment of end groups and ethylene glycol moieties was evaluated by comparing the ^{13}C NMR spectra obtained prior and post addition of small amounts of trichloroacetyl isocyanate (TAI) derivatizing reagent. Upon the addition of TAI, the terminal hydroxyl groups are transformed into urethane groups. Consequently, the ^{13}C NMR signals of carbons in α and β positions to the urethane groups shift downfield and upfield, respectively, thus allowing the identification of signals corresponding only to the polymer backbone.
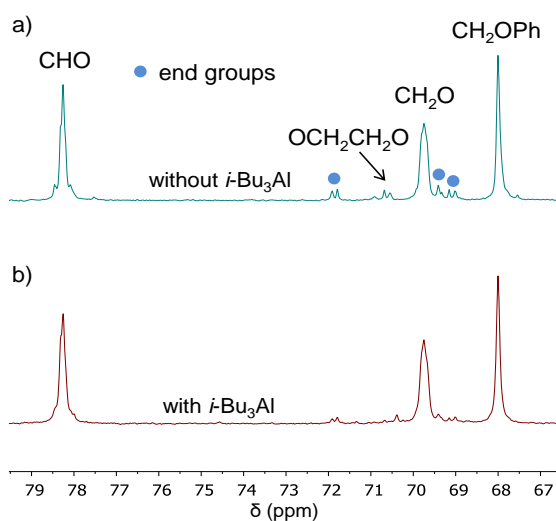

Figure 8. ^{13}C NMR (in acetone-d_6) of PGPE samples of similar molecular weights obtained in the a) absence and b) presence of iBu$_3$Al (Entries 3 and 8, respectively).

4. <u>BDS analysis of chain dipolar microstructure</u>

Figure 9 shows the BDS results in a wide frequency and temperature range for PGPE obtained in the absence of iBu$_3$Al (Entry 3, Table 1), as a representative sample.
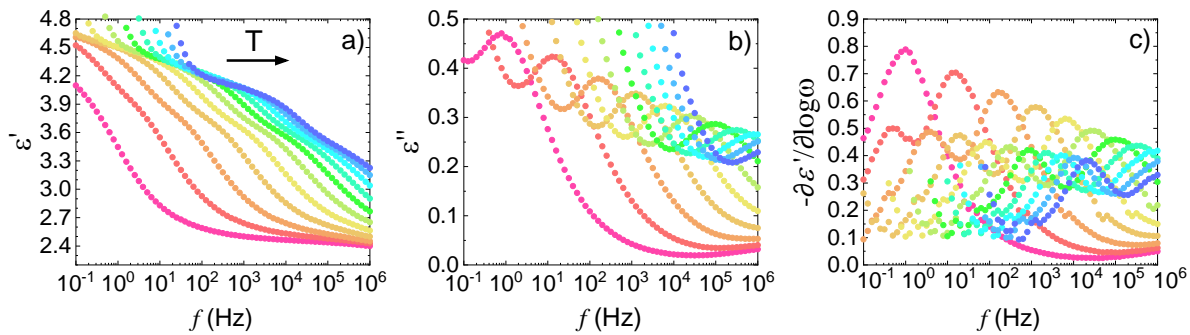
Figure 9. BDS data corresponding to a PGPE sample (Entry 3) in the temperature range 285 K – 335 K (5 K steps). a) Real part of the complex permittivity. b) Imaginary part of the complex permittivity. c) Data in the -∂ε'/∂logω representation.

Figure 9a depicts the real part (ε') of the complex dielectric permittivity, where the relaxation processes are observed as steps. Figure 9b shows the imaginary part (ε") of the complex dielectric permittivity. Here, relaxation processes are present as peaks. In this representation, conductivity from free charge carriers has contributions also, affecting the definition of the lower frequency relaxation peaks strongly. To ease the analysis of the dielectric spectra, van Turnhout and Wübbenhorst proposed the following relation:[20,25]

$$-\frac{\partial \varepsilon'}{\partial \log \omega} \approx \varepsilon''^2 \qquad\qquad \text{Eq. 1}$$

where $\omega = 2\pi f$. This relation holds that a relaxation peak in ε'' gives a maximum in $-\partial \varepsilon'/\partial \log \omega$. Because of the square in ε'' in Eq. 1, the derived maxima will be narrower than its corresponding peak in the raw ε'' data. Therefore, closely adjacent peaks will be better resolved. Finally, dc conductivity contributions following $\varepsilon'' \propto 1/\omega$ do not contribute to this formalism. Moreover, possible interfacial polarization phenomena overlap less on the dipolar contributions. Figure 9c shows the BDS data in the $-\partial \varepsilon'/\partial \log \omega$ representation. In this representation a lower frequency relaxation peak is better resolved, in contrast to ε'', since the low-frequency increase is dramatically reduced.

In the temperature range depicted in Figure 9c, the sample showed two relaxation processes. The peaks located at high frequencies (around 10^4-10^5 Hz), correspond to the segmental (α) relaxation of PGPE. The peaks located at lower frequencies (10^1-10^3 Hz range) were assigned to the NM relaxation. This assignment is based on previous reports on PGPE dielectric relaxations. [17,21] All the samples presented in the current work showed these two relaxation processes, with the following general features. First, the α-relaxation peak appeared at higher frequencies the lower the molecular mass was. This dependence relates to variations in T_g, as expected in this M_n range,[21] *i.e.* polymers with lower M_n have lower T_g and thus faster dynamics. Second, BDS results showed that the NM relaxation was also faster, the lower the molecular

weight was. This is in line with the predictions of the Rouse model for unentangled polymer chains ($f_{NM} \propto M_n^{-2}$).[26]

Figure 10 shows BDS data at 305 K for a *l*-2a-PGPE sample (Entry 4, Table 1) and a *l*-1a-PGPE sample generated by initiation with N_3TBAN (Entry 7, Table 3, chapter II). The two samples have comparable molecular weight (around 7 kDa). For both samples, the maxima of the α-relaxation peaks are in the same position. This result indicates that a possible change in the dipolar microstructure does not affect the segmental relaxation of the chain as expected. However, the maxima of the NM relaxation peaks are clearly in different positions. This first observation already suggests the formation of two distinct dipolar microstructures for the two initiation systems as described below.
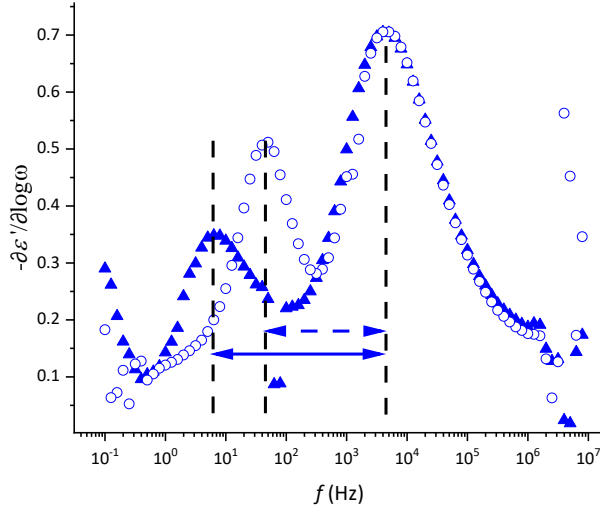
Figure 10. Comparison of the dielectric response at 305 K of a *l*-2a-PGPE (Entry 4, Table 1) open circles and a *l*-1a-PGPE (Entry 7, Table 3, *C*hapter II) solid triangles.

An analysis of the PGPE dielectric relaxations for all the samples presented in Table 1 was performed. For each one, the relaxation time (τ) of the segmental and NM relaxations as a function of the temperature (280 $\leq$ *T* (K) $\leq$ 380) was evaluated. The relaxation time was estimated from the frequency of the maximum (f_{max}) of each relaxation peak ($\tau = \frac{1}{2\pi f_{max}}$).

In particular, the segmental relaxation peak was observed in the temperature range of 280 $\leq$ *T* (K) $\leq$ 320. Its temperature dependence was analyzed under the Vogel-Tamman-Fulcher (VFT) law:

$$\tau_\alpha(T) = \tau_0 \exp\left[\frac{D\,T_0}{T - T_0}\right] \qquad\qquad \text{Eq. 2}$$

where τ_0 is the pre-exponential factor and D the fragility parameter. In the case of PGPE those parameters were fixed as $\tau_0 = 10^{-14}$ s and D = 6.1 as previously reported.[17,21] The so-called Vogel temperature (T_0) was the only free parameter for the fitting procedure. From the VFT results, the dynamic glass transition temperature ($T_{\text{g-BDS}}$) was calculated as the temperature at which the relaxation time (τ_α in Eq. 2) equals 100 s (Table 3). Slightly higher $T_{\text{g-BDS}}$ values were found for samples synthesized in the absence of iBu$_3$Al. The results obtained from the VFT analysis indicate that possible changes in the dipolar microstructure do not have a detectable impact on the segmental relaxation of this polymer, as expected.

The NM relaxation appeared in the temperature range of 300 $\leq T$ (K) $\leq$ 380. Its temperature dependence was analyzed under the Williams-Lander-Ferry (WLF) law:

$$\tau_{\text{NM}}(T) = \tau_{\text{NM}}(T_{\text{Ref}}) \exp\left[-\frac{C_1(T - T_{\text{Ref}})}{C_2 + T - T_{\text{Ref}}}\right] \qquad\qquad \text{Eq. 3}$$

where C_1 and C_2 are the WLF constants, and T_{ref} is the reference temperature. C_1 and C_2 parameters are found to take values which are not changing much from polymer to polymer when the $T_{\text{Ref}} = T_{\text{g}}$.[20] In the current study T_{Ref} was taken as the dynamic glass transition ($T_{\text{g-BDS}}$). In the case of PGPE, C_1 = 30 and C_2 = 34.8 were found to be adequate values. From these fittings, the NM relaxation time at the glass transition temperature

($\tau_{NM}(T_{g\text{-BDS}})$) was obtained, which is the single fitting parameter in Eq. 3. Table 3 presents the summary of all the obtained results. As it can be seen, samples prepared with t-Bu-P_4 / ethylene glycol in the absence of iBu$_3$Al showed lower values of $\tau_{NM}(T_{g\text{-BDS}})$, in comparison to those prepared in the presence of iBu$_3$Al. Considering that the NM relaxation can account for changes in the PGPE architecture, as reported previously,[17,21] the changes in $\tau_{NM}(T_{g\text{-BDS}})$ serve as an indication that different synthesis routes affect the resulting PGPE molecular structure.

Table 3. Relaxation time of the NM at the dynamic glass transition temperature.

Entry	iBu$_3$Al	n_{arms} (BDS)[c]	$T_{g\text{-BDS}}$ (K $\pm$ 0.5)	$\tau_{NM}(T_{g\text{-BDS}})$ (s)	$\tau_{NM}(T_{g\text{-BDS}})/M_n^2$ (s/kg^{2}mol^{-2})
1			275.0	195	29
2			278.5	1380	37
3	No	2	277.0	1072	37
4			278.0	1549	29
5			278.0	1820	43
6			277.0	10233	173
7			277.0	3631	101
8	Yes	m	276.0	3548	106
9			277.0	2884	62
10			278.5	12023	109

[c]Number of arms determined by BDS. m = mixture of 1 and 2 arms

To further evaluate the PGPE topology from BDS data, Figure 11 shows $\tau_{NM}(T_{g\text{-}BDS})/M^2$ as a function of M, in an ln-ln graph, M being the molecular mass. In this plot, error bars were calculated taking into consideration the uncertainties in the evaluation of τ_{NM}, as well as the corresponding values of Đ (Table 1). In this representation, the Rouse model predicts that for a given monodisperse molecular structure the data-points must lie within a horizontal line.
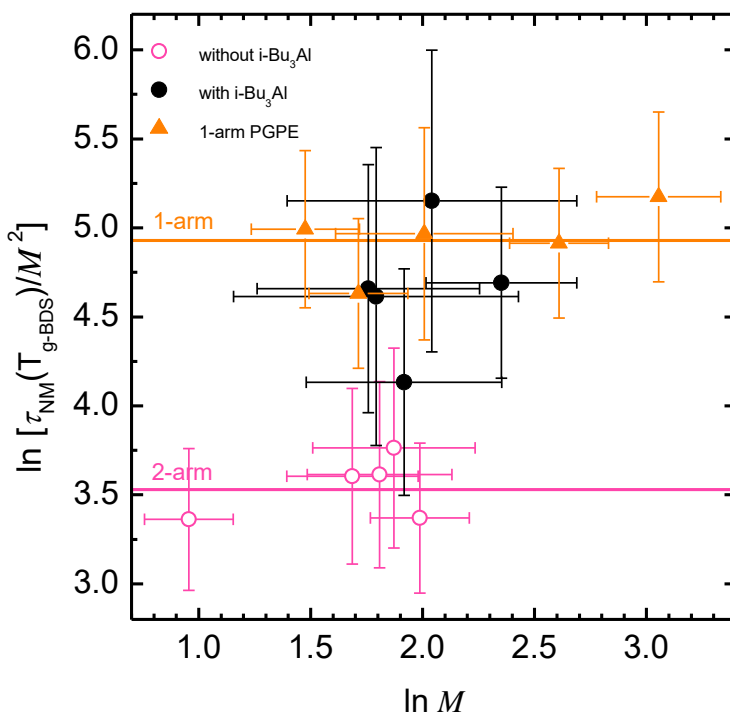

Figure 11. Architecture evaluation for PGPE samples under the Rouse model. Error bars correspond to the propagation of the experimental errors from $\tau_{NM}(T_{g\text{-}BDS})$ and Đ.

Solid triangles in Figure 11 show the NM analysis of *l*-1a-PGPE samples presented in chapter II. The straight line at $\ln[\tau_{NM}(T_{g\text{-}BDS})/M^2]$ = 4.93 corresponds to the trend expected from the Rouse model in this case. Taking the 1-arm result as a reference, it is possible to determine the topology of PGPE samples synthesized in presence/absence of iBu₃Al. Briefly, if for purely symmetric dipole-inverted 2-arm polymers only even-numbered Rouse modes contribute to the NM relaxation, then the NM dynamics should be faster by a factor of 4.[27] In other words, the trend $\ln[\tau_{NM}(T_{g\text{-}BDS})/M^2]$ = 4.93 of the *l*-1a-PGPE must be reduced by ln[4] ≈ 1.4. This corresponds to the line drawn at $\ln[\tau_{NM}(T_{g\text{-}BDS})/M^2]$ = 3.53 in Figure 11. Samples prepared in the absence of iBu₃Al (open circles) agree very well with this expectation. This confirms that these polymers are mostly made by 2 symmetric arms, each containing half of the monomers. Solid circles in Figure 11 show the PGPE samples prepared in the presence of iBu₃Al. These points deviate from the 2-arm expectation, mostly lying in between the two trends. According to BDS data, samples synthesized in the presence of iBu₃Al are either composed of asymmetric 2 arm chain or a mixture of one and two arm polymers.

The impurities observed in PGPE samples initiated with *t*-BuP₄/ethylene glycol in the absence of iBu₃Al corresponded to water initiation. However, as it will be presented in Chapter IV, these water-initiated chains are also composed of two symmetric arms. For that reason, these impurities did not cause deviations of the expected $\ln[\tau_{NM}(T_{g\text{-}BDS})/M^2]$ value for two-arm PGPE.

5. <u>Conclusions</u>

Taking advantage of the dielectric relaxation associated with the chain mode exhibited by some linear regio-regular polyethers, broadband dielectric spectroscopy was used to assess and verify the symmetrical bidirectional growth of α,ω-dihydroxy telechelic poly(glycidyl phenyl ether) obtained by initiation with ethylene glycol and t-BuP$_4$. Such verification can hardly be performed with other conventional spectroscopic techniques, demonstrating the complementarity of BDS with other commonly used methods for the characterization of polymer architectures. The combination of BDS and MALDI-ToF MS confirmed that in the absence of the well-known monomer activator iBu$_3$Al, the synthesized polymer is mainly composed of two symmetric arms but in the presence of iBu$_3$Al, the polymerization leads to a number of byproducts characterized by unidirectional growth.

6. __References__

(1)   Schwesinger, R.; Schlemper, H. Peralkylated Polyaminophosphazenes— Extremely Strong, Neutral Nitrogen Bases. *Angew. Chemie Int. Ed. English* **1987**, *26* (11), 1167–1169.

(2)   Xia, Y.; Zhao, J. Macromolecular Architectures Based on Organocatalytic Ring-Opening (Co)Polymerization of Epoxides. *Polymer.* **2018**, *143*, 343–361.

(3)   Misaka, H.; Tamura, E.; Makiguchi, K.; Kamoshida, K.; Sakai, R.; Satoh, T.; Kakuchi, T. Synthesis of End-Functionalized Polyethers by Phosphazene Base-Catalyzed Ring-Opening Polymerization of 1,2-Butylene Oxide and Glycidyl Ether. *J. Polym. Sci. Part A Polym. Chem.* **2012**, *50* (10), 1941–1952.

(4)   Misaka, H.; Sakai, R.; Satoh, T.; Kakuchi, T. Synthesis of High Molecular Weight and End-Functionalized Poly (Styrene Oxide) by Living Ring-Opening Polymerization of Styrene Oxide Using the Alcohol / Phosphazene Base Initiating System. *Macromolecules* **2011**, *44*, 9099–9107.

(5)   Kwon, W.; Rho, Y.; Kamoshida, K.; Kwon, K. H.; Jeong, Y. C.; Kim, J.; Misaka, H.; Shin, T. J.; Kim, J.; Kim, K. W.; et al. Well-Defined Functional Linear Aliphatic Diblock Copolyethers: A Versatile Linear Aliphatic Polyether Platform for Selective Functionalizations and Various Nanostructures. *Adv. Funct. Mater.* **2012**, *22* (24), 5194–5208.

(6)   Satoh, Y.; Matsuno, H.; Yamamoto, T.; Tajima, K.; Isono, T.; Satoh, T. Synthesis of Well-Defined Three- and Four-Armed Cage-Shaped Polymers via "Topological Conversion" from Trefoil- and Quatrefoil-Shaped Polymers. *Macromolecules* **2017**, *50* (1), 97–106.

(7)   Isono, T.; Satoh, Y.; Miyachi, K.; Chen, Y.; Sato, S. I.; Tajima, K.; Satoh, T.; Kakuchi, T. Synthesis of Linear, Cyclic, Figure-Eight-Shaped, and Tadpole-Shaped Amphiphilic Block Copolyethers via t-Bu-P$_4$-Catalyzed Ring-Opening Polymerization of Hydrophilic and Hydrophobic Glycidyl Ethers. *Macromolecules*

2014, *47* (9), 2853–2863.

(8) Satoh, Y.; Miyachi, K.; Matsuno, H.; Isono, T.; Tajima, K.; Kakuchi, T.; Satoh, T. Synthesis of Well-Defined Amphiphilic Star-Block and Miktoarm Star Copolyethers via t-Bu-P$_4$-Catalyzed Ring-Opening Polymerization of Glycidyl Ethers. *Macromolecules* **2016**, *49* (2), 499–509.

(9) Isono, T.; Kamoshida, K.; Satoh, Y.; Takaoka, T.; Sato, S. I.; Satoh, T.; Kakuchi, T. Synthesis of Star- and Figure-Eight-Shaped Polyethers by t-Bu-P$_4$-Catalyzed Ring-Opening Polymerization of Butylene Oxide. *Macromolecules* **2013**, *46* (10), 3841–3849.

(10) Eßwein, B.; Steidl, N. M.; Möller, M. Anionic Polymerization of Oxirane in the Presence of the Polyiminophosphazene Base t-BuP$_4$. *Macromol. Rapid Commun.* **1996**, *17* (2), 143–148.

(11) Brocas, A. L.; Deffieux, A.; Le Malicot, N.; Carlotti, S. Combination of Phosphazene Base and Triisobutylaluminum for the Rapid Synthesis of Polyhydroxy Telechelic Poly(Propylene Oxide). *Polym. Chem.* **2012**, *3* (5), 1189–1195.

(12) Polymeropoulos, G.; Zapsas, G.; Ntetsikas, K.; Bilalis, P.; Gnanou, Y.; Hadjichristidis, N. 50th Anniversary Perspective: Polymers with Complex Architectures. *Macromolecules* **2017**, *50* (4), 1253–1290.

(13) Hu, S.; Dai, G.; Zhao, J.; Zhang, G. Ring-Opening Alternating Copolymerization of Epoxides and Dihydrocoumarin Catalyzed by a Phosphazene Superbase. *Macromolecules* **2016**, *49* (12), 4462–4472.

(14) Erberich, M.; Keul, H.; Möller, M. Polyglycidols with Two Orthogonal Protective Groups: Preparation, Selective Deprotection, and Functionalization. *Macromolecules* **2007**, *40* (9), 3070–3079.

(15) Billouard, C.; Carlotti, S.; Desbois, P.; Deffieux, A. "Controlled" High-Speed Anionic Polymerization of Propylene Oxide Initiated by Alkali Metal Alkoxide/Trialkylaluminum Systems. *Macromolecules* **2004**, *37* (11), 4038–4043.

(16) Labbé, A.; Carlotti, S.; Billouard, C.; Desbois, P.; Deffieux, A. Controlled High-

Speed Anionic Polymerization of Propylene Oxide Initiated by Onium Salts in the Presence of Triisobutylaluminum. *Macromolecules* **2007**, *40* (22), 7842–7847.

(17)   Ochs, J.; Veloso, A.; Martínez-Tong, D. E.; Alegria, A.; Barroso-Bujans, F. An Insight into the Anionic Ring-Opening Polymerization with Tetrabutylammonium Azide for the Generation of Pure Cyclic Poly(Glycidyl Phenyl Ether). *Macromolecules* **2018**, *51* (7), 2447–2455.

(18)   Schmitt, B.; Stauf, W.; Müller, A. H. E. Anionic Polymerization of (Meth)Acrylates in the Presence of Cesium Halide-Trialkylaluminum Complexes in Toluene. *Macromolecules* **2001**, *34* (6), 1551–1557.

(19)   Hirao, A.; Hayashi, M.; Ito, S.; Goseki, R.; Higashihara, T.; Hadjichristidis, N. Star-Branched Polymers (Star Polymers). In *Anionic Polymerization: Principles, Practice, Strength, Consequences and Applications*; Hadjichristidis, N., Hirao, A., Eds.; 2015; pp 659–718.

(20)   Kremer, F.; Schönhals, A. *Broadband Dielectric Spectroscopy*, Springer-V.; Berlin, Heidelberg, New York, 2003.

(21)   Gambino, T.; Martínez De Ilarduya, A.; Alegría, A.; Barroso-Bujans, F. Dielectric Relaxations in Poly(Glycidyl Phenyl Ether): Effects of Microstructure and Cyclic Topology. *Macromolecules* **2016**, *49* (3), 1060–1069.

(22)   Roland, C. M.; Bero, C. A. Normal Mode Relaxation in Linear and Branched Polyisoprene. *Macromolecules* **1996**, *29* (23), 7521–7526.

(23)   Haque, F. M.; Alegria, A.; Grayson, S. M.; Barroso-bujans, F. Detection, Quanti Fi Cation, and " Click-Scavenging " of Impurities in Cyclic Poly(Glycidyl Phenyl Ether) Obtained by Zwitterionic Ring- Expansion Polymerization with $B(C_6F_5)_3$. *Macromolecules* **2017**, *50*, 1870–1881.

(24)   Ronda, J. C.; Serra, A.; Mantecón, A.; Cádiz, V. Studies on the Microstructure of Poly(Phenyl Glycidyl Ether) Using the ^{13}C Nuclear Magnetic Resonance Technique. *Polymer.* **1995**, *36* (3), 471–478.

(25)   Wübbenhorst, J.; van Turnhout, J. "Conduction-Free" Dielectric Loss de/dlnf - A

Powerful Tool for the Analysis of Strong (Ion) Conducting Dielectric Materials. *Novocontrol Dielectr. Newsl.* **2000**, *No.14*.

(26) Rubinstein, M.; Colby, R. H. *Polymer Physics*; Oxford University Press, 2003.

(27) Watanabe, H.; Urakawa, O.; Kotaka, T. Slow Dielectric Relaxation of Entangled Linear Cis-Polyisoprenes with Asymmetrically Inverted Dipoles. 1. Bulk Systems. *Macromolecules* **1993**, *26* (19), 5073–5083.

Chapter IV

Cyclic poly(glycidyl phenyl ether) with a
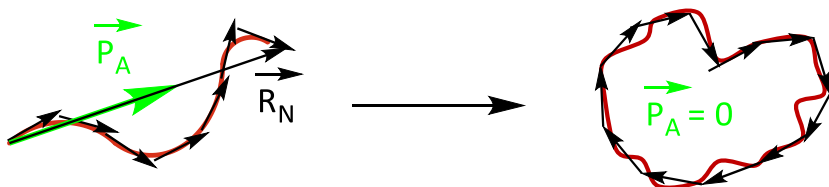
dipole-inverted microstructure

Table of Contents

As seen in Chapter III, the initiation of residual water is difficult to avoid when using phosphazene base as a catalyst for the polymerization of epoxide monomers. In this Chapter, water is directly used to initiate the polymerization of glycidyl phenyl ether in the presence of a phosphazene base (t-BuP$_4$). The formation of polymer chains displaying a dipole inversion along the chain contour is demonstrated and the obtained linear polymers are used as precursor for the synthesis of macrocyclic polymers displaying a normal mode relaxation.

1. <u>Introduction</u>

In contrast to macrocycles having all monomers oriented the same way (Figure 1a), dipole-inverted macrocycles present a net dipole moment proportional to the ring diameter vector, $\overrightarrow{P_A} \propto \overrightarrow{R_{N/2}}$ where $\overrightarrow{P_A}$ is the dipole moment associated to the main chain and $\overrightarrow{R_{N/2}}$ is the end-to-end vector of the subchain or arm (Figure 1b). Consequently, dipole-inverted macrocycles will exhibit a dielectric normal mode (NM) relaxation, which specifically reflects the fluctuations of the ring diameter. Moreover, this characteristic will enable the evaluation of macrocyclic chain dynamics in a broad time-frequency domain by broadband dielectric spectroscopy (BDS), which is otherwise more difficult with other frequency-dependent techniques (e.g. rheology, neutron scattering).[1–6]

a) one arm (without dipole inversion)

b) two arms (with dipole inversion)
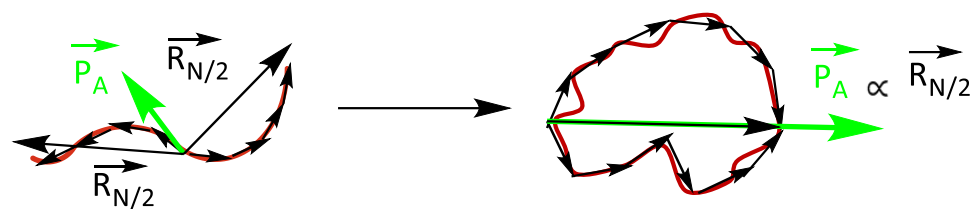
Figure 1. Dipolar microstructures for macrocyclic chains generated from linear chains constituted by a) one arm or b) two arms with dipole inversion.

As presented in Chapter III, the combination of ethylene glycol with the phosphazene base t-BuP$_4$, allows the preparation of poly(glycidyl phenyl ether) (PGPE) with two symmetric arms. In these structures, the ethylene glycol moiety marks the center of the chain and the chain dipolar inversion, as demonstrated by BDS analysis.[7] In that polymerization system, co-initiation from residual water was sometimes unavoidable, even by working with the outmost care.[7] This undesired initiation has been frequently found in polymerization systems catalyzed by t-BuP$_4$.[8,9]

Because of the dihydrogenated nature of water, it should be able to initiate the polymerization of epoxide monomers upon deprotonation with a phosphazene base

(PB) to produce a two-arm polymer structure. It is expected that initiation first occurs by the attack of a PB-activated water molecule (or a hydroxide)[10] to the epoxide ring and then to the formation of a dihydroxide molecule. This bifunctional molecule will then have identical probability to promote the chain growth in both directions from the deprotonated hydroxyl functionalities and to form the desired two-arm polymer structure. Shimada and coworkers[11] found that the ring opening polymerization (ROP) of cyclotrisiloxane initiated by water and a PB catalyst generated hydroxyl telechelic polysiloxanes as a result of the activation of water molecules by the PB during initiation and the subsequent activation of terminal silanol groups during propagation. The ROP of epoxides such as ethylene oxide, propylene oxide or allyl glycidyl ether using a combination of water as initiator, organobases as catalyst and triethylborane as monomer activator was reported by Zhang et al.[12] However, t-BuP$_4$ was not considered due to its extremely high basicity promoting transfer reactions.

In this Chapter, the combination of t-BuP$_4$ and water is used to initiate the polymerization of glycidyl phenyl ether (GPE) and generate monodisperse PGPE polymers formed by two symmetric arms (l-2a-PGPE). Then, macrocyclic structures are prepared via end group modification and ring closure through Glaser coupling. This series of samples will be named c-2a-PGPE. The structural chemical analysis was performed by matrix-assisted laser desorption ionization–time-of-flight mass spectrometry (MALDI-ToF MS), nuclear magnetic resonance (NMR), and size exclusion chromatography (SEC). However, only BDS analysis of the synthesized linear polymer was capable to validate the formation of dipole-inverted two-arm structures and therefore to confirm the symmetrical growth of two PGPE subchains initiated by water. Moreover, BDS analysis of dipole-inverted macrocycles showed slower NM relaxations

at the glass transition temperature than their linear dipole inverted analogues. This important result implies that the cyclic topology presents slower fluctuations of the $\overrightarrow{R_{N/2}}$ vector than the linear chain, a result that has not been anticipated by theory/simulations for these relatively small ring sizes.[13,14] This finding has been possible thanks to the fact that the dielectric relaxation of the dipole inverted ring reflects directly the fluctuation of the ring diameter vector $\overrightarrow{R_{N/2}}$ without any additional contributions that are very relevant for other experimental methods applied in the investigation of the cyclic chain dynamics.

2. <u>Experimental section</u>

GPE, THF and toluene (Sigma-Aldrich) were distilled from CaH_2 under reduced pressure and stored under a nitrogen atmosphere. 1-*tert*-Butyl-4,4,4-tris(dimethylamino)-2,2-bis[tris(dimethylamino)-phosphoranylidenamino]-2λ^5,4λ^5-catenadi(phosphazene) (*t*-BuP$_4$) (Sigma-Aldrich) was stored in a glovebox and used as received. Dichloromethane, propargyl alcohol (Sigma-Aldrich) and 1,8-diazabicyclo[5.4.0]undec-7-ene (DBU) (Fluka) were used as received.

2.1.   Synthesis of α,ω-hydroxy poly(glycidyl phenyl ether)

In a typical experiment, distilled water (3 mg; 1.7×10^{-4} mol) and 180 μL of *t*-BuP$_4$ solution (0.8 mol/L in hexane) were transferred to a round-bottom flask containing 0.9 mL of THF and equipped with a magnetic stirrer in a glovebox. The obtained solution was stirred at room temperature for 30 min. GPE (1 mL; 7.0×10^{-3} mol) was added under a nitrogen atmosphere. The reaction was performed at room temperature for ≥48 h. After reaction, the highly viscous liquid was dissolved in THF (2 mL) and the reaction was quenched by addition of an HCl solution in methanol (0.5 M). The polymer was precipitated into hexane, recovered and dried at 40 °C under vacuum. Different molecular weight polymers were prepared by adjusting the monomer to water ratio.

2.2.   Propargylation of end groups: formation of α,ω-alkyne poly(glycidyl phenyl ether)

Propargylation of *l*-2a-PGPE samples was performed as follows. A solution of α,ω-hydroxy poly(glycidyl phenyl ether)   (194 mg; 3.6×10^{-5} mol) and NaH (52 mg; 2.2×10^{-3} mol) was stirred at 40 °C for 1 h in THF (30 mL) under an inert atmosphere. Then, propargyl bromide (200 mg; 1.68×10^{-3} mol) was added. The reaction was stirred for 24 h at room temperature. Then 10 mL of a 0.1 M HCl solution was added to the flask, the THF was evaporated under reduced pressure, and the polymer was extracted

with dichloromethane. Finally, the solution was concentrated and precipitated into hexane.

2.3.   Cyclization of α,ω-alkyne poly(glycidyl phenyl ether)

Cyclization of propargylated *l*-2a-PGPE samples was performed as follows. In a round-bottom flask, CuBr (14 mg; 9.8 x 10^{-5} mol), PMDETA (0.02 mL; 1 x 10^{-4} mol) and DBU (0.01 mL; 6.7 x 10^{-5} mol) were dissolved in dichloromethane (3 mL). In a second flask, α,ω-alkyne poly(glycidyl phenyl ether) (25 mg; 3.2 x 10^{-6} mol) was dissolved in dichloromethane (3 mL). This solution was slowly added (at 2 mL/h) via a syringe pump to the CuBr solution. After all the solution was added (1.5 h) the reaction was stirred at room temperature for 2 h. The copper catalyst and the amine were removed by extraction with a saturated ammonium chloride solution. The organic phase was dried with magnesium sulfate. Finally, the solution was concentrated and precipitated into hexane. To remove high molecular weight impurities coming from interchain coupling, cyclic polymer samples were fractionated by using a recycling preparative GPC.

2.4. **Characterization**

SEC measurements were performed using two different SEC equipment, a SEC-MALS-RI located at the University of the Basque Country, Spain, and a SEC-RI located at Tulane University, USA. SEC–MALS-RI data were acquired with an Agilent G-1310A HPLC pump connected to miniDAWN MALS and Optilab rEX dRI detectors from Wyatt. All the detectors were at 25°C. PLgel 5μm 500Å and PLgel 5μm Mixed-C columns were used for separation, both kept in a column heater at 30 °C. THF (1.0 mL/min) was used as an eluent. ASTRA software (Wyatt, version 6.1.2.84) was used for data collection and processing. A differential refractive index (dn/dc) value for PGPE of 0.136 mL/g was used, as previously determined.[15]

SEC-RI data were acquired with a Waters model 1515 isocratic pump (Milford, MA). THF (1.0 mL/min) was used as the eluent with columns heated at 30 °C by a column oven. This system was operated with a set of two columns in series from Polymer Laboratories Inc., consisting of PSS SDV analytical linear M (8 × 300 mm) and PSS SDV analytical 100 Å (8 × 300 mm) columns. A model 2487 differential refractometer detector was used as a refractive index detector. The instrument was calibrated with Waters polystyrene ReadyCal standards.

Fractionation of *c*-2a-PGPE samples was performed using two different GPC equipment. The first one is located at Tulane University, USA and the second one at the University of the Basque Country, Spain. The first equipment is a Waters model 1515 isocratic pump (Milford, MA). THF (8.0 mL/min) was used as the eluent with columns heated at

a constant 30 °C by a column oven. This system was operated with three columns in series from Polymer Laboratories Inc. consisting of three PSS SDV analytical 5 µm 500 Å (8 × 300 mm) columns. A model 2487 differential refractometer detector was used as a refractive index detector. 50 mg of *c*-2a-PGPE was dissolved in 2 mL of THF and filtered through an AGILENT 0.2 µm filter before injection.

The second equipment is a recycling preparative GPC LaboACE LC-5060 from Japan Analytical Industry (JAI) equipped with an UV-VIS4ch LA detector. To fractionate the sample, 40 mg of *c*-2a-PGPE was dissolved in 4 mL of chloroform and filtered through an AGILENT 0.2 µm filter. Then, the polymer solution was injected into the equipment and separated by a combination of JAIGEL 2.5 HR and JAIGEL 3 HR columns at a flow rate of 10 mL/min. After 3 cycles, the desired fraction was collected. The solvent was evaporated and the polymer fraction was dried in a vacuum oven.

MALDI-ToF MS measurements were performed on a Bruker Autoflex III MALDI–TOF mass spectrometer (Bruker Daltonics, Billerica, MA. Spectra were acquired in reflector mode. *Trans*-2-[3-(4-*tert*-Butylphenyl)-2-methyl-2-propenylidene]malononitrile (DCTB, Fluka) was used as a matrix. Sodium trifluoroacetate (NaTFA) (Aldrich) was added as the cationic ionization agent (~2 mg/mL dissolved in THF). The matrix was dissolved in THF at a concentration of 20 mg/mL. Polymer samples were also dissolved in THF at a concentration of ~10 mg/mL. In a typical MALDI experiment, the matrix, salt, and polymer solutions were premixed at a 20:5:10 ratio. Approximately 1 µL of the obtained mixture was hand spotted on the ground steel target plate. MALDI–TOF MS data were calibrated against SpheriCal dendritic calibrants (Polymer Factory, Sweden). For each spectrum 10000 laser shots were accumulated.

^{1}H NMR spectra were acquired at 25 °C on a Bruker Avance 400 in deuterated chloroform.

Differential scanning calorimetry (DSC) measurements were carried out on ~5 mg specimens using a Q2000 TA Instruments. All samples were measured by placing the samples in sealed aluminum pans, cooling to −100 °C at 20 °C/min, and heating to 150 °C at 20 °C/min (first run). Then, samples were cooled back to −100 °C at 20 °C/min (second run) and finally heated to 150 °C at 20 °C/min (third run). A helium flow rate of 25 mL/ min was used throughout. The glass transition temperature (T_g) was evaluated in the third run.

BDS experiments were carried out over the frequency range (f) 10^{-1} - 10^{7} Hz using a Novocontrol Alpha spectrometer. The typical BDS protocol was as follows. First, the sample was heated in the BDS cell from room temperature to 420K at 3 K/min. This final temperature was kept for 15 min to dry the sample and let the evaporation of possible residual solvent. Then, dielectric experiments started in 5 K isothermal steps from 420 K to 180 K. To maintain the sample capacitor thickness, a teflon cross-shaped spacer (100 μm thick) was used. The frequency dependent complex permittivity $\varepsilon^*(\omega) = \varepsilon'(\omega) - i\,\varepsilon''(\omega)$ characterizing the dielectric properties of the material was measured, where $\omega = 2\pi f$, $\varepsilon'(\omega)$ is the dielectric dispersion and $\varepsilon''(\omega)$ the dielectric loss.

The relaxation times from BDS measurements were obtained from the maximum of the isothermal relaxation loss peaks ($\tau_{max} = 1/\omega_{max}$). The temperature dependence of the segmental (α) relaxation times was fitted to a Vogel-Fulcher- Tamman (VFT) equation,[16–18]

$$\tau_{max}^{\alpha} = \tau_0 \exp\left[\frac{DT_0}{T - T_0}\right] \qquad\qquad \text{Eq. 1}$$

where τ_0 is a pre-exponential factor of the order of the vibrational times, D is usually referred to as fragility parameter, and T_0 is the so-called Vogel temperature. Eq. 1 provides a way of evaluating the dynamics glass transition temperature $T_{g\text{-}BDS}$ as that corresponding to a segmental relaxation time of 100 s, i.e., $T_{g-BDS} = T_0 + \frac{DT_0}{\ln(100/\tau_0)}$.

The NM relaxation characterizes the slowest dipole moment fluctuation. Its temperature dependence was fitted to a Williams-Lander-Ferry (WLF) equation,[19,20] which is commonly used to describe the temperature dependence of the terminal relaxation of the polymer:

$$\tau_{max}^{NM} = \tau_{NM}(T_{ref}) \exp\left[-\frac{C_1(T - T_{ref})}{C_2 + T - T_{ref}}\right] \qquad\qquad \text{Eq.2}$$

C_1 and C_2 are the WLF constants, and T_{ref} is the reference temperature. In the current study $T_{ref} = T_{g\text{-}BDS}$ was used. It is important to note that Eq. (1) and Eq. (2) are mathematically equivalent, but they are applied for the analysis of different processes only for convenience.[21,22]

For the fittings of BDS data $\tau_0 = 10^{-14}$ s, D = 6.1, C_1 = 30, and C_2 = 34.8 K were used, as previously found in the dielectric analysis of PGPE samples.[15,23]

3. <u>Results and discussion</u>

3.1. <u>Synthesis of α,ω-hydroxy poly(glycidyl phenyl ether)</u>

The polymerization of GPE was performed in dry THF at room temperature by using t-BuP$_4$ / H$_2$O as initiation system. Table 1 shows the molecular characteristics of synthesized samples.

Initially, 0.8 equivalents of t-BuP$_4$ per 1 equivalent of water were used, and then, the amount of t-BuP$_4$ was lowered to 0.3 and 0.1 to reduce the basicity of the system, as explained below. Different molecular weights with low polydispersity indexes (Đ) were obtained by adjusting the monomer to water ratio. The reaction time depended on the target molecular weight and the initial amount of t-BuP$_4$. Although the molecular weight could be controlled for low molecular weight targets (i.e. 2 kDa < M_n < 6 kDa), when higher molecular weights were targeted (i.e. M_n > 6 kDa), the observed molecular weight reached a plateau around 6 kDa, as for the polymerization of GPE initiated by ethylene glycol and t-BuP$_4$ presented in Chapter III and reported in reference [7].

Table 1. Polymerization of GPE initiated by t-BuP$_4$ / H$_2$O. Molecular characteristics of l-2a-PGPE samples.

Entry	[GPE]$_0$/[H$_2$O] /[t-BuP$_4$]	[GPE]$_0$ (mol/L)	$M_{n(obs)}$[a] (kDa)	$M_{n(theo)}$ (kDa)	Đ	Time[b] (h)	Yield (wt%)
1	66/1/0.8	7.8	6.2	10	1.09	120	99
2	66/1/0.8	3.5	6.6	10	1.02	320	97
3	39/1/0.8	7.8	5.7	5.8	1.06	48	98
4	39/1/0.8	7.8	5.5	5.8	1.03	48	96
5	13/1/0.8	7.8	2.2	2.0	1.12	48	98
6	13/1/0.8	3.5	2.5	2.0	1.05	48	95
7	13/1/0.3	7.8	2.5	2.0	1.04	48	97
8	13/1/0.1	7.8	6.2	2.0	1.06	80	98

[a] Determined by SEC-MALS-RI
[b] Time at which the reaction was stopped after observing high viscosity.

Figure 2 depicts a likely mechanism of polymerization of GPE with t-BuP$_4$ / H$_2$O following the hypothesis suggested in the introductory part. In the scheme, the t-BuP$_4$ forms activated water molecules (or hydroxide species)[10] that are able to attack the epoxide ring and to form a dihydroxyl molecule. Deprotonation of one of two hydroxides generates two different monoalkoxides, a secondary alkoxide and a primary alkoxide. Each alkoxide will be able to attack other epoxide ring and to propagate the polymerization. Taking into account that the most probable attack occurs to the methylene carbon of epoxide, the primary alkoxide will form a symmetric molecule with dipolar inversion and the secondary alkoxide an asymmetric molecule that does not

exhibit dipolar inversion. The equilibrium of protonation-deprotonation provided by the PB will favor that both hydroxide groups at the chain ends will be equivalent and that a two-arm PGPE structure (*l*-2a-PGPE) with dipolar inversion will be formed. This hypothesis is demonstrated below.
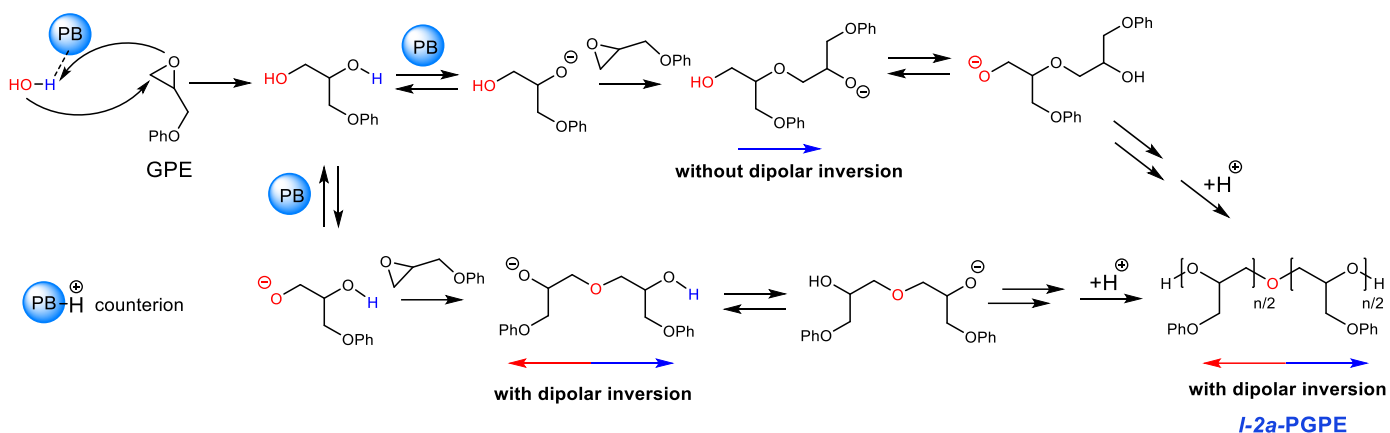

Figure 2. Polymerization mechanism of glycidyl phenyl ether (GPE) initiated by water in the presence of *t*-BuP$_4$ phosphazene base (PB).

MALDI-ToF MS analysis of synthesized *l*-2a-PGPE samples confirmed the formation of chains terminated by two hydroxyl groups. Adequate parameters for MALDI-ToF MS analysis were obtained as described in Appendix 2. High intensity signals corresponding to sodium-complexed *l*-2a-PGPE of mass = 150 n + 18 + 23 (n times the unit mass of GPE + the mass of one water molecule + the mass of one sodium cation) revealed the formation of a unique polymer population (Figure 3).
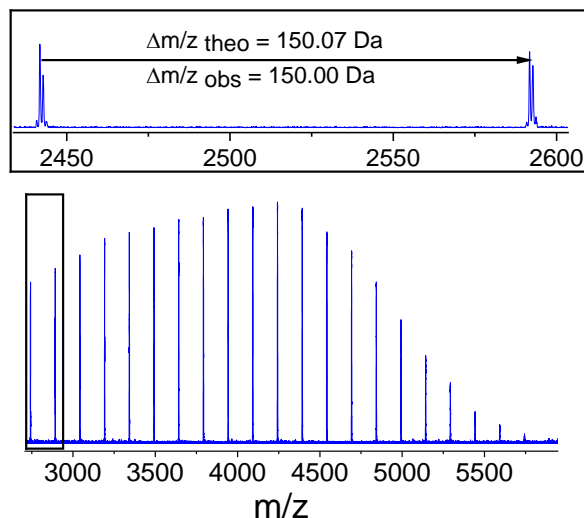
Figure 3. MALDI-ToF MS of water-initiated PGPE (Table 1, Entry 3).

When low molecular weight polymers were targeted, a second population was formed. Figure 4a shows the MALDI-ToF MS data of a sample of 2.2 kg/mol (Entry 5, Table 1) exhibiting two main mass populations. The highest intensity signals correspond to the sodium-complexed PGPE terminated in two hydroxyl groups. The second signal distribution exhibits a shift of -17.98 Da with respect to previous dihydroxide species, which can be assigned to sodium complexed PGPE chains terminated in alkene moieties (A-PGPE, Figure 5). These species are known to be formed by transfer to monomer reaction under basic conditions[24,25] and are highly undesired for two reasons: a) the chain ends cannot be transformed in clickable groups and therefore these chains cannot form macrocyclic structures, and b) A-PGPE chains do not have a two-arm structure with chain dipolar inversion.
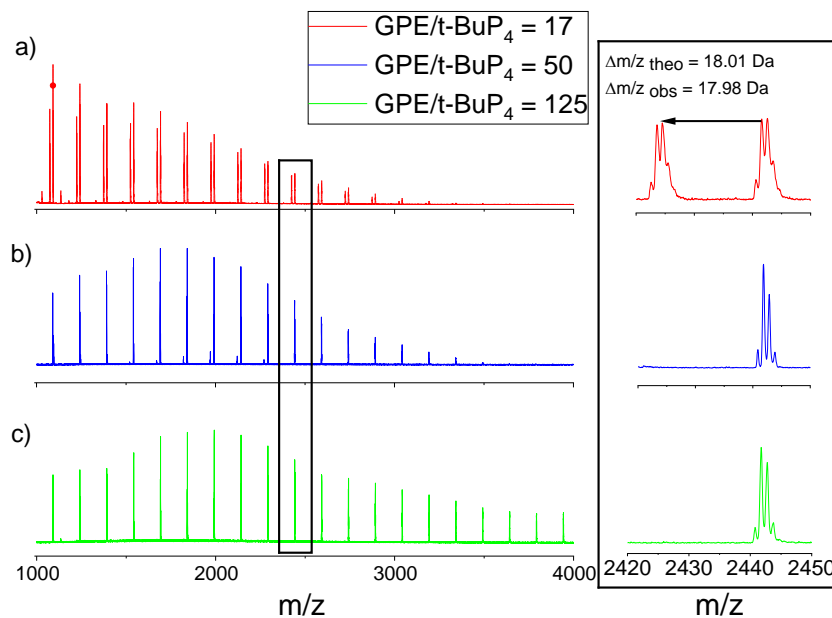
Figure 4. MALDI-ToF MS spectra of a) Entry 5, b) Entry 7 and c) Entry 8 of Table 1 showing the influence of the relative amount of GPE / t-BuP$_4$ on the transfer to monomer reactions.
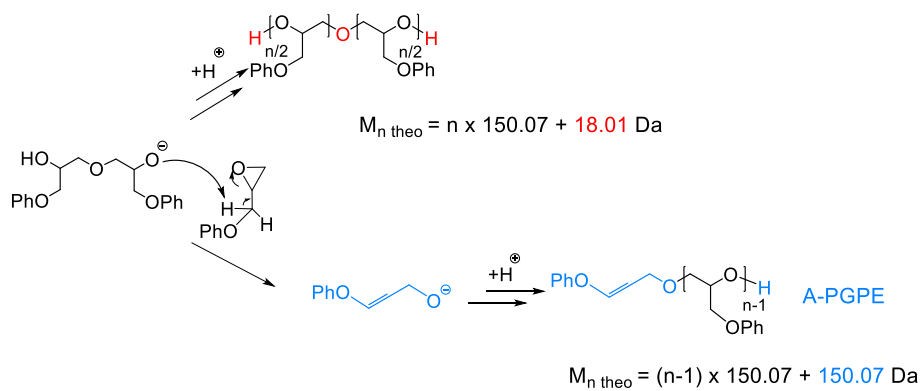

Figure 5. Transfer to monomer reaction leading to A-PGPE.

145

By reducing the amount of t-BuP$_4$ in low molecular weight samples, the transfer to monomer reaction was notably decreased, which was not the case when higher monomer dilution was used (entry 6, Table 1, data not shown). MALDI-ToF MS spectra of samples obtained with 0.3 and 0.1 equivalents of t-BuP$_4$ per 1 equivalent of water (entries 7 and 8, Table 1) are exhibited in Figure 4b and 4c, respectively. The data show a significant decrease of the relative peak intensity of A-PGPE specimens indicating that by reducing the amount of PB in the system, the transfer to monomer reaction can be avoided. This result was further confirmed by ^{1}H NMR (Figure 6). The signals h and g assigned to the alkene group at 5.4 ppm and 6.6 ppm respectively, decreased in intensity with the reduction of t-BuP$_4$. The signal h' and g' at 5.0 ppm and 6.5 ppm respectively correspond to the trans alkene proton.[24] However, the reduction of t-BuP$_4$ led to larger polymerization times likely due to slower initiation caused by lower amounts of active species. As a consequence, the molecular weight of l-2a-PGPE increased twice than that calculated theoretically indicating the loss of control over the polymerization reaction.

The analysis of the regiosequences in water initiated PGPE was performed by by ^{13}C NMR (Figure 7). The data revealed the appearance of signals that correspond to a configuration produced by only head-to tail or tail-to-head enchainment as observed by the appearance of sharp methylene (CH$_2$O) and methine (CHO) peaks of GPE repeated units in the main chain. Assignment of triad regiosequences was done according to previous study.[15] End groups were identified by comparing the ^{13}C NMR spectra obtained prior and post addition of small amounts of trichloroacetyl isocyanate (TAI) derivatizing reagent. Upon the addition of TAI, the terminal hydroxyl groups are transformed into urethane groups, allowing their identification.
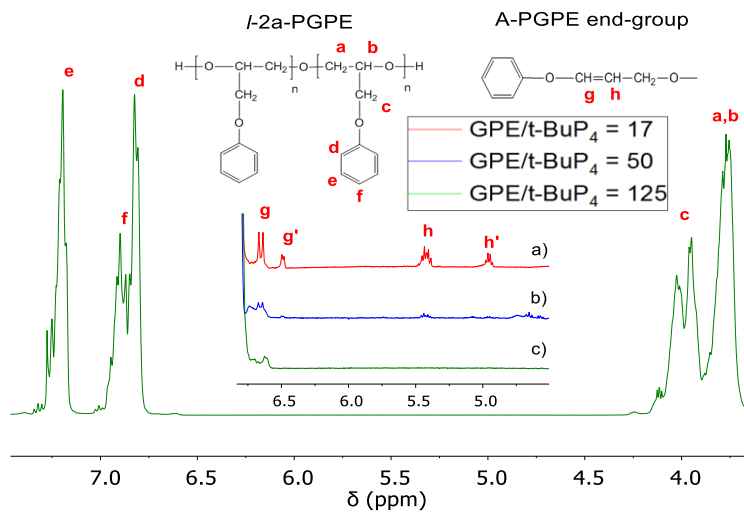
Figure 6. ^{1}H NMR data of low molecular weight PGPE obtained with different amounts of *t*-BuP$_4$ a) Entry 5 b) Entry 7 and c) Entry 8 of Table 1.
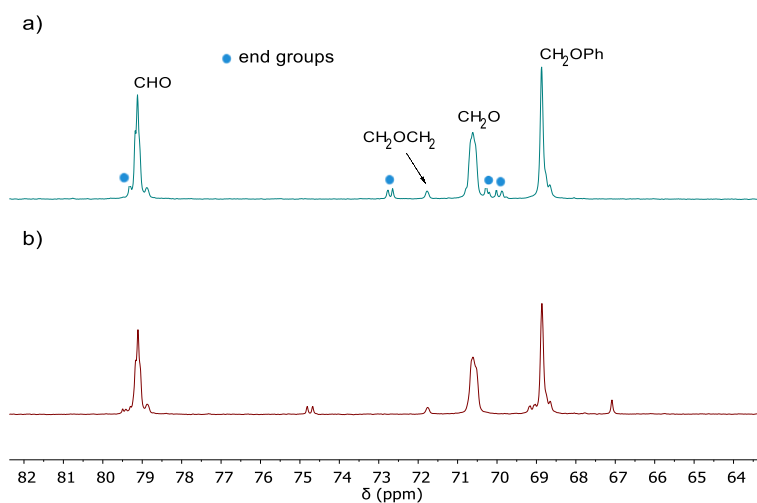

Figure 7. ^{13}C NMR (in acetone-d$_6$) of PGPE samples initiated by H$_2$O/tBuP$_4$ (Entry 4, Table 1). a) In the absence of TAI and b) in the presence of TAI.

Finally, to elucidate whether the growth of water-initiated *l*-2a-PGPE occurred in one or two directions (without or with dipole inversion), the obtained polymers were analyzed by BDS. As a remainder, according to the Rouse model for unentangled polymers, only odd modes contribute to the end-to-end chain relaxation. For linear and regio-regular samples, the end-to-end chain motions involve the dipole moment fluctuation, which results in a dielectric relaxation with a main relaxation time $\boldsymbol{\tau_{NM}} \propto \left(\frac{\boldsymbol{M}}{\boldsymbol{p}}\right)^{\boldsymbol{2}}$, with p = 1.[22,23,26] However, for polymers composed by two symmetric dipole-inverted arms, the NM relaxation would be described by even modes. In this case, the main dielectric relaxation time is $\boldsymbol{\tau_{NM}} \propto \left(\frac{\boldsymbol{M}}{\boldsymbol{p}}\right)^{\boldsymbol{2}}$, with p = 2.[23,27] Consequently, the dielectric NM relaxation should be faster by a factor of 4 than the end-to-end vector fluctuation.

For a proper comparison of different samples, the NM relaxation at $T_{g\text{-}BDS}$ was evaluated. This parameter takes into account the small but significant changes in the glass transition temperature. For one-arm regio-regular linear PGPE samples a mass-independent value of $\ln[\tau_{NM}(T_{g\text{-}BDS})/M^2] \approx 4.9$ is expected.[7,23] Correspondingly, a mass-independent value of $\ln[\tau_{NM}(T_{g\text{-}BDS})/M^2] \approx 3.5$ is expected for polymers constituted by two symmetric dipole-inverted arms.[7,23]

Figure 8a shows the relaxation spectra at 310 K for two water-initiated *l*-2a-PGPE of different molecular weights. The results are very similar to those of ethylene glycol-initiated *l*-2a-PGPE presented in Chapter III and in reference [7], suggesting that water-initiated PGPE also contains a dipole-inverted structure. Note that for an easiest spectral analysis, the data of $-\frac{\partial \varepsilon'}{\partial \ln f}$ as a function of f are also represented.[28] In this

representation the derived maxima will be narrower than its corresponding peak in the raw ε'' data. In addition, the obtained data will be free of direct current conductivity, importantly contributing to ε'', mainly at low frequencies (Figure 9).
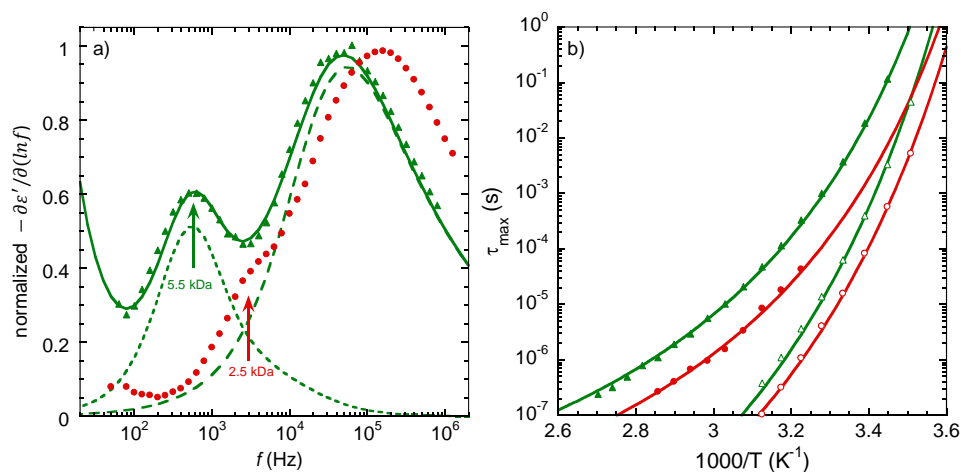

Figure 8. a) BDS spectra at 310 K of *l*-2a-PGPE of different molecular weight (Entries 4 and 7, Table 1). Solid line is a fitting of the higher molecular weight sample as a superposition of NM (dotted line), α-relaxation components (dashed line) and a low frequency power law. b) Corresponding relaxation plot exhibiting the α-relaxation (open symbols) and the NM (close symbols) for both samples. Solid lines were obtained by fitting the data to Eqs. 1 and 2, respectively.
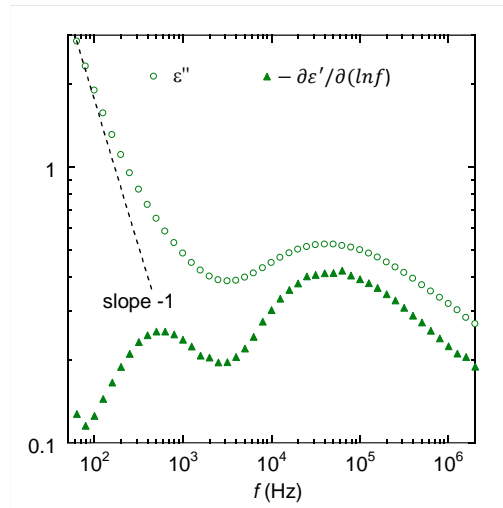
Figure 9. BDS data of *l*-2a-PGPE (Entry 8, Table 1). Comparison between ε'' and $-\frac{\partial \varepsilon'}{\partial lnf}$ representations.

The dielectric relaxation spectra of Figure 8a exhibit two well resolved relaxation peaks corresponding to the NM and segmental α relaxation of PGPE[7,15,24] in going from lower to higher frequency. The peak maxima of the α relaxation appear at frequencies (f_{max}) that are similar for the two samples, as expected from their close glass transition temperatures. Contrarily, the peak maxima of the NM relaxation clearly depend on the molecular weight (see arrows in Figure 8a). A way to visualize this information in the whole temperature range where samples were analyzed is by plotting the relaxation times from the peak maxima for both, the α and the NM (Figure 8b). As observed, the two samples exhibit similar time-temperature dependence of both relaxations. The analysis of the dielectric data by means of Eq.1 and Eq.2 for the two *l*-2a-PGPE samples resulted in values of $\ln[\tau_{NM}(T_{g\text{-}BDS})/M^2] \approx 3.5$ (Table 2, see fitting curves in Figure 8b),

which confirms both, the two-arm architecture and the high regio-regularity of each arm. A detailed analysis of the NM peak component has been performed in reference [29] to confirm the symmetric nature of the two arms in agreement with previous study. Namely, a Havriliak-Negami (HN) function was used to account for the α-relaxation contribution whereas the NM was described according to the Rouse model with mode components symmetrically broadened (see fitting curves in Figure 8a).[7,23]

Table 2. Parameters obtained from DSC and BDS analysis for water-initiated *l*-2a-PGPE. Comparison to previous results on ethylene glycol-initiated *l*-2a-PGPE.[7]

Entry	Initiation	$M_{n(obs)}$[a] (kDa)	$T_{g\text{-}DSC}$ (K)	$T_{g\text{-}BDS}$ (K)	$\tau_{NM}(T_{g\text{-}BDS})$ (s)	$\ln[\tau_{NM}(T_{g\text{-}BDS})/M^2]$
3	H_2O	5.7	274	275	11×10^2	3.5
4	H_2O	5.5	276	275	9.7×10^2	3.5
7	H_2O	2.5	271	271	2.2×10^2	3.6
8[b]	ethylene glycol	5.9	277	277	1.1×10^3	3.4

[a] Determined by SEC-MALS-RI
[b] Table 1, Entry 3, Chapter III

3.2.   <u>Cyclization of α,ω-alkyne poly(glycidyl phenyl ether)</u>

After modification of the hydroxide end groups of *l*-2a-PGPE into alkyne with propargyl bromide and NaH (Figure 10), Glaser coupling was used to form cyclic 2-arm PGPE (*c*-2a-PGPE). The experimental conditions of this reaction were adjusted as described below.
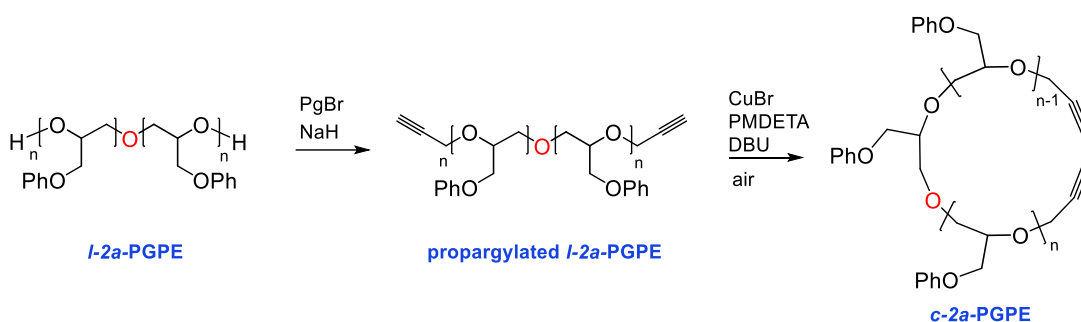
Figure 10. Propargylation of end groups and cyclization leading to *c*-2a-PGPE.

3.2.1. Optimization of the cyclization reaction

In order to minimize intermolecular coupling, different parameters were examined and their influence on cyclic purity was verified by GPC. PGPE samples of 5 kDa were used in all the experiments. The influence of the atmosphere was first evaluated by performing the Glaser coupling reaction under nitrogen or air. For this first set of

experiments, the concentration of the linear precursor solution was fixed at 4.10^{-3} M in 2 mL of dichloromethane (DCM). In a second flask, 50 equivalents of Cu(I)Br respect to the alkyne function were dissolved in 2 mL of DCM. Then, the polymer solution was added to the copper solution at 6 mL/h (20 µmol/h) under nitrogen atmosphere or under air. Figure 11a shows the GPC of the obtained products and the linear precursor.

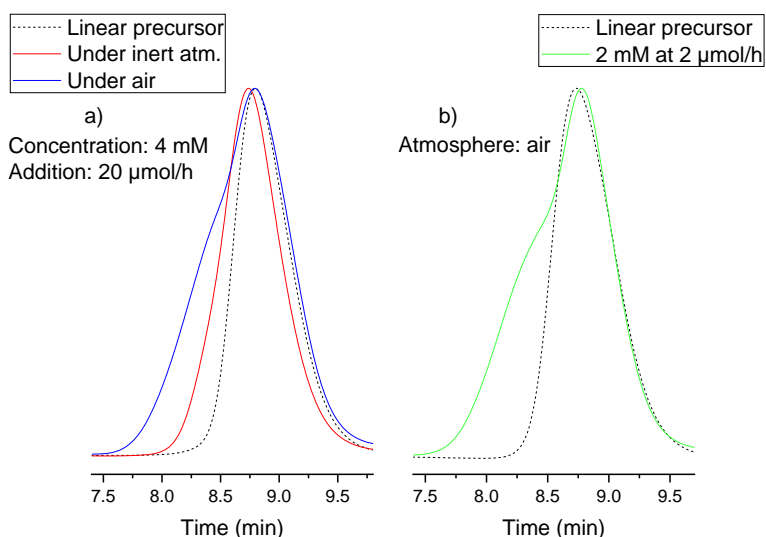**Figure 11.** SEC data (nomalized RI) showing the influence of a) the atmosphere and b) the concentration on the Glaser coupling reaction. Data recorded on a SEC-MALS-RI.

A shift toward lower retention time was observed when the reaction was performed under an inert atmosphere. Under those conditions, only intermolecular coupling occurred increasing the molecular weight of the polymer chains. When performed

153

under air, no clear shift was observed, and an intense shoulder indicated the presence of a large proportion of higher molecular weight impurities. Nevertheless, the Glaser coupling was faster when performed under air than under nitrogen likely because the presence of oxygen allows the oxidation of Cu(I) into Cu(II).[30] When the concentration of the linear precursor solution was lowered to 2 mM and the addition speed to 1 mL/h (2 µmol/h) (Figure 11b), a very slight shift of the main peak toward higher retention time was observed suggesting a minor formation of cyclic chains contaminated with a large amount of high molecular weight impurities.

According to Bolhmann et al.,[31] the first step of the Glaser coupling is the π–coordination of triple bound to a copper (I) species followed by the activation of the terminal C-H bound by an external base. Although the exact explanation is yet to be elucidated, various studies showed a faster kinetics for the Glaser coupling under basic conditions,[32,33] even in the absence of metal catalyst.[34] Based on this, for the second set of experiments, DBU was added to the copper solution. The linear precursor solution (2 mM) was added to the copper catalyst solution at 1 mL/h (2 µmol/h) in air, as in previous experiment of Figure 11b. Figure 12 shows the GPC data of cyclic polymers synthesized in the presence of 5 equivalents and 50 equivalents of DBU respect to the alkyne groups.
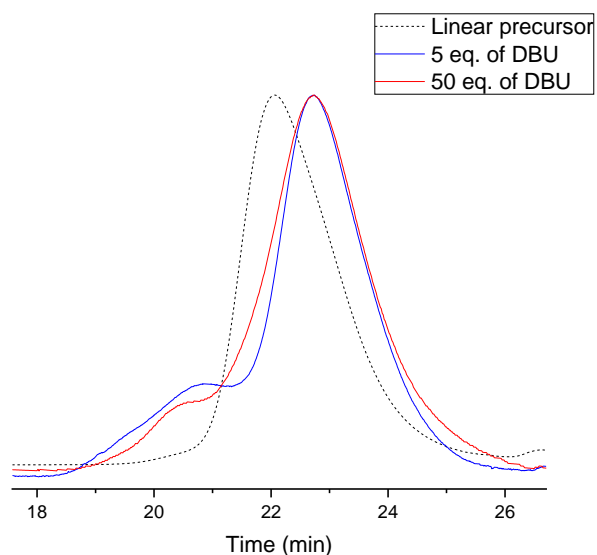
Figure 12. SEC data (nomalized RI) showing the influence of the organic base DBU on the Glaser coupling reaction. Data recorded on a SEC-RI.

A clear shift toward higher retention time was observed for both samples indicating the formation of cyclic chains. The shoulder at the high molecular weight side was less intense in the case where 50 equivalents of DBU were added to the copper solution. This result confirms the faster kinetics of Glaser coupling under basic conditions. Although intermolecular coupling could not be completely avoided for samples of 5 kDa, the addition of DBU improved drastically the cyclic purity. Moreover, this set of conditions allowed the synthesis of pure cyclic polymers of lower molecular weight (M_n = 2.5 kDa) as shown below.

3.2.2. Preparation of pure cyclic poly(glycidyl phenyl ether) by Glaser coupling

Based on the results obtained during the optimization of the Glaser coupling reaction, cyclic PGPEs were prepared as follows. Cu(I)Br was used as a catalyst and the amine PMDETA was used to increase the solubility of the copper salt into dichloromethane. The reaction was performed under air to allow the oxidation of Cu(I) into Cu(II) and speed up the reaction.[30] Finally, DBU was also added to the catalyst solution to further increase the reaction rate.[32,33] The solution containing the propargylated *l*-2a-PGPE was slowly added (2 μmol/h) to the copper catalyst solution, using a syringe pump, based on Huang et al. work.[35] *c*-2a-PGPE up to 2.5 kDa with a very low proportion of linear chains was generated, as observed in the GPC trace of Figure 13a. The data exhibits a higher retention time for the cyclic polymer compared to its linear precursor as a result of its lower hydrodynamic volume. The lack of any distinguishable shoulder at the higher molecular mass side indicates the absence of intermolecular coupling.
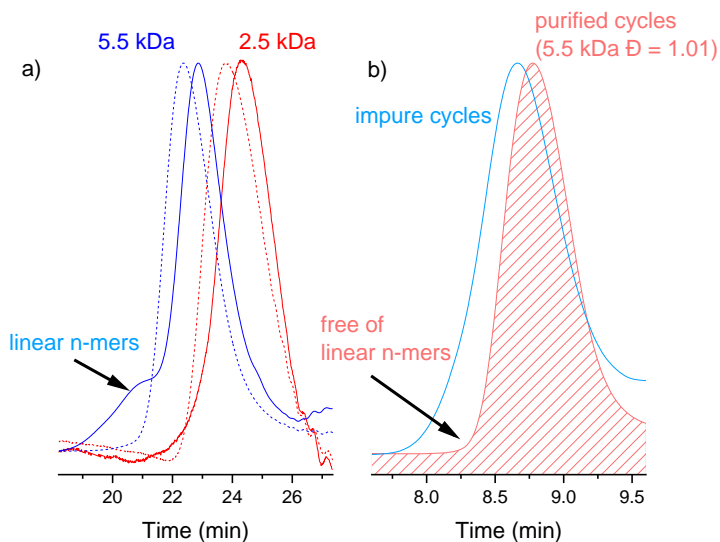
Figure 13. a) SEC of *c*-2a-PGPE (solid line) and its propargylated *l*-2a-PGPE precursor (dash line) of two molecular weights (data recorded on a SEC-RI). b) SEC of *c*-2a-PGPE purified by fractionation on a preparative GPC (data recorded on a SEC-MALS-RI).

Increasing the chain length decreases the probability of the two ends to meet and, as a consequence, the percentage of pure cycle polymer decreases.[36] To limit the probability of two linear chains to react, the synthesis of higher molecular weight *c*-2a-PGPE samples was performed with a larger dichloromethane volume in the copper solution compared to that used for 2.5 kDa polymer sample. In those conditions, higher molecular weight *c*-2a-PGPE (M_n = 5.5 kDa) was successfully obtained as observed by a clear shift in the retention time of Figure 13a. However, a shoulder at shorter retention time suggests the formation of higher molecular weight impurites indicating intermolecular coupling.

The successful formation of cycles *via* Glaser coupling was also confirmed by MALDI-ToF MS. Figure 14 shows the mass spectra of *c-2a*-PGPE and its linear precursors before and after end group modification with propargyl bromide (Entry 4, Table 1). Figure 14a shows the data corresponding to the propargylated *l-2a*-PGPE. After end group modification, a shift of +75.92 mass units confirmed the quantitative propargylation of hydroxyls at both end groups. Upon cyclization *via* Glaser coupling the loss of two protons (-2 m/z) was detected (Figure 14b).
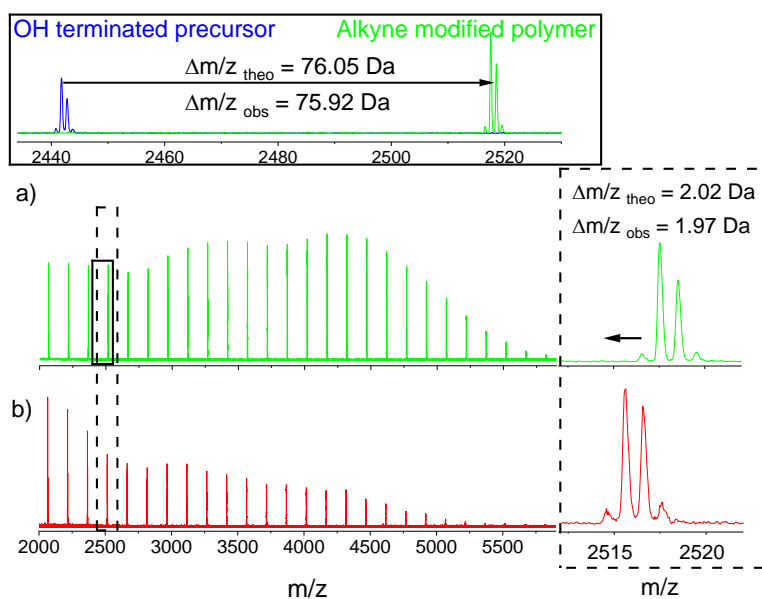

Figure 14. MALDI-ToF MS of (a) propargylated *l*-2a-PGPE and (b) *c*-2a-PGPE. The spectra were recorded in reflector mode.

To identify the nature of species appearing at shorter retention times upon cyclization, a *c-2a*-PGPE species was fractionated using a preparative GPC and the collected fraction (between 33 and 35 min) was analyzed by MALDI ToF MS (Figure 15). The figure shows the mass data of pure macrocyclic structure, its linear propargylated precursor and the collected GPC fraction. The latter exhibits a shift of + 91.82 m/z from the propargylated *l-2a*-PGPE and +93.70 from the cyclic structure. The mass distribution of the collected fraction can be assigned to sodium complexed PGPE dimer terminated in two alkyne groups (Figure 16). This impurity was successfully removed with a preparative GPC allowing the BDS analysis of a pure cyclic sample with very low polydispersity, Đ = 1.01 (Figure 13b). It is worth to note that cyclic dimers were not detected.
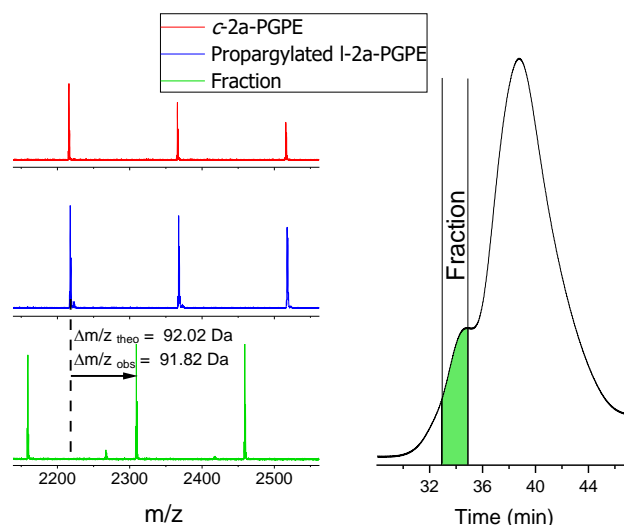

Figure 15. Identification of linear dimers in a *c*-2a-PGPE sample generated from that of Entry 8, Table 1 using MALDI-ToF MS and preparative GPC fractionation (at Tulane University).

M_{theo} = 2n x 150.07 + 94.04 Da M_{theo} = 4n x 150.07 + 94.04 + 92.02 Da
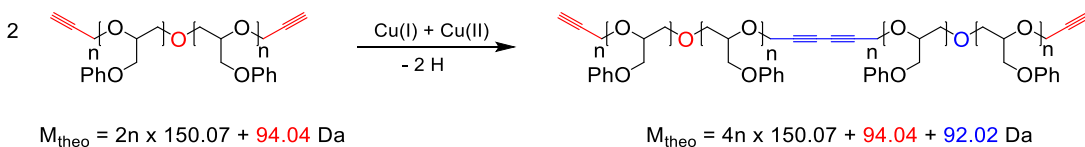
Figure 16. Linear dimer formed upon intermolecular of two linear chains during Glaser coupling.

3.3. <u>Ring dynamics study by BDS analysis</u>

Figure 17 shows the BDS results obtained on a purified cyclic sample *c-2a*-PGPE (M_n = 5.5 kDa, Đ = 1.01) in comparison with that of its corresponding propargylated linear counterpart, *l-2a*-PGPE. The overall aspect of the BDS data in Figure 17a is the same in both polymers, with a small shift in the α-peak frequency as it would reflect the expected increase of T_g upon cyclization. This change in T_g is confirmed in Figure 17b when fitting the peak relaxation times of these two samples. A difference of about 3 K in T_g was observed, the cyclic polymer presenting a higher value (Table 3). This result is in line with previous finding on PGPE polymers without dipole inversion.[24]

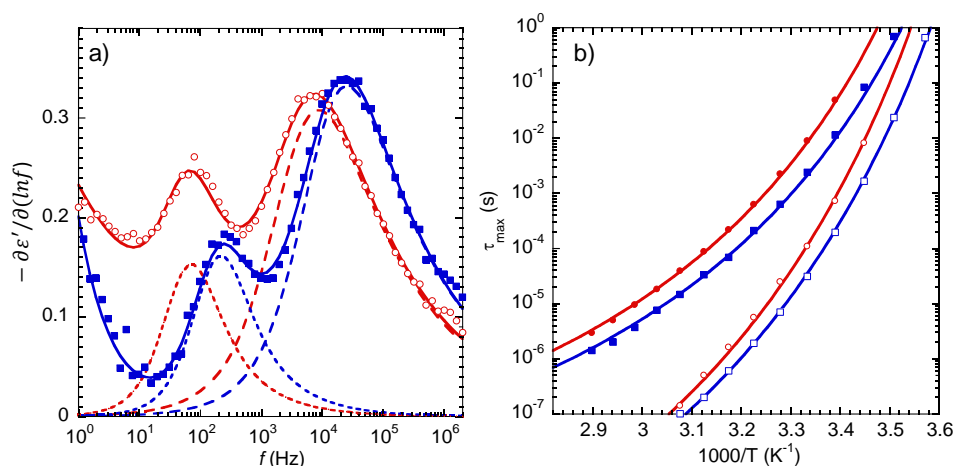**Figure 17.** a) BDS spectra at 305 K for *c*-2a-PGPE (red circles) and propargylated *l*-2a-PGPE (blue squares) of Mn = 5.5 kDa (Entry 4). Solid line is a fitting as a superposition of NM (dotted line), α-relaxation components (dashed line) and a low frequency power law. b) Relaxation plot exhibiting the α-relaxation (open symbols) and the NM (close symbols) for both samples. Solid lines were obtained by fitting the data to Eqs. 1 and 2, respectively.

Table 3. Parameters obtained from BDS analysis for propargylated *l*-2a-PGPE and *c*-2a-PGPE.

Entry	Structure	M_n (kDa)	$T_{g\text{-}DSC}$ (K)	$T_{g\text{-}BDS}$ (K)	$\tau_{NM}(T_{g\text{-}BDS})$ (s)	$\ln[\tau_{NM}(T_{g\text{-}BDS})/M^2]$
Entry 4	linear	5.5	274	274	9.0×10^2	3.4
	cyclic	5.5	277	277	14×10^2	3.8
Entry 3	linear	5.7	274	275	11×10^2	3.5
	cyclic	5.7	276	276	15×10^2	3.8

The fitting lines in Figure 17b also allowed the comparison of the NM relaxation time at T_g. In the case of dipole-inverted chains, the NM represents the fluctuations of $\overrightarrow{R_{N/2}}$ (Figure 1). Whereas in the linear polymer both arms share a single end at the dipole inversion point, in the cyclic structure both ends of the two arms are linked together. BDS results show that the NM of cyclic chains at T_g is a factor of 1.5 slower than that of linear chains (Table 3), which clearly indicates a slower fluctuation of $\overrightarrow{R_{N/2}}$ in the rings. In order to analyze in more detail other possible effects of the chain topology on the NM relaxation, the BDS data of both samples were fitted following the same procedure used above (see Figure 8a). The same fitting approach worked well for both linear and cyclic topologies. Moreover, the fitting parameters were very similar for both topologies except the relaxation times (see relaxation components in Figure 17a). These results confirm, on one hand, previous findings concerning the effect of cyclic topology on the α-relaxation of this type of polymers,[15] as expected from ring polymer theory.[37] On the other hand, the fact that the NM of rings can be well described in terms of the Rouse model is in agreement with theoretical expectations[13] and molecular dynamic simulations[14] on relatively short polymer rings. However, it is expected (from both theory and simulations) that the relaxation times of the ring diameter vector will be ¼ of the whole end-to-end vector of the linear chain.[7] This is also the expectation for the relaxation of the $\overrightarrow{R_{N/2}}$ of the two-arm linear chain. Contrarily to those expectations, it was found that the relaxation of $\overrightarrow{R_{N/2}}$ in the ring is 1.5 times slower than in the linear analogue. Note that this comparison is made at T_g, which represents an iso-frictional situation. This 1.5 factor results in a value of $\ln[\tau_{NM}(T_{g\text{-}BDS})/M^2] \approx 3.5 + \ln 1.5 \approx 3.8$ for the cyclic polymer, which would be independent of the molecular weight of rings. Moreover, this characteristic 3.8 value for rings was confirmed in a second batch of

sample of similar molecular weight (Table 3). These results evidence the presence of additional constrains associated to the ring topology for ring sizes far below the entanglement mass of linear PGPE (M_e=39 kDa).[23] The role played by side groups in these results deserves further investigation.

4. Conclusions

Two-arm linear poly(glycidyl phenyl ether)s with an inverted-dipole microstructure were synthesized using t-BuP$_4$ phosphazene base and water as initiation system. Transfer to monomer reactions were completely avoided by adjusting the initial amount of phosphazene base yielding hydroxyl-terminated chains with high end-group fidelity. BDS analysis of the generated linear structures confirmed the formation of regio-regular microstructures composed by two symmetric subchains with opposite dipole moment orientation. This result supports a polymerization mechanism dominated by t-BuP$_4$ driven protonation-deprotonation allowing that both hydroxide groups at the chain ends are equivalent. It is important to note that the validation of such structures can hardly be performed with other conventional techniques, demonstrating the complementarity of BDS for the characterization of polymer architectures.

Once validated both, the formation of two symmetric arms and the high end-group fidelity, the two terminal hydroxyl groups in poly(glycidyl phenyl ether)s were quantitatively modified into alkyne groups. Finally, macrocycles with inverted-dipole microstructure were generated at high dilution in the presence of Cu(I) and Cu(II)

through intramolecular alkyne-alkyne coupling (i.e. Glaser coupling). The optimization of cyclization reaction was achieved by using PMDETA, DBU and air conditions. Low molecular weight cycles of 2.5 kDa were generated with high cyclic purity, although intermolecular coupling could not be avoided at molecular weights higher than ~5 kDa. Nevertheless, pure rings (used in BDS analysis) were attained by fractionation in a preparative GPC.

Finally, thanks to the fact that the dielectric relaxation of dipole-inverted polymer chains directly reflects the fluctuations of the ring diameter vector, it was demonstrated that the topological constrains affect the dynamics for ring lengths far below the entanglement mass of linear PGPE. These results, although exemplified in a specific polyether structure, provides some general and physically sound directives for the study of fundamental questions in polymer ring dynamics.

5. **References**

(1)   Pasquino, R.; Vasilakopoulos, T. C.; Jeong, Y. C.; Lee, H.; Rogers, S.; Sakellariou, G.; Allgaier, J.; Takano, A.; Brás, A. R.; Chang, T.; et al. Viscosity of Ring Polymer Melts. *ACS Macro Lett.* **2013**, *2* (10), 874–878.

(2)   Richter, D.; Gooßen, S.; Wischnewski, A. Celebrating Soft Matter's 10th Anniversary: Topology Matters: Structure and Dynamics of Ring Polymers. *Soft Matter* **2015**, *11* (44), 8535–8549.

(3)   Doi, Y.; Matsubara, K.; Ohta, Y.; Nakano, T.; Kawaguchi, D.; Takahashi, Y.; Takano, A.; Matsushita, Y. Melt Rheology of Ring Polystyrenes with Ultrahigh Purity. *Macromolecules* **2015**, *48* (9), 3140–3147.

(4)   Gooßen, S.; Brás, A. R.; Krutyeva, M.; Sharp, M.; Falus, P.; Feoktystov, A.; Gasser, U.; Pyckhout-Hintzen, W.; Wischnewski, A.; Richter, D. Molecular Scale Dynamics of Large Ring Polymers. *Phys. Rev. Lett.* **2014**, *113* (16), 1–5.

(5)   Kapnistos, M.; Lang, M.; Vlassopoulos, D.; Pyckhout-Hintzen, W.; Richter, D.; Cho, D.; Chang, T.; Rubinstein, M. Unexpected Power-Law Stress Relaxation of Entangled Ring Polymers. *Nat. Mater.* **2008**, *7* (12), 997–1002.

(6)   Yan, Z. C.; Costanzo, S.; Jeong, Y.; Chang, T.; Vlassopoulos, D. Linear and Nonlinear Shear Rheology of a Marginally Entangled Ring Polymer. *Macromolecules* **2016**, *49* (4), 1444–1453.

(7)   Ochs, J.; Martínez-Tong, D. E.; Alegria, A.; Barroso-Bujans, F. Dielectric Relaxation as a Probe To Verify the Symmetrical Growth of Two-Arm Poly(Glycidyl Phenyl Ether) Initiated by t-BuP$_4$ /Ethylene Glycol. *Macromolecules* **2019**, *52* (5), 2083–2092.

(8)   Tezgel, Ö.; Puchelle, V.; Du, H.; Illy, N.; Guégan, P. Modification of Proline-Based 2,5-Diketopiperazines by Anionic Ring-Opening Polymerization. *J. Polym. Sci. Part A Polym. Chem.* **2019**, *57* (9), 1008–1016.

(9)   Rassou, S.; Illy, N.; Tezgel, O.; Guégan, P. Anionic Ring-Opening Polymerization of N-Glycidylphthalimide: Combination of Phosphazene Base and Activated Monomer Mechanism. *J. Polym. Sci. Part A Polym. Chem.* **2018**, *56* (10), 1091–1099.

(10)   Weitkamp, R. F.; Neumann, B.; Stammler, H. G.; Hoge, B. Generation and Applications of the Hydroxide Trihydrate Anion, [OH(OH$_2$)$_3$]$^-$, Stabilized by a Weakly Coordinating Cation. *Angew. Chemie - Int. Ed.* **2019**, *58* (41), 14633–14638.

(11)   Fuchise, K.; Sato, K.; Shimada, S. Organocatalytic Controlled/Living Ring-Opening Polymerization of Cyclotrisiloxanes Initiated by Water with Strong Organic Base Catalysts. *Chem. Sci.* **2018**, *9*, 2879–2891.

(12)   Chen, Y.; Shen, J.; Liu, S.; Zhao, J.; Wang, Y.; Zhang, G. High Efficiency Organic Lewis Pair Catalyst for Ring-Opening Polymerization of Epoxides with Chemoselectivity. *Macromolecules* **2018**, *51*, 8286–8297.

(13)   Wiest, J. M.; Burdette, S. R.; Liu, T. W.; Bird, R. B. Effect of Ring Closure on Rheological Behavior. *J Non-newt. Fluid* **1987**, *24* (3), 279–295.

(14)   Tsolou, G.; Stratikis, N.; Baig, C.; Stephanou, P. S.; Mavrantzas, V. G. Melt Structure and Dynamics of Unentangled Polyethylene Rings: Rouse Theory, Atomistic Molecular Dynamics Simulation, and Comparison with the Linear Analogues. *Macromolecules* **2010**, *43* (24), 10692–10713.

(15)   Gambino, T.; Martínez De Ilarduya, A.; Alegría, A.; Barroso-Bujans, F. Dielectric Relaxations in Poly(Glycidyl Phenyl Ether): Effects of Microstructure and Cyclic Topology. *Macromolecules* **2016**, *49* (3), 1060–1069.

(16)   Vogel, H. The Law of the Relationship between Viscosity of Liquids and the Temperature. *Phys. Zeitschrift* **1921**, *22*, 645–646.

(17)   Fulcher, G. S. Analysis of Recent Measurements of the Viscosity of Glasses. *J. Am. Ceram. Soc.* **1925**, *8* (6), 339–355.

(18)   Tammann, G.; Hesse, W. Die Abhängigkeit Der Viscosität von Der Temperatur Bie

Unterkühlten Flüssigkeiten. *Zeitschrift für Anorg. und Allg. Chemie* **1926**, *156* (1), 245–257.

(19) Ferry, J. D. *Viscoelastic Properties of Polymers 3rd Edition*, John Wiley.; New York, 1980.

(20) McCrum, N. G.; Read, B. E.; Williams, G. *Anelastic and Dielectric Effects in Polymeric Solids*, Dover publ.; 1991.

(21) Kremer, F.; Schönhals, A. *Broadband Dielectric Spectroscopy*, Springer-V.; Berlin, Heidelberg, New York, 2003.

(22) Rubinstein, M.; Colby, R. H. *Polymer Physics*; Oxford University Press, 2003.

(23) Martínez-Tong, D. E.; Ochs, J.; Barroso-Bujans, F.; Alegria, A. Broadband Dielectric Spectroscopy to Validate Architectural Features in Type-A Polymers: Revisiting the Poly(Glycidyl Phenyl Ether) Case. *Eur. Phys. J. E* **2019**, *42* (7).

(24) Ochs, J.; Veloso, A.; Martínez-Tong, D. E.; Alegria, A.; Barroso-Bujans, F. An Insight into the Anionic Ring-Opening Polymerization with Tetrabutylammonium Azide for the Generation of Pure Cyclic Poly(Glycidyl Phenyl Ether). *Macromolecules* **2018**, *51* (7), 2447–2455.

(25) Billouard, C.; Carlotti, S.; Desbois, P.; Deffieux, A. "Controlled" High-Speed Anionic Polymerization of Propylene Oxide Initiated by Alkali Metal Alkoxide/Trialkylaluminum Systems. *Macromolecules* **2004**, *37* (11), 4038–4043.

(26) Watanabe, H. Dielectric Relaxation of Type-A Polymers in Melts and Solutions. *Macromol. Rapid Commun.* **2001**, *22* (3), 127–175.

(27) Watanabe, H.; Urakawa, O.; Kotaka, T. Slow Dielectric Relaxation of Entangled Linear Cis-Polyisoprenes with Asymmetrically Inverted Dipoles. 1. Bulk Systems. *Macromolecules* **1993**, *26* (19), 5073–5083.

(28) Wübbenhorst, J.; van Turnhout, J. "Conduction-Free" Dielectric Loss de/Dlnf - A Powerful Tool for the Analysis of Strong (Ion) Conducting Dielectric Materials. *Novocontrol Dielectr. Newsl.* **2000**, *No.14*.

(29)   Ochs, J.; Alegría, A.; Gónzalez de San Román, E.; Grayson, S. M.; Barroso-Bujans, F. Synthesis of Macrocyclic Poly(Glycidyl Phenyl Ether) with a Dipole-Inverted Microstructure via Ring Closure of Two-Arm Linear Precursors Obtained by Initiation with t-BuP$_4$ /Water (under Preparation).

(30)   Leophairatana, P.; Samanta, S.; De Silva, C. C.; Koberstein, J. T. Preventing Alkyne-Alkyne (i.e., Glaser) Coupling Associated with the ATRP Synthesis of Alkyne-Functional Polymers/Macromonomers and for Alkynes under Click (i.e., CuAAC) Reaction Conditions. *J. Am. Chem. Soc.* **2017**, *139* (10), 3756–3766.

(31)   Bohlmann, F.; Schönowsky, H.; Inhoffen, E.; Grau, G. Ferdinand Bohlmann, Hubert. *Chem. Ber.* **1963**, *97*, 794–800.

(32)   Jover, J.; Spuhler, P.; Zhao, L.; McArdle, C.; Maseras, F. Toward a Mechanistic Understanding of Oxidative Homocoupling: The Glaser-Hay Reaction. *Catal. Sci. Technol.* **2014**, *4* (12), 4200–4209.

(33)   Li, L.; Wang, J.; Zhang, G.; Liu, Q. A Mild Copper-Mediated Glaser-Type Coupling Reaction under the Novel CuI / NBS / DIPEA Promoting System. *Tetrahedron Lett.* **2009**, *50* (28), 4033–4036.

(34)   Schörgenhumer, J.; Waser, M. Transition Metal-Free Coupling of Terminal Alkynes and Hypervalent Iodine-Based Alkyne-Transfer Reagents to Access Unsymmetrical 1,3-Diynes. *Org. Biomol. Chem.* **2018**, *16* (41), 7561–7563.

(35)   Zhang, Y.; Wang, G.; Huang, J. Synthesis of Macrocyclic Poly (Ethylene Oxide) and Polystyrene via Glaser Coupling Reaction. *Macromolecules* **2010**, *43*, 10343–10347.

(36)   Jacobson, H.; Stockmayer, W. H. Intramolecular Reaction in Polycondensations. I. The Theory of Linear Systems. *J. Chem. Phys.* **1950**, *18*, 1600–1606.

(37)   Di Marzio, E. A.; Guttman, C. M. The Glass Temperature of Polymer Rings. *Macromolecules* **1987**, *20*, 1403–1407.

Chapter V

Conclusions

In this thesis, cyclic poly(glycidyl phenyl ether)s (PGPEs) having controlled dipolar microstructures were synthesized via the ring closure technique. An important part of this work focused on the characterization of linear precursors to ensure their high end-group fidelity, since it is an essential parameter for the synthesis of pure monocyclic chains via the ring closure technique. Anionic ring opening polymerization of glycidyl phenyl ether (GPE) was chosen as a strategy for the synthesis of linear PGPE precursors. Matrix assisted laser desorption ionization - time of flight mass spectrometry (MALDI-ToF MS) and NMR were used to verify the end-group fidelity of the polymer chains after synthesis.

In particular, two cases were studied. First, polymers having every monomer unit aligned in the same direction resulting in a non-inverted dipole microstructure. Second, polymer chains presenting a dipole inversion in the middle of the chain. For the first series of samples, it was demonstrated that α-azide, ω-hydroxy PGPEs with high end-group fidelity were obtained when using tetrabutylammonium azide and the well-known monomer activator triisobutylaluminum (iBu$_3$Al) to avoid transfer to monomer reactions during polymerization. However, for the second series of polymers this strategy was inappropriate. Indeed, it was found that in the presence of the phosphazene base t-BuP$_4$, used for the preparation of α, ω-hydroxy PGPEs, iBu$_3$Al promoted several side reactions resulting in poor end-group fidelity. In this case, transfer to monomer reactions were completely avoided by maintaining a ratio of GPE / t-BuP$_4$ > 50, thus guaranteeing high end-group fidelity. Finally, using broadband

dielectric spectroscopy (BDS), the dipole orientation along the chain contour was evaluated directly after synthesis.

After modification of the hydroxy end groups of linear precursors into alkynes, cyclic polymers without dipole inversion were prepared either by copper(I)-catalyzed azide-alkyne cycloaddition, while cyclic chain presenting a dipole inversion were synthesized by intramolecular alkyne-alkyne coupling (i.e. Glaser coupling). The formation of high molecular weight chains by intermolecular coupling is one of the major sources of impurities during cyclization by the ring closure technique. To tackle this problem, a series of experiments was performed to monitor the influence of different parameters over the cyclic purity. Ultimately, the importance of the oxidation state of the copper catalyst was highlighted in both coupling reactions and the optimum experimental conditions for the preparation of pure monocyclic chains were determined as demonstrated by GPC and MALDI-ToF MS.

Finally, the BDS study of the alpha dielectric relaxation and the normal mode relaxation of the synthesized cyclic regio-regular polymers allowed to clearly identify the formation of the desired dipole microstructures. In cyclic polymers with non-inverted dipoles, the dipole moment along the chain is canceled, leading to disappearance in the normal mode. These results were used to validate the cyclic purity of these polymers, which further showed for the first time the utility of BDS for this unconventional purpose. In the case of cyclic polymers presenting a dipole inversion, they exhibit a normal mode relaxation that specifically reflects fluctuations of the diameter of the ring. This important characteristic allowed evaluation of ring dynamics, which resulted in a relaxation 1.5 times slower than the analogous relaxation in the linear precursor at

the glass transition temperature. These results show the potential of inverted dipole macrocycles in the study of fundamental physical problems in cyclic polymers.

Appendix 1

Synthesis of cyclic polymers

Table of Contents

Cyclic polymers are typically synthesized by three main approaches, ring chain equilibration, ring expansion polymerization and ring closure. During the last few decades, enormous efforts have been made to produce rings in high yields and high purity. The development of a large variety of chemical reactions has allowed the preparation of cyclic polymers having different backbones. In this section, some examples of cyclization reactions are presented with the intention to show the extended literature available in this field of polymer chemistry.

1. <u>Ring chain equilibration</u>

Step growth polymerization is a type of mechanism where polymer chains are formed upon reaction between functional groups of the monomer. The first theory on step growth polymerization comes from the work of Carothers[1] and Flory.[2,3] It is assumed that linear monomers react to form linear oligomers and later linear polymers. Even though no cyclization reaction was first taken into account, it was later observed that cyclic oligomers were formed by backbiting of linear chains. This process is occurring throughout the whole step growth polymerization and includes a ring chain equilibration. Therefore, as an equilibration reaction, the population of reaction products represents the thermodynamic minimum energy. For that reason, step growth polymerization can be classified as a thermodynamically controlled polymerization. Years later, Jacobson and Stockmayer, observed that in every thermodynamically controlled polymerization cyclic chains were formed via backbiting,[4,5] but preparation of cyclic samples with such a strategy remained difficult because of the large amount of

linear chains formed and the broad molecular weight distribution of the final product. For that reason, extensive purification is required and low yields are achievable. Only low molecular weights cyclic chains were obtained with high polydispersity. Moreover, the linear precursor could not be properly isolated making the characterization of the cyclic chains complicated.

One early example of cyclic polymers prepared by ring chain equilibration is cyclic poly(dimethylsiloxane)s (PDMS) (Figure 1).[6] Since then, this synthesis strategy was used to synthesize a wide range of cyclic PDMS.[7,8] The reaction product is composed of linear PDMS of high molecular weight and low molecular weight cyclic chains, mostly tetramers, pentamers and hexamers.

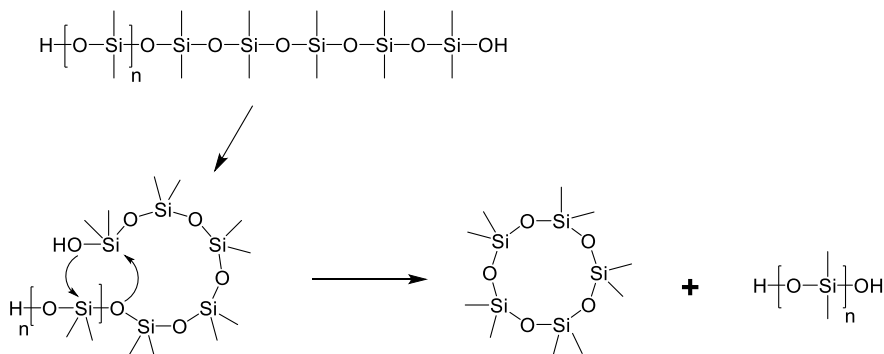**Figure 1.** Formation of cyclic PDMS by ring chain equilibration reaction

Although a large set of physical properties of cyclic polymers could be studied thanks to those works, the presence of linear chains in a cyclic sample, even at low concentration, can modify the physical properties of the polymer sample.[9,10] For that reason, it is crucial to synthesize ring polymers with high topological purity.

2. <u>Ring expansion polymerization</u>

2.1. <u>Ring expansion polymerization with metal-based catalysts</u>

Originally, Kricheldorf and Lee prepared macrocycles of different (thio)lactones using tin heterocyclic initiators.[11,12] The monomer units were inserted into the Sn-O bond of the initiator, which is highly reactive toward various electrophilic reagents (Figure 2). The cyclic structure was confirmed by size exclusion chromatography (SEC) and ^{1}H nuclear magnetic resonance (NMR) analysis. Similar method was used to prepare complex cyclic topologies using lactone and lactide based monomers.[13–15] The use of the same tin based catalyst was expanded for the synthesis of cyclic poly(ethylene glycol),[16] cyclic poly(tetrahydrofurandiol)[17] and cyclic poly(siloxane),[18] as well as the corresponding copolymers. In order to stabilize the macrocyclic product, Kricheldorf and co-workers replaced the tin catalyst by a bis-functional phthalate thioester after polymerization.[19] A ring-exchange process allowed the formation of a more stable macrocycle without intermediate ring opening reaction.
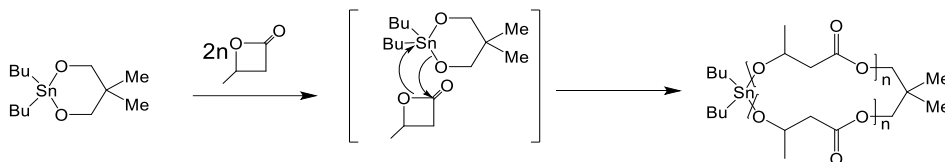
Figure 2. First synthesis of cyclic lactone by ring expansion polymerization

Other metal alkoxides have been used for the successful preparation of macrocycles. The insertion of lactide into an aluminum based catalyst[20] (Figure 3) yielded cyclic polymers of 39 kDa with polydispersity index around 1.5. The molecular weight was dependent of the monomer over catalyst ratio and could be controlled by adjusting this parameter. The same mechanism of insertion-coordination followed by transesterification led to the formation of cyclic chains.[21] It was demonstrated that the rate-determining step was the rearrangement of the aluminum based catalyst during insertion of the monomer unit.
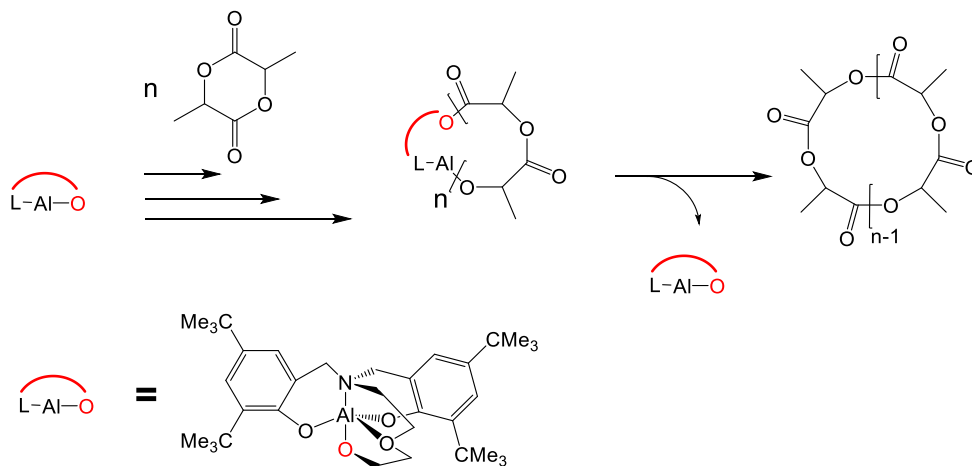

Figure 3. Aluminum based catalyst for the ring expansion polymerization of lactide

Continuous efforts on the development of new catalysts opened new possibilities for the synthesis of cyclic polymers. Salicylaldiminato tin(II) complex was used to catalyze the REP of L-lactide and ε-caprolactone in solvent free polymerizations.[22] Tin is known to favor transesterification at high conversion, making it a metal of choice for the synthesis of high molecular weight cyclic polymers. The tin complex contains an alkoxy side chain that initiates the polymerization (Figure 4). The length of this side chain determines the distance between the tin atom and the growing polymer chain. This parameter will impact the intramolecular transesterification reaction at the end of the propagation step leading to the final cyclic product. Complexes with a shorter alkoxy chain were found to successfully promote the REP of both L-lactide and ε-caprolactone. This result highlights the importance of the transesterification reaction for the formation of ring polymers by REP, a reaction that is usually undesired in regular polymerizations. Matrix assisted laser desorption ionization - time of flight mass spectrometry (MALDI-ToF MS) analysis showed an increase of the amount of macrocycles with reaction time, confirming that transesterification leading to the formation of the final macrocyclic product took place at high conversion.
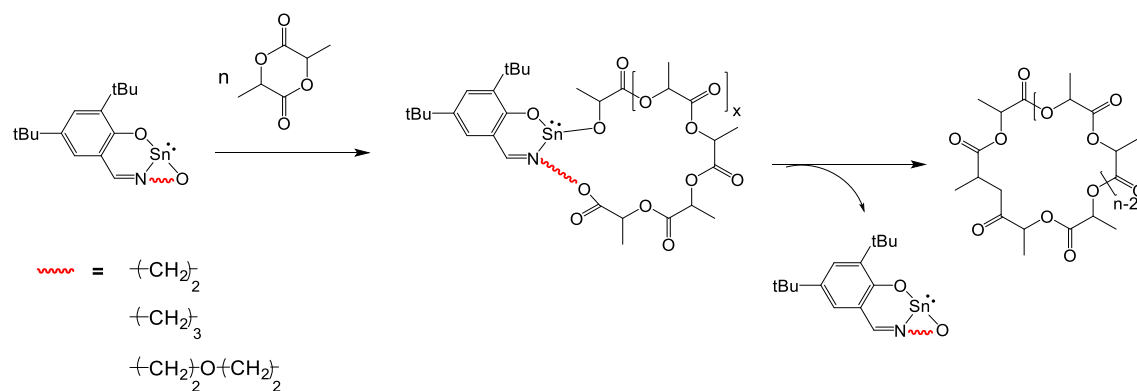
Figure 4. Tin-based catalyst containing an alkoxy side chain that initiates the REP of lactide

The organotin-based ring expansion was then adapted for the preparation of catenated rings (Figure 5). A newly synthesized catenated initiator allowed the ring expansion polymerization of lactide and ε-caprolactone.[23] Later, the same authors expanded this strategy for the preparation of more complex structures using a bis-copper templated initiator.[24]
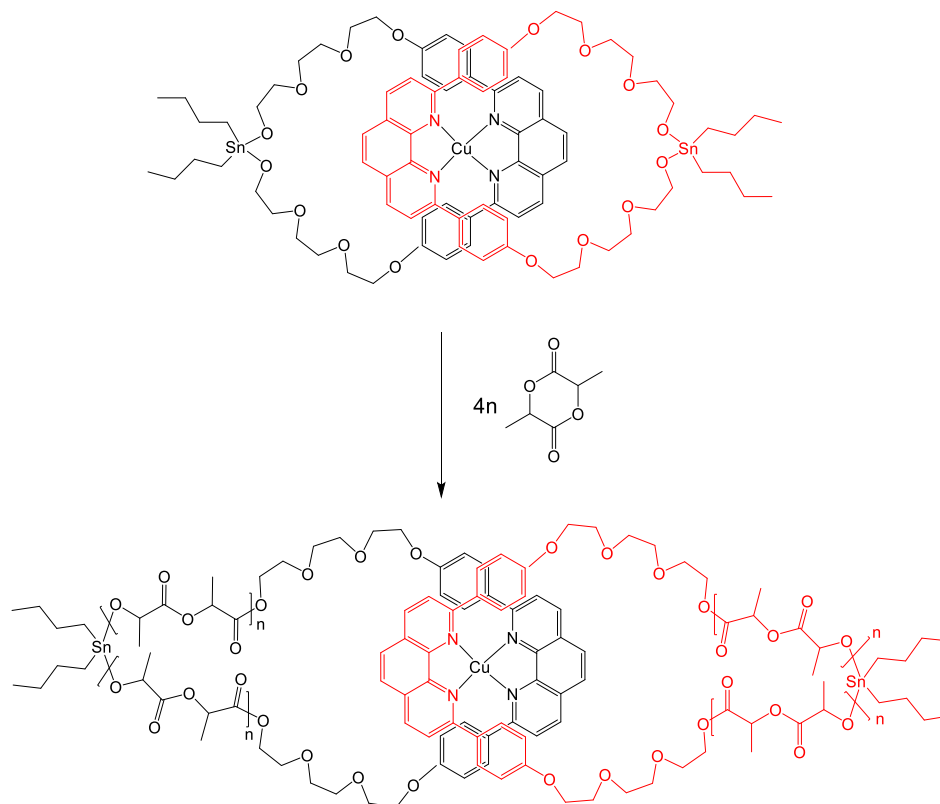
Figure 5. Catenated cyclic poly(lactide) departing from a tin based catenated catalyst

In 2015, borohydride complex catalysts of group II metals and lanthanides have been used for the REP of lactide.[25] Bulk polymerization of L-lactide at 130 °C afforded the synthesis of cyclic polymers with molecular weights as high as 30 kDa. Interestingly, the high activity of the lanthanide complexes made this process viable for extrusion polymerization. The purity of the cyclic polymer was confirmed by MALDI-ToF mass spectrometry and NMR spectroscopy.

2.2. <u>Ring expansion methathesis polymerization</u>

The ring expansion methathesis polymerization (REMP) is applicable in solution and in the melt. The potential of this method to achieve high molecular cyclic polymer was demonstrated by Grubbs et al. with the REMP of cis-cyclooctene using a ruthenium-based catalyst[26] (Figure 6). This approach relies on the metathesis of alkenes for inserting the monomer into the metallacycle ring. In other worlds, the double bonds of the monomer and the ruthenium catalyst rearrange, linking the catalyst and the monomer to form a cyclic molecule that will grow into a macrocycle upon addition of monomer. During the final step, the macrocyclic ruthenium complex undergoes an intramolecular cross-metathesis to regenerate the ruthenium catalyst and yield the cyclic polybutadiene. This work established the first route to extremely high molecular weight cyclic polybutadiene, over 100 kDa, although with a relatively high polydispersity (around 2).
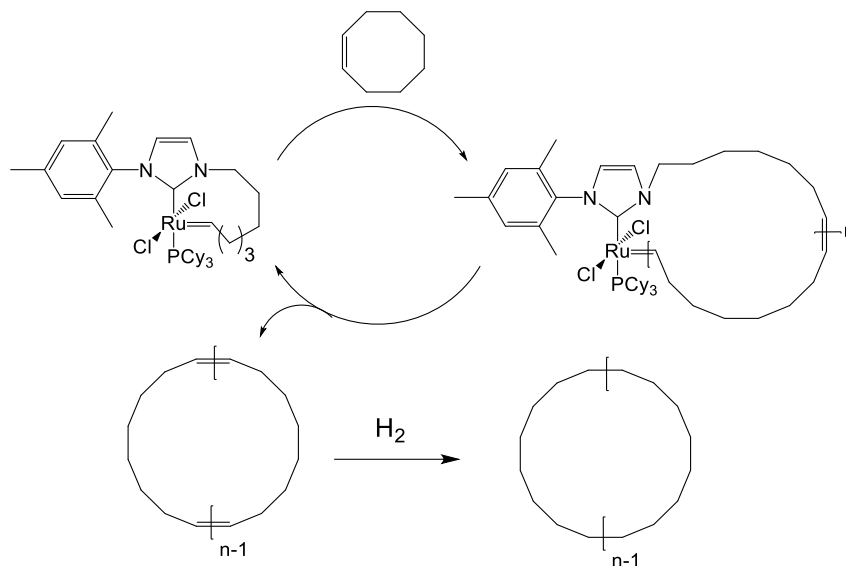
Figure 6. Ring expansion metathesis using a Ru-based catalyst for the synthesis of high molecular weight cyclic polyolefin

Later, the same authors extended this approach to the REMP of 1,5-cyclooctadiene (COD).[27] Linear byproducts were formed by polymerization of 4-vinylcyclohexane (4VC), an impurity contained in COD. The formation of those linear impurities was avoided when using 1,5,9- trans-cis-trans-cyclododecatriene (CDT) as monomer, since it is free of 4VC and form the same cyclic polybutadiene upon REMP.[27]

Veige and coworkers,[28] developed a tungsten catalyst for the REMP of norbornenes. The reaction of a trianionic pincer-supported tungsten alkyliyne complex with CO_2 generated an active tungsten-oxo alkylidene catalyst. The obtained cyclic polymers showed great control over their structures, cis-selectivity and syndiotacticity over 98%, and molecular weights up to 578 kDa with relatively low polydispersity (around 1.2).

The insertion of the monomer unit into the highly hindered metal complex is believed to provide cis selectivity, whereas the change of configuration of the metal center after each monomer unit addition gives a syndiotactic cyclic polymer. Shortly after, the same authors demonstrated that CO_2 was not mandatory to obtain a tungsten catalyst capable to initiate the REMP, while producing polymers with high cis selectivity and syndiotacticity.[29] This method presents the advantages of the controlled polymerization of norbornenes by ring opening metathesis (ROMP) and of the synthesis of ring polymers. Optimization of the synthesis of the tungsten catalyst allowed the polymerization of alkynes via the same method.[30] A variety of poly(acetylene)s could be obtained with molecular weights up to 350 kDa.

2.3. Radical ring-expansion polymerization

Radical polymerization involves a reversible hemolytic bound cleavage, propagation and radical recombination. For that reason, it is a suitable strategy to prepare cyclic polymers by ring-expansion strategy. In 2003, Pan et al.[31] used a modified reversible addition-fragmentation chain-transfer (RAFT) technique where ^{60}Co γ–rays where used to trigger the polymerization of methyl acrylate. A cyclic dithioester initiated the polymerization at a low temperature (- 30 °C) to avoid the intermolecular recombination of radicals (Figure 7). Thanks to the great versatility of controlled radical polymerization, a large variety of monomers can be polymerized through this method including copolymers. Although a significant amount of linear impurities was detected

184

by MALDI-ToF mass spectrometry, this study represents an early example of ring-expansion by radical polymerization.
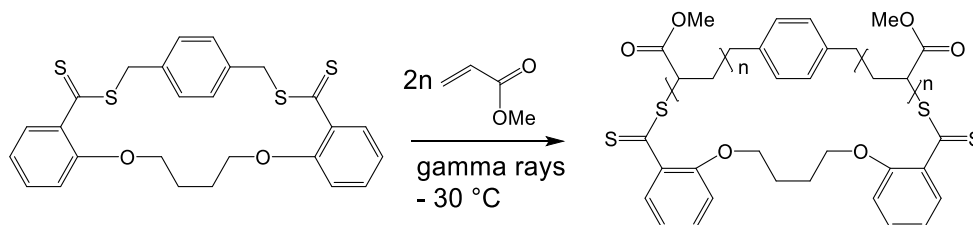

Figure 7. Radical polymerization triggered by [60]Co γ–rays for the synthesis of cyclic poly(methyl acrylate)

Nitroxide-mediated controlled radical polymerization was found to be viable for the synthesis of cyclic polystyrene via ring-expansion.[32] A cyclic initiator prepared by a multistep synthesis initiated the polymerization and yielded cyclic polymers with molecular weight up to 65 kDa. Linear impurities were detected by SEC and MALDI-ToF MS and were attributed to the intermolecular recombination of radicals. In 2016, the same authors reported a modified version of the initiator which also allowed the preparation of cyclic polymers.[33]

Advincula et al. used xanthate-based cyclic chain transfer agent for the synthesis of cyclic poly(vinylcarbazole).[34] Molecular weights up to 33 kDa were obtained and the living character of the polymerization was demonstrated by the linear increase of molecular weight as a function of time. In this example, the presence of linear impurities caused by the intermolecular recombination of radicals was also detected.

Because the two chain ends are neither ionically nor covalently bound during polymerization, the radical mediated ring-expansion technique is subject to the entropic constrains of ring closure. For that reason, linear impurities are more likely to be obtained when synthetizing cyclic polymers by this method.

2.4. Zwitterionic ring opening polymerization (ZROP)

For a large majority of polymerization reactions, the counterion is ionically bounded to the chain end. In the case where each counterion is covalently bounded to the chain, the polymerization is considered macrozwitterionic.[35] This polymerization route offers new possibilities for the synthesis of cyclic polymers. As early as 1960, Szwarc suggested that the charge cancellation of the zwitterionic chain may lead to cyclic structures.[36]

2.4.1. Nucleophilic zwitterionic ring opening polymerization

The reaction between a neutral nucleophile and a neutral cyclic monomer, leads to the formation of a zwitterionic species. After propagation and monomer depletion, the cyclic product is obtained following the charge cancelation between the two chain ends. In 2007 Waymouth described the synthesis of cyclic poly(lactide) using N-Heterocyclic carbene (NHC) organocatalysts as nucleophiles.[37] Attack to the carbonyl of the lactide

monomer by the N-heterocyclic carbene formed the zwitterionic active chain (Figure 8). After the release of the catalyst, the cyclization of macrozwitterions resulted in cyclic structures. MALDI-ToF MS, SEC and NMR confirmed the cyclic topology of the obtained material.
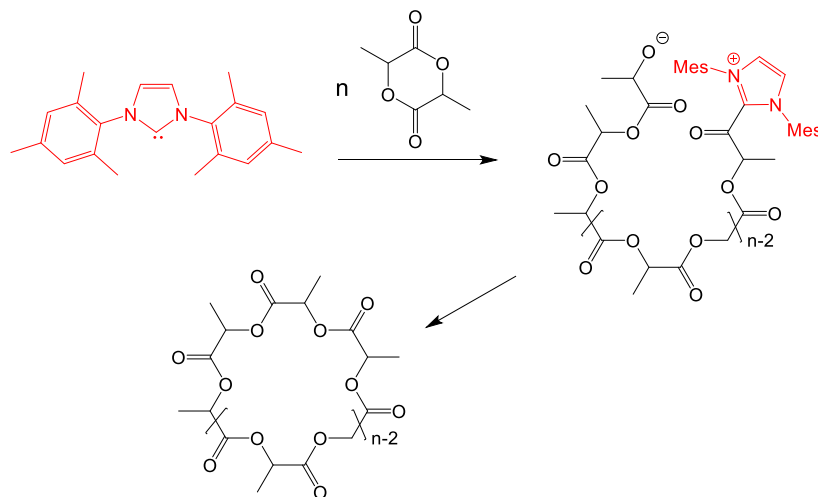
Figure 8. Zwitterionic ring-opening polymerization of lactide to yield cyclic chains

Although the ZROP initiated by N-heterocyclic carbenes is fast, high molecular weights are difficult to obtain. Other nucleophiles such as amidine[38] and pyridine[39] were used for the synthesis of cyclic poly(lactide) and poly(thioglycolide) respectively. However, linear chains were formed as well during polymerization.

For a successful cyclization of high molecular weight polymers during ZROP, propagation must by faster than the cyclization process by charge cancellation. This is

favored when the electrophile formed after the first attack of the nucleophile initiator contains a poor living group.[40] On the other hand, if the zwitterionic intermediate is not capable of cyclization, other termination steps will lead to linear polymer chains. Kricheldorf demonstrated this case for the polymerization of pivalactone initiated by pyridine, where cyclic chains were not obtained.[41]

The combination of different monomers and initiators were then investigated to increase the purity of final cyclic products. 1,8- diazabicycloundec-7-ene (DBU) was successfully used for the polymerization of N-butyl N-carboxyanhydride leading to cyclic poly(N-butylglycine).[42] The cyclic polymer exhibited controlled molecular weight and narrow polydispersity. Additionally, the growing chain was successfully extended with N-propargyl N-carboxyanhydride, a monomer that contains an alkyne group allowing post polymerization reactions. The authors reported that the polymerization of N-butyl N-carboxyanhydrides proceeded via ZROP reaction mechanism although they noted higher rates of reaction as well as improved moisture/air stability compared to previously reported NHCs initiated ZROP. Later, Waymouth et al.[43] found out that the use of bicyclic isothioureas, which are less nucleophilic than DBU, helped minimizing the formation of linear chains due to a proton abstraction of the DBU moiety by the chain end as depicted in Figure 9. Following this strategy, cyclic polymers of M_n = 66 kDa were synthesized.

Bicyclic isothioureas
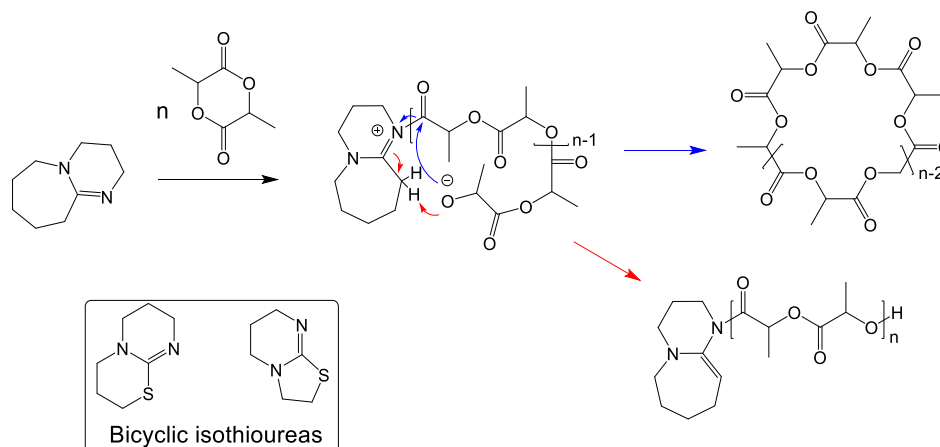
Figure 9. DBU as initiator for the ZROP of lactide leading to a mixture of linear and cyclic chains

Highly active N-heterocyclic carbine has been used to prepare cyclic poly(alkylene phosphates)[44] and cyclic poly(carbonate)s[45] with molecular weights as high as 200 kDa and 96 kDa respectively.

2.4.2. Electrophilic zwitterionic ring opening polymerization

As opposed to the nucleophilic ZROP, the electrophilic ZROP (EZROP) involves an electrophile which will activate a cyclic constrained monomer towards ring-opening. This process generates a zwitterionic species capable of growing and undergoing cyclization. In 2014, the first successful EZROP allowed the preparation of cyclic

poly(glycidyl phenyl ether)[46] under anhydrous conditions. The catalyst $B(C_6F_5)_3$ activated the epoxide monomer initiating the polymerization. The cyclic topology was maintained throughout the whole process via ionic bound of the two chain ends (Figure 10). It is worth to mention that the presence of adventitious water led to the formation of linear chains. When the polymerization was performed in THF or 1,4-dioxane, a copolymer of the solvent and the monomer was obtained. However, homopolymers of the solvent molecules could not be synthesized by this method. The following year, same authors, Barroso-Bujans et al., reported the synthesis of cyclic copolymers of THF and glycidyl phenyl ether.[47] Molecular weights ranging from 31 kDa to 330 kDa were achieved. However, MALDI-ToF MS revealed the presence of a high percentage of linear chains for higher molecular weight samples. In that case the very long polymer chains were less likely to undergo cyclization.
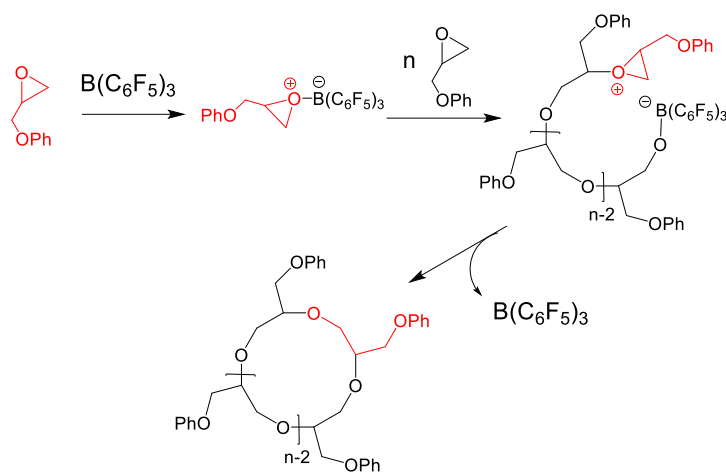

Figure 10. EZROP of glycidyl phenyl ether catalyzed by $B(C_6F_5)_3$

In 2013, Sawamoto et al.[48] combined ring-expansion cationic polymerization initiated by a hemiacetal cyclic initiator and the use of a Lewis acid, SnBr$_4$. After activation of the initiator a zwitterionic species was formed. This strategy was used for the synthesis of cyclic poly(isobutyl vinyl ether) (Figure 11). The living character of the polymerization was demonstrated by a kinetic study and sequential monomer addition. Cyclic polymers with broad polydispersity were obtained. Upon hydrolysis, monodispersed linear chains were recovered. This result suggested the fusion of rings during polymerization. Later, it was demonstrated that the fusion of cyclic chains can be suppressed by tuning the initiator concentration.[49] Further investigation by the same authors proved that pure monodisperse cyclic polymers can be prepared by diluting the reaction system.[50]
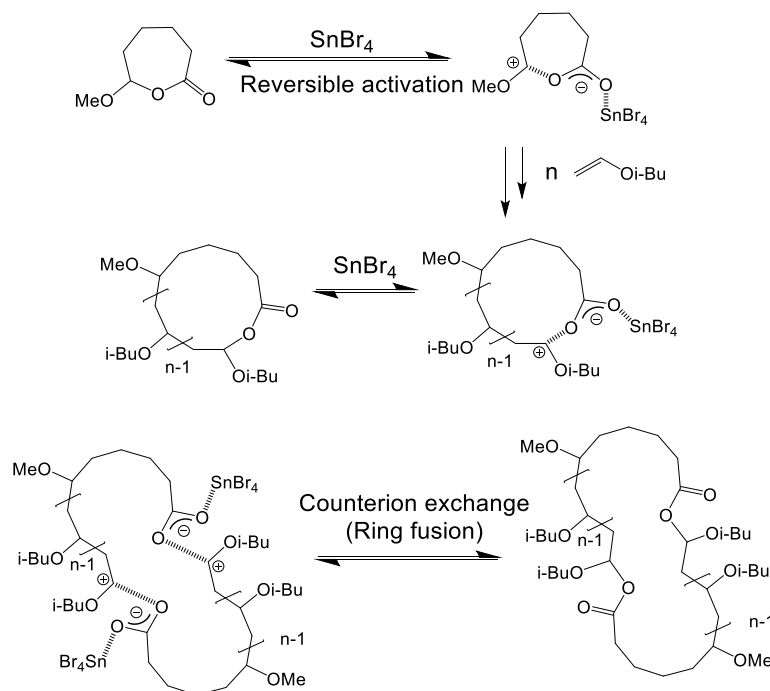

Figure 11. "Ring fusion" during ring expansion polymerization of poly(isobutyl vinyl ether) using SnBr$_4$ as Lewis acid catalyst

A similar strategy was used by Moore et al. for the synthesis of cyclic poly(phthalaldehyde).[51] Using BF_3OEt_3 and tin chloride catalyst, cyclic polymers of 109 kDa were obtained with a high polydispersity (> 2.0). Interestingly, it was demonstrated that the cyclic chains could be reopened and extended to higher molecular weight or even depolymerized to lower molecular weights.

2.4.3. Lewis pair-mediated zwitterionic ring opening polymerization

The use of organic Lewis acid/base pairs for the polymerization of lactones and methacrylates is already well documented in the literature.[52,53] In 2013, Bourissou et al. used this synthetic route for the preparation of cyclic poly(lactide), cyclic poly(ε-caprolactone) and their copolymers.[54] The combination of $Zn(C_6F_5)_2$ with an organic base (an amine or a phosphine) catalyzed the ring-opening of the cyclic monomer. Different rate of reaction were observed depending on the used base. The cyclic topology was proved by MALDI-ToF MS and NMR analysis, as no linear chains were detected. Concerning the copolymers, NMR analysis revealed the absence of heterodyads. This proved a sequential polymerization of the two monomers, with no monomer alternation and therefore the formation of a di-block copolymer. This work demonstrated that a chain extension rather than a reinitiation is possible when using Lewis acid/base pairs.

Following the work of Bourissou, Li and coworkers[55] extended this strategy to other Lewis bases such as 7-methyl-1,5,7-triazabicyclo[4.4.0]decane-5-ene (MTBD),

1,3-bis(2,4,6-trimethylphenyl)imidazol-2-ylidene (^{Mes}NHC) and DBU. The more sterically hindered bases DBU and MTBD showed a higher polymerization activity. The authors proposed a mechanism of reaction where the Lewis pair dissociates to activate the monomer towards ring-opening and to form a zwitterionic species that will maintain the cyclic topology during polymerization (Figure 12).
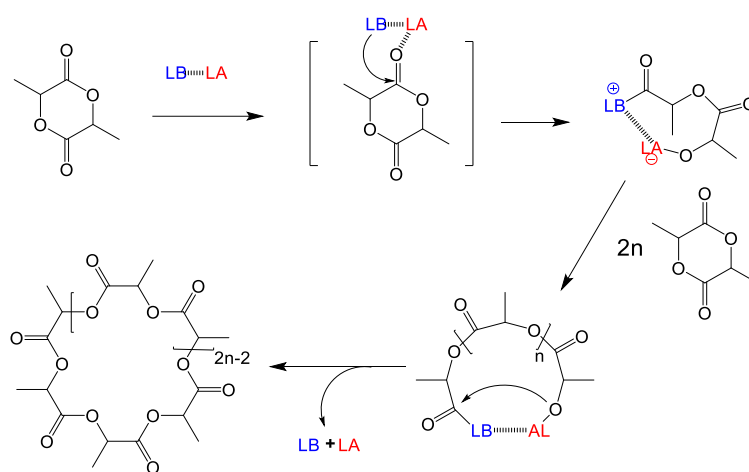

Figure 12. Proposed mechanism for the ring-expansion of lactide catalyzed by Lewis pair

3. <u>Ring closure approach</u>

3.1. <u>Bimolecular homodifunctional coupling</u>

In 1980, Höcker et al.[56] and Rempp et al.[57] reported simultaneously the first cyclic polystyrene with α,α'-dihalo-p-xylene as bifunctional coupling agent (Figure 13). To generate a dianionic "living" chain, the anionic polymerization of styrene with sodium naphthalene was performed under argon atmosphere. A solution of the obtained polymer was then added simultaneously with an equimolar solution of the coupling agent into pure tetrahydropyran, where cyclization took place under high dilution. Cyclic polymers from 3 to 25 kDa with polydispersities below 1.2 were obtained, but with rather low yields of cyclization (< 50%). After the addition of one equivalent of coupling agent, the presence of styryl anion was still detected by means of colorimetry. The presence of unreacted anions is a sign of acyclic living chains. By adding an excess of coupling agent, linear chains with much greater molecular weight than the cyclic product were formed and could be efficiently separated by fractionation. A few years later, a similar method was used to synthesize cyclic polystyrene of 450 kDa by replacing the α,α'-dihalo-p-xylene by dimethyldichlorosilane.[58] However, the yields of cyclization remained low.
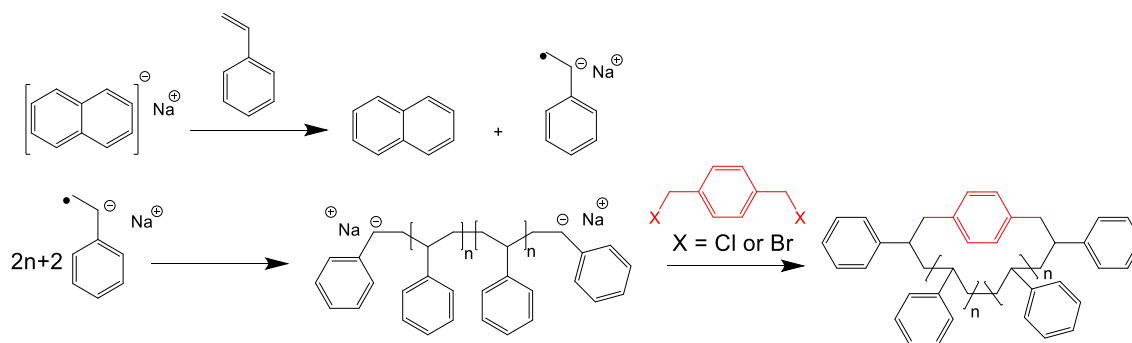
Figure 13. Synthesis of the first cyclic polystyrene via bimolecular ring closure using α,α'-dihalo-p-xylene as bifunctional coupling agent

Following a similar procedure, many groups have synthesized a diversity of cyclic homopolymers such as: poly(butadiene),[59] poly(2-vinylpyridine)[60] and poly(isoprene).[61]

In order to increase the yields of cyclization, Ishizu et al. proposed an interesting variant of the bimolecular ring closure technique.[62] In this study, intermolecular oligomerization was limited by the use of a biphasic system. Linear dibromobutyl polystyrene was first prepared by direct coupling of the polystyryl dianion with a large excess of 1,4-dibromobutane (Figure 14). Then, the cyclization of dibromobutyl polystyrene with hexamethylene diamine as coupling agent was performed via interfacial polymerization. This term refers to a step-reaction polymerization carried out at the interface between two immiscible liquid phases. The organic phase, a mixture of toluene and dimethyl sulfoxide (DMSO) contained the difunctional polystyrene while the coupling agent was dissolved in an aqueous solution of sodium hydroxide. The two liquid phases were stirred at 80 °C. The polymer was obtained after concentrating the organic phase. The authors demonstrated high yields of cyclization (> 90 %). Moreover,

with this strategy the concentration of linear precursor was as high as 10^{-3} M, while other coupling strategies typically require much lower concentration (around 10^{-6} M) to avoid intermolecular coupling. The same authors extended this strategy to the synthesis of polystyrene-b-poly(isoprene) copolymer.[63]
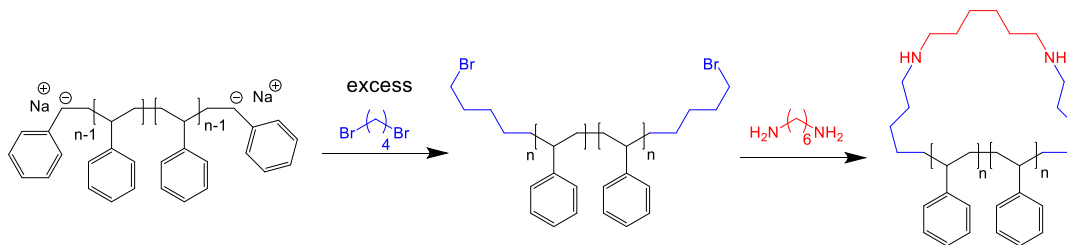
Figure 14. Cyclization of polystyrene using interfacial polymerization

The bimolecular approach was used for the preparation of cyclic block copolymers such as cyclic polystyrene-b-poly(2-vinylpyridine),[64] cyclic polystyrene-b-poly(ethylene oxide),[65] cyclic poly(propylene oxide)- b- poly(ethylene oxide),[66] cyclic poly(butadiene)-b-polystyrene[67] and cyclic poly(dimethylsiloxane)-b-polystyrene [68,69]

Tezuka et al.[70] proposed a strategy minimizing the intermolecular oligomerization and giving access to other complex structures besides monocyclic architectures. A bifunctional poly(tetrahydrofuran) [poly(THF)] was synthesized by cationic ring opening polymerization of THF with trifluoromethanesulfonic anhydride as initiator

(Figure 15).[71] The termination reaction with N-phenylpyrrolidine produced the bifunctional poly(THF) with N-phenylpyrrolidinium salt end groups. An ion exchange reaction was performed to replace the trifluoromethanesulfonate counteranion by a dicarboxylate previously synthesized. High dilution conditions favored the formation of electrostatic pre-assembly with the smallest number of components and having a balanced charge as represented in Figure 15. The formation of this particular electrostatic pre-assembly composed of one poly(THF) chain and one dicarboxylate counteranion allowed the preparation of highly pure cyclic product. Upon heating the dilute solution, the attack of the carboxylate to the pyrrolidium end-group was triggered, forming the neutral diester cyclic product. The authors have then extended this method to other cyclic polymers such as cyclic polystyrene.[72] The electrostatic self-assembly helped to minimize the formation of linear impurities, however only polymers with molecular weights below 5 kDa were achievable with this strategy.
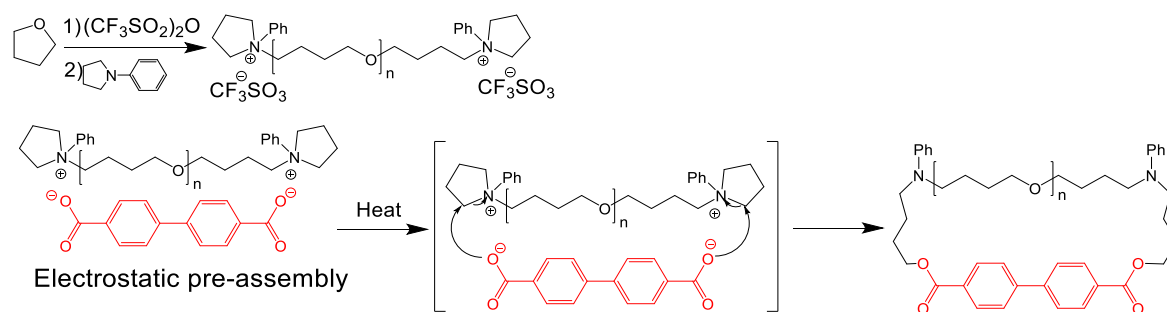

Figure 15. Cyclization via electrostatic self-assembly covalent fixation (ESA-CF)

Figure 16 shows how the use of higher functionality for the poly(THF) with N-phenylpyrrolidinium end-groups (represented in red) and the carboxylate species with the corresponding functional groups (represented in blue) allowed the synthesis of more complex polymer structures.[70]
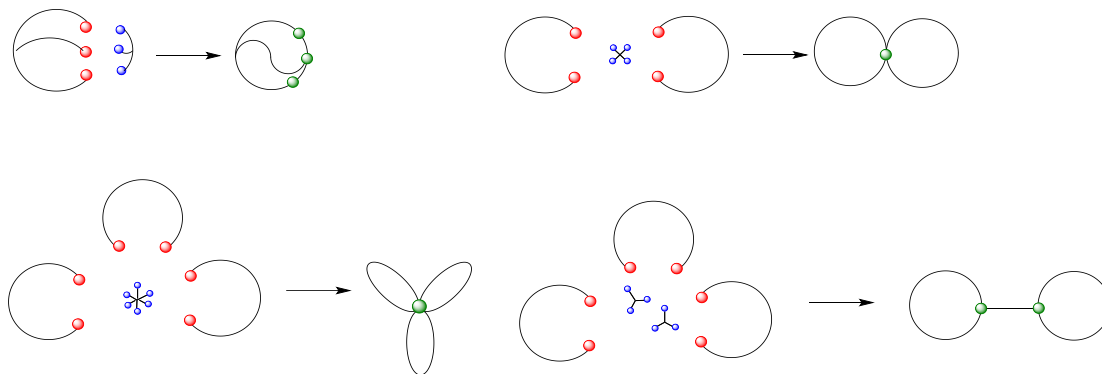
Figure 16. Different architectures accessible via electrostatic self-assembly covalent fixation (ESA-CF)

The use of the extremely fast thiol-Michael coupling reaction for the preparation of cyclic poly(lactide) was first reported by Stanford et al.[73] Under high dilution, high yield of cyclization (>95 %) was obtained. An advantage of using the thiol-ene "click" reaction is the absence of copper catalyst and the mild conditions that are compatible with sensitive polymer backbones containing ester functions for example.

More recently a self-accelerating double strain-promoted azide–alkyne cycloaddition (DSPAAC) reaction was used for the preparation of cyclic polystyrene (Figure 17).[74] An

α,ω dibromo polystyrene was prepared by atom transfer radical polymerization (ATRP). The two terminal bromides were modified into azide upon reaction with sodium azide. Cyclic polystyrene was then synthesized via DSPAAC reaction using sym-dibenzo-1,5-cyclooctadiene-3,7-diyne (DBA) as coupling agent. The intermolecular coupling between one end of the polymer chain and DBA activated the second alkyne group, which reacted much faster than the original alkyne. Thanks to this process, exact stoichiometry between the polymer chain and the coupling agent was no longer necessary. Therefore, an excess of DBA can be introduced to accelerate the first intermolecular reaction and to increase the efficiency of the cyclization reaction. Using the same strategy, multicyclic structures were obtained by using linear precursors with higher functionality.
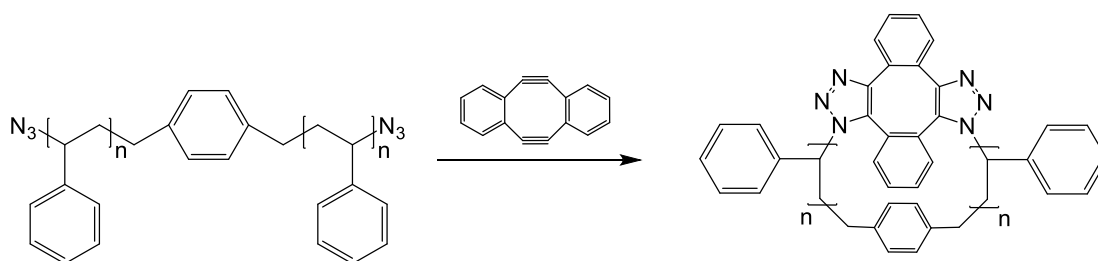

Figure 17. Cyclization of polystyrene via double-strain-promoted azide–alkyne click reaction

Later, this strategy was extended to the preparation of cyclic poly(L-lactide)[75] as well as several vinyl monomers.[76–78] Finally in 2019, a combination of ring-opening metathesis polymerization (ROMP) and DSPAAC reaction was developed for the synthesis of well-

defined cyclic poly(norbornenes)[79] with molecular weight around 8000 Da and low polydispesity index < 1.1.

3.2. <u>Homodifunctional unimolecular ring closure</u>

An early example of homocoupling cyclization was demonstrated by Tezuka et al.[80] This study involved the metathesis condensation of allyl end group of a bifunctional poly(THF). The reaction was performed under high dilution using Grubb's Ru-based catalyst. Cyclization was demonstrated via a clear shift in retention time in SEC measurements. The quantitative conversion of the allyl groups was monitored by ^{1}H NMR and MALDI-ToF MS. Concentration below 0.2 g/L was required to minimize the formation of linear impurities. This method was then extended to the preparation of cyclic poly(methyl acrylate) (PMA).[81] The linear PMA precursor was first prepared via ATRP using dimethyl-2,6-dibromoheptanedioate as initiator to yield a telechelic polymer ended in allyl groups. Then, the cyclization was realized via ring closure metathesis (RCM) using the Grubb's Ru-based catalyst, as in Tezuka work[80] (Figure 18). Later, the RCM was adapted to the synthesis of cyclic polystyrene,[82] poly(ε-caprolactone)[83] and poly(phosphoesters).[84]
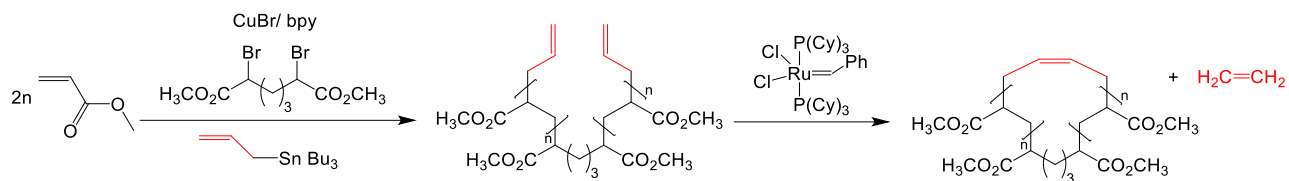
Figure 18. Synthesis of cyclic poly(methyl acrylate) combining ATRP and RCM

The formation of a carbodiimide bound through the coupling of isocyanate-terminated poly(propylene oxide) allowed the formation of cyclic polymers of low molecular weights, below 2000 Da (Figure 19).[85]
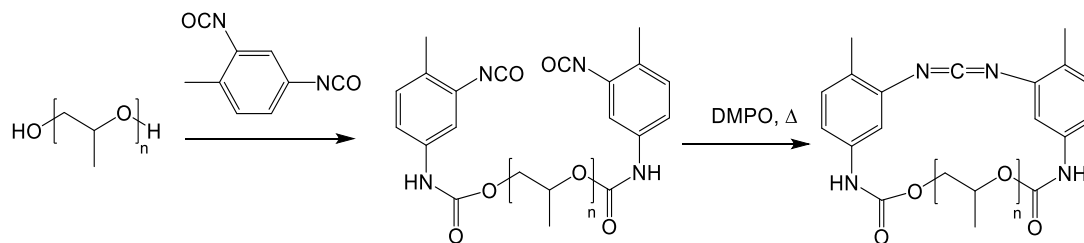
Figure 19. Isocyanate coupling for the synthesis of cyclic poly(propylene oxide)

In 2010 the coupling of radicals was also used for the preparation of cyclic polystyrene.[86] Later, a radical trap-assisted atom transfer radical coupling (RTA-ATRC) was developed to increase the yield of polymerization.[87] A nitroso radical trap was included at one end on the chain, which increased the reaction rate of the intramolecular coupling. Interestingly, the linear precursor could be recovered by heating the obtained cyclic product.

3.3. <u>Heterodifunctional unimolecular ring closure</u>

The first example of successful cyclization via this approach was performed by Deffieux et al.[88] Linear poly(2-chloroethyl vinyl ether) (PCEVE) was synthesized using 1-vinyl-4-(((vinyloxy)methoxy)methyl)benzene in the presence of hydrogen iodide to form a well-defined linear precursor containing an iodo group at one end of the chain and a styrenyl group on the other end (Figure 20). Then, the iodo end group was activated towards terminal styrenyl group with $SnCl_4$ under high dilution to produce cyclic PCEVE. Finally, the reaction was quenched with sodium methoxide to yield a stable macrocyclic polymer. Later, similar approach was used for the synthesis of cyclic polystyrene[89] with molecular weights as high as 12 kDa and high purity > 95 %. This work afforded cyclic polymers without needing further purification.
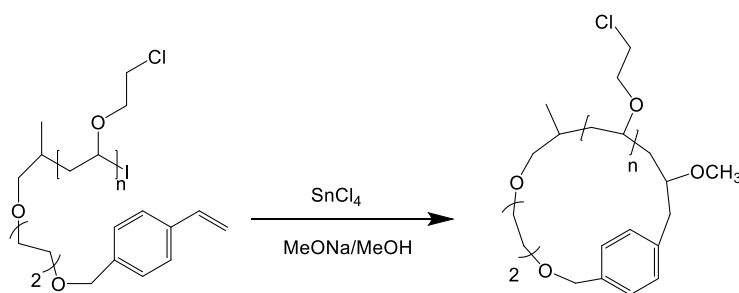
Figure 20. Synthesis cyclic PCEVE via heterocoupling of a difunctional linear precursor

In 2001, Schappacher and Deffieux[90] synthesized α-acetal,ω-bis(hydroxymethyl) heterodifunctional linear polystyrene by living anionic polymerization of styrene using 3-lithiopropionaldehyde diethyl acetal as initiator. The coupling of the two complementary chain ends gave the desired cyclic product forming a cyclic acetal linkage.

The coupling of amine and carboxylic acid was reported by Kubo et al.[91] to prepare cyclic polystyrene. The polymerization of the linear precursor was initiated by 3-lithiopropionaldehyde diethyl acetal to introduce the acetal functionality, further converted into carboxylic acid. The amine functionality was introduced using 2,2,5,5-tetramethyl-1-(3-bromopropyl)-1-aza-2,5-disilacyclopentane. The coupling of the two end groups was done under high dilution in the presence of 1-methyl-2-chloropyridium iodide as catalyst (Figure 21). The formation of the amide linkage was confirmed by ^{1}H NMR.
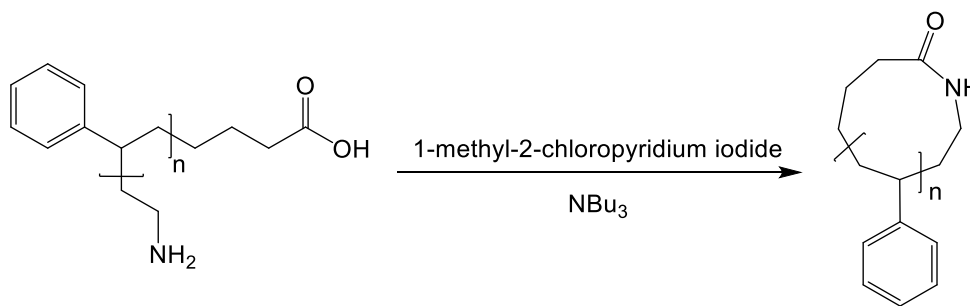
Figure 21. Amide linkage for the formation of cyclic polystyrene

The synthesis of linear polystyrene precursor by NMP for the preparation of cyclic polymer was reported by Lepoittevin et al.[92] The controlled polymerization was mediated by 4-hydroxy-2,2,6,6-tetramethylpiperidinyloxyl (4-hydroxy-TEMPO) (Figure 22). The obtained α-hydroxy-ω-carboxyl polystyrene was added dropwise into a solution containing 1-methyl-2-chloropyridium iodide to yield cyclic chains of very high purity.
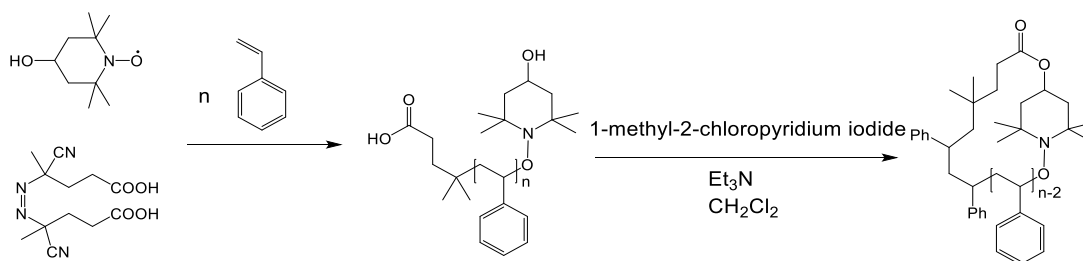
Figure 22. Linear polystyrene synthesized via NMP for the preparation of cyclic chains

Other polymerization techniques such as NMP[93] of styrene and ROP of lactones[83,94–96] have been reported in combination with copper(I)-catalyzed alkyne-azide cycloaddition (CuAAC) "click" chemistry to prepare cyclic polymers. Cyclic poly(N-isopropylacrylamide)[97] and cyclic polystyrene[98] were synthesized combining RAFT polymerization and CuAAC. The azide end group was directly incorporated by using an azide containing chain transfer agent. The complementary alkyne group was introduced at the other chain end upon end group modification. A similar strategy was employed by Monteiro et al.[99] for the synthesis of cyclic and multicyclic polystyrene (Figure 23).

Multicyclic structures were obtained from propargylated moieties linking a previously synthesized cyclic chain.
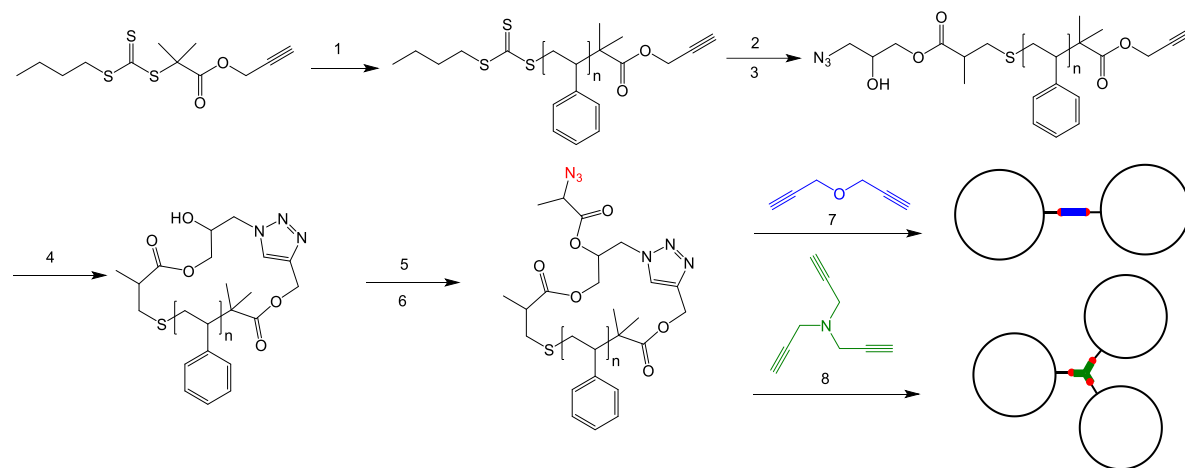
Figure 23. Combination of RAFT polymerization and CuAAC "click" chemistry to generate cyclic and multicyclic polystyrene. 1) AIBN, bulk polymerization at 65 °C for 15.5 h, 2) glycidyl methacrylate, hexylamine, TEA and TCEP in DMF at 25 °C, 3) NaN3-NH4Cl in DMF at 50 °C, 4) CuBr, PMDETA in toluene at 25°C, feed rate = 0.1 mL/min over 4.17 h and then kept for 3 h, 5) 2-bromo-propionyl bromide, TEA in THF at 0 °C-RT for 48 h, 6) NaN$_3$ in DMF at 25 °C for 16 h 7) CuBr in DMF, at 25 °C for 1 h, and 8) CuBr-triazole in toluene at 25 °C for 12 h.

Furthermore, the CuAAC "click" chemistry was also compatible for the preparation of cyclic block copolymers such as cyclic poly(methyl methacrylate)-b-polystyrene,[100] cyclic poly(2-(2-methoxyethoxy)ethyl methacrylate)-b-poly((ethylene glycol) methyl ether methacrylate),[101] cyclic polystyrene-b-poly(isoprene),[102] and cyclic poly(ethylene gylcol)-b-poly(caprolactone).[103]

The Diels-Alder reaction discovered in 1928[104] is known to be one of the simplest reactions forming carbon-carbon bonds.[105] Mizawa et al.[106] prepared cyclic poly(methyl methacrylate) via Diels-Alder reaction. A complex synthesis of the linear precursor made the overall cyclization process difficult. Years later, a more efficient procedure combining living radical polymerization and Diels-Alder coupling was reported (Figure 24).[107] The linear α-anthracene-ω-bromide polystyrene was prepared by ATRP. An end group modification reaction was performed to introduce an azide function at the ω-end of the chain. A maleimide function was then clicked to the polymer using the CuAAC reaction. Finally, Diels-Alder coupling between the anthracene and the maleimide end-groups was performed to generate the cyclic polymer.
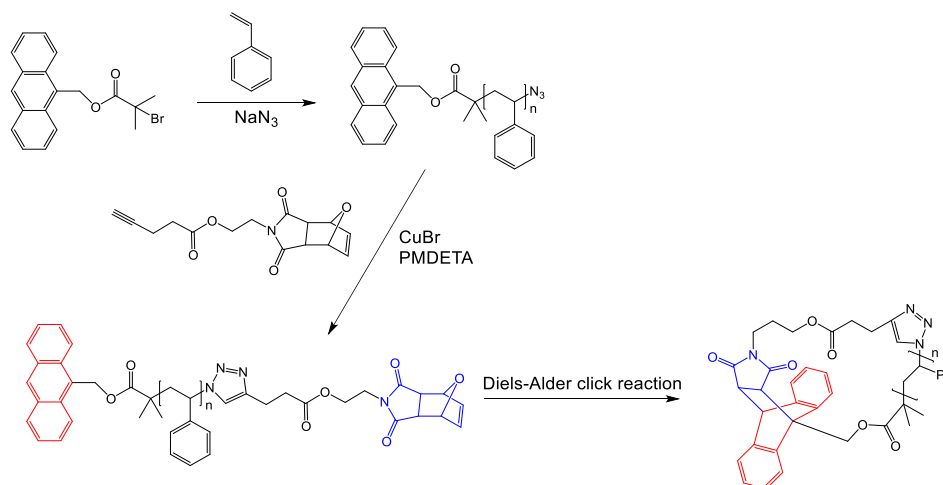
Figure 24. Diels-Alder click reaction for the synthesis of cyclic polystyrene

The cyclization was confirmed by means of SEC and ^{1}H NMR. However, the low reactivity of the diene resulted in a long reaction time (48 h) and low amounts of cyclic polymer.

Glassner et al.[108] palliated to this problem by preparing α-maleimide-ω-cyclopentadienyl functionalized precursors of poly(methyl methacrylate) and poly(tert-butyl acrylate) via ATRP using a protected maleimide containing ATRP initiator. After modification of the bromide end-group into cyclopentadiene, intramolecular Diels-Alder coupling yielded the corresponding pure monocyclic polymers. The cyclic structure was clearly identified by SEC, mass spectrometry and NMR.

One of the main advantages of Diels-Alder coupling over the CuAAC "click" reaction is its catalyst-free aspect. Indeed, the Diels-Alder reaction can be photo-induced.[109] In

2014, Josse et al.[110] used this feature for the synthesis of cyclic polyesters (Figure 25). The linear precursors were prepared by ROP of lactone monomers using 2-((11-hydroxyundecyl)oxy)-6-methyl-benzaldehyde to yield a linear chain bearing a photo-sensitive group at the α-chain end. The hydroxyl group at the ω-chain end was subsequently converted into acrylate, which upon irradiation with UV-light in diluted solution (25 mg/L) gave the corresponding cyclic polymer.
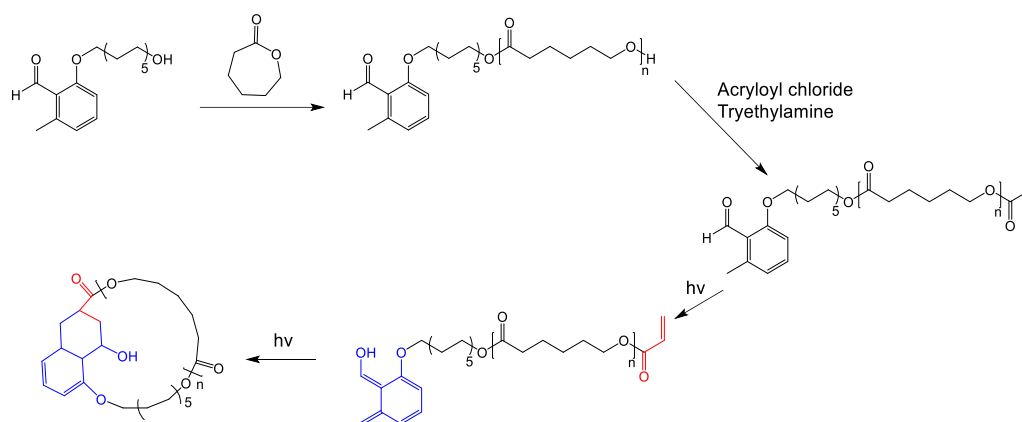
Figure 25. Photo-induced Diels-Alder coupling for the synthesis of cyclic poly(ε-caprolactone)

Cyclic polymers synthesized through this route were recovered in high yield. Indeed, since only the polymer is present in solution, simple solvent evaporation was enough and no post reaction purification steps were necessary. Moreover, the photo-initiated cycloaddition was irreversible and the product was not susceptible to undergo retro-Diels-Alder reactions.[111,112]

Since then, this route toward highly pure cyclic polymer has been intensively investigated. The mild reaction conditions make this strategy adaptable to a wide range of polymer backbones. In 2014, RAFT was combined with the light-induced Diels-Alder reaction to generate pure monocyclic chains.[113] The photosensitive moiety was introduced by a dithioester RAFT agent. A large range of polymer backbones was obtained including vinylic, acrylic and styrenic. The rapid kinetics of this ring closure technique allowed the preparation of pure cyclic polymers from a 5 g/mL solution of linear precursor. Interestingly, this method could also be used as a one-pot technique to obtain linear chains in a dilute medium before irradiation to form the corresponding cyclic product. In that way intermediate purification steps were avoided. Finally, a significant amount of material could be prepared when successive additions of the linear polymer were performed after a period of irradiation. A year later, Coulembier et al.[114] extended the use of this chemistry under sunlight irradiation.

The base-catalyzed thiol-Michael reaction already used to prepare cyclic polymers via the bimolecular approach[73] was also used by Monteiro and coworkers in the unimolecular approach.[115] In this study, the combination of RAFT with thiol-ene or thio-bromo reactions was used for the synthesis of different cyclic polymers. A previously synthesized heterofunctional trithiocarbonate RAFT agent mediated the polymerization of styrene, tert-butyl acrylate, N-isopropylacrylamide and N,N-dimethylacrylamide (Figure 26). An activated acrylate or bromide function was introduced at one chain end via post polymerization modification. The cyclization of the linear chains was performed in a one-pot reaction, via hexylamine-catalyzed cascade aminolysis and thiol-ene Michael or thio-bromo addition sequence. As a result, cyclic polymers of around 4 kDa in high yields (>80 %) were generated.
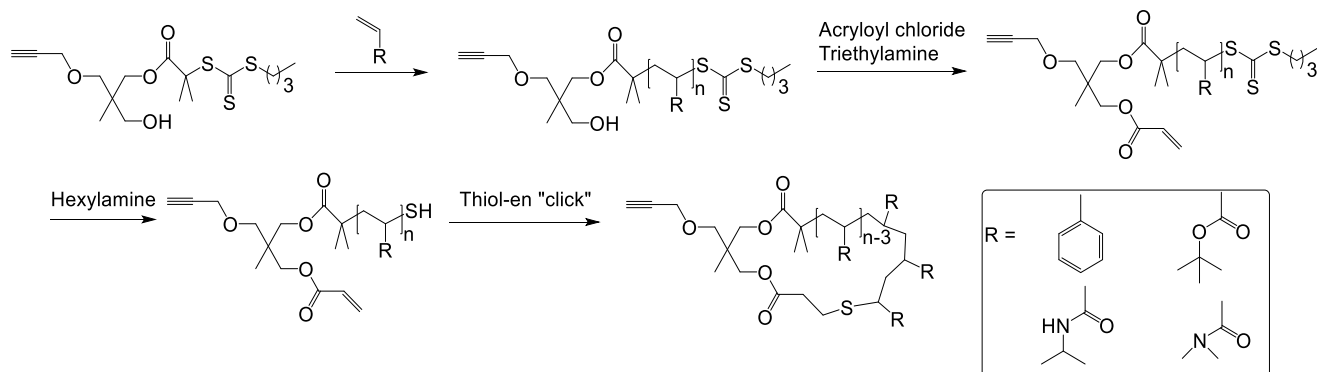
Figure 26. RAFT polymerization combined with tiol-Michael reaction for the synthesis of cyclic polymers

A similar strategy has been employed for the preparation of cyclic poly(N-isopropylacrylamide).[116] An α-anthracene-ω-thiol linear precursor was synthesized by RAFT polymerization followed by an aminolysis sequence. Finally, the intramolecular coupling of the two end groups was performed under high dilution.

In this context of finding alternatives to the CuAAC "click" chemistry, the group of Zhang explored the use of thiol-bromomaleimide substitution click reaction.[117,118] Using this method, cyclic water soluble poly(N-isopropylacrylamide) and poly(N,N-dimethylacrylamide) were prepared. The linear precursors were synthesized by RAFT polymerization (Figure 27). After reduction of the thiocarbonylthio group, the efficient thiol-bromomaleimide substitution click reaction afforded pure cyclic polymers.
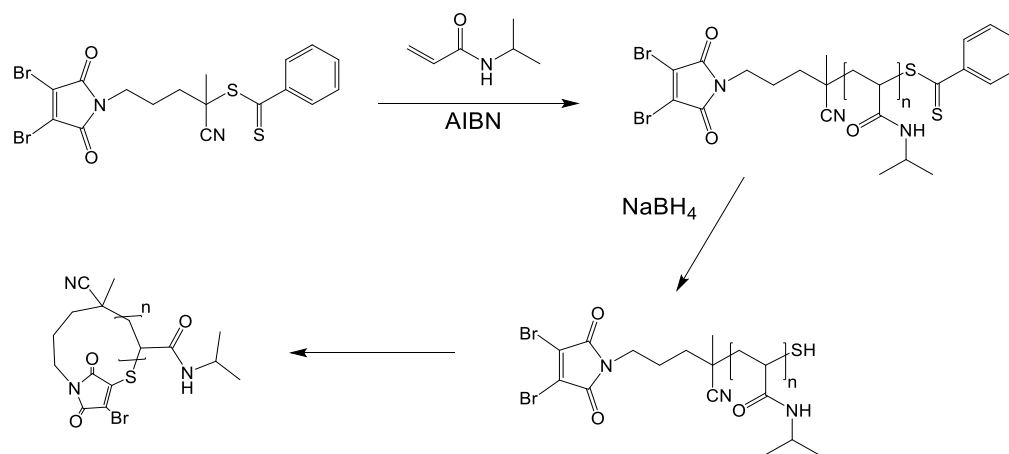
Figure 27. RAFT polymerization combined with thiol-bromomaleimide substitution click reaction for the synthesis of cyclic poly(N-isopropylacrylamide)

In the effort to eliminate the use of copper-based catalyst in click reactions for biological applications, while retaining the high efficiency of the CuAAC reaction, the strain promoted azide-alkyne cycloaddition (SPAAC) reaction was developed. It was demonstrated that this new strategy shares the same efficiency as CuAAC.[119,120] This synthetic route was extended to the preparation of cyclic polymers.[121] Well defined linear polystyrene having a bromo at one chain end and a cyclopropenone-masked dibenzocyclooctyne at the other was prepared by ATRP (Figure 28). The bromo group was modified into azide following the reaction scheme. Then, under UV-irradiation and high dilution the cyclopropenone-masked dibenzocyclooctyne was deprotected allowing the strained alkyne to react with the complementary azide and to yield the corresponding cyclic polymer. Interestingly, a batch procedure where three successive additions of the linear precursor (7 mg) into 30 mL of solvent followed by UV-irradiation for 5 h gave pure cyclic polymer in high amounts.
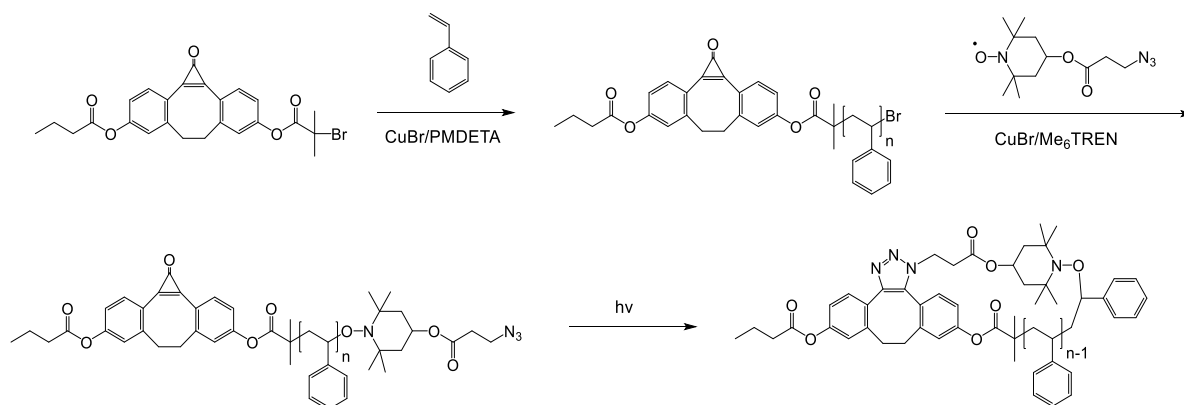
Figure 28. UV-promoted SPAAC reaction for the synthesis of cyclic polystyrene

More recently, RAFT polymerization was combined for the first time with sulfur(VI)-fluoride exchange (SuFEx) click reaction[122] to synthesize cyclic poly(N-isopropylacrylamide) and cyclic poly(N-vinylpyrrolidone).[123] A new RAFT agent containing both ether and sulfonyl fluoride moieties was developed in order to incorporate the two complementary end groups at both ends of the chain (Figure 29). The SuFEx click reaction presents the advantages of being inert to UV light, insensitivity to oxygen and water. Its fast reaction rates at room temperature, high yields, high tolerance toward various functional groups, and easy manipulation allow the preparation of a large library of cyclic polymers. Moreover, the use of a metal-catalyst is not required. The linear precursor was added slowly into a catalyst solution to maintain high dilution. Cyclic polymers of 5 kDa with a polydispersity <1.2 were obtained.
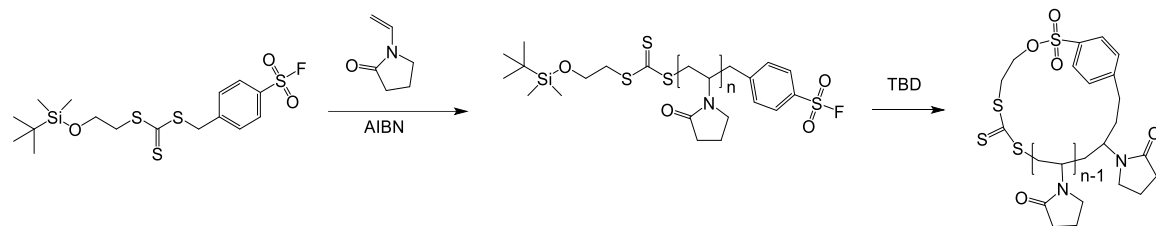
Figure 29. RAFT polymerization and sulfur(VI)-fluoride exchange click reaction for the synthesis of cyclic poly(N-vinylpyrrolidone)

4. <u>References</u>

(1)   Carothers, W. H. Studies on Polymerization and Ring Formation. I. An Introduction to the General Theory of Condensation Polymers. *J. Am. Chem. Soc.* **1929**, *51* (1833), 2548–2559.

(2)   Flory, P. J. Fundamental Principles of Condensation Polymerization. *Chem. Rev.* **1946**, *39* (1), 137–197.

(3)   Flory, P. J. Molecular Weight Distributions in Linear Polymers. In *Principles of Polymer Chemistry*; 1953; pp 317–346.

(4)   Jacobson, H.; Stockmayer, W. H. Intramolecular Reaction in Polycondensations. I. The Theory of Linear Systems. *J. Chem. Phys.* **1950**, *18*, 1600–1606.

(5)   Jacobson, H.; Beckmann, C. O.; Stockmayer, W. H. Intramolecular Reaction in Polycondensations. II. RingChain Equilibrium in Polydecamethylene Adipate. *J. Chem. Phys.* **1950**, *18*, 1607–1612.

(6)   Dodgson, K.; Semlyen, J. A. Studies of Cyclic and Linear Poly (Dimethyl Siloxanes): 1. Limiting Viscosity Number- Molecular Weight Relationships. *Polymer.* **1977**, *18*, 1265–1268.

(7)   Wright, P. V; Beevers, M. S. Preparation of Cyclic Polysiloxanes. In *Cyclic Polymers*; Semlyen, J. A., Ed.; New York, 1986; pp 85–133.

(8)   Clarson, S. J. Cyclic Polysiloxanes. In *Cyclic Polymers 2nd edition*; Semlyen, J. A., Ed.; 2000; pp 161–183.

(9)   Kapnistos, M.; Lang, M.; Vlassopoulos, D.; Pyckhout-Hintzen, W.; Richter, D.; Cho, D.; Chang, T.; Rubinstein, M. Unexpected Power-Law Stress Relaxation of Entangled Ring Polymers. *Nat. Mater.* **2008**, *7* (12), 997–1002.

(10)   Ricardo, A. P.; Zhang, B.; Grayson, S. M. The Influence of Small Amounts of Linear

Polycaprolactone Chains on the Crystallization of Cyclic Analogue Molecules. *RSC Advances* **2016**, 6, 48049–48063.

(11) Kricheldorf, H. R.; Lee, S. Polylactones. 35. Macrocyclic and Stereoselective Polymerization of B-D,L-Butyrolactone with Cyclic Dibutyltin Initiators. *Macromolecules* **1995**, *28*, 6718–6725.

(12) Kricheldop, H. R.; Lee, S.; Schittenhelm, N. Macrocycles, 1 Macrocyclic Polymerizations of (Thio)Lactones - Stepwise Ring Expansion and Ring Contraction. *Macromol. Chem. Phys.* **1998**, *199*, 273–282.

(13) Kricheldorf, H. R.; Lee, S.; Bush, S. Polylactones 36 . Macrocyclic Polymerization of Lactides with Cyclic Bu 2 Sn Initiators Derived from 1 , 2-Ethanediol , 2-Mercaptoethanol, and 1,2-Dimercaptoethane. *Macromolecules* **1996**, *29*, 1375–1381.

(14) Kricheldorf, H. R. Biodegradable Polymers with Variable Architectures via Ring-Expansion Polymerization. *J. Polym. Sci. Part A Polym. Chem.* **2004**, *42*, 4723–4742.

(15) Kricheldorf, H. R.; Weidner, S. M.; Scheliga, F. Cyclic Poly(L-Lactide)s via Ring-Expansion Polymerizations Catalysed by 2,2-Dibutyl-2-Stanna-1,3-Dithiolane. *Polym. Chem.* **2017**, *8*, 1589–1596.

(16) Kricheldorf, H. R.; Langanke, D. Macrocycles, 7: Cyclization of Oligo- and Poly(Ethylene Glycol)s with Dibutyltin Dimethoxide - A New Approach to (Super)Macrocycles. *Macromol. Chem. Phys.* **1999**, *200* (5), 1174–1182.

(17) Kricheldorf, H. R.; Langanke, D. Macrocycles, 8: Multiblock Copoly(Ether-Esters) of Poly(THF) and e-Caprolactone via Macrocyclic Polymerization. *Macromol. Chem. Phys.* **1999**, *200*, 1183–1190.

(18) Kricheldorf, H. R.; Langanke, D. Polylactones, 56. ABA Triblock Copolymers Derived From ε-Caprolactone or L-Lactide and a Central Polysiloxane Block. *Macromol. Biosci.* **2001**, *1* (8), 364–369.

(19) Kricheldorf, H. R.; Al-masri, M.; Schwarz, G. Macrocycles. 20. Cyclic Poly(Ethylene

Glycol) Phthalates via Ring-Exchange Substitution. *Macromolecules* **2002**, *35*, 8936–8942.

(20) Weil, J.; Mathers, R. T.; Getzler, Y. D. Y. L. Lactide Cyclopolymerization by an Alumatrane-Inspired Catalyst. *Macromolecules* **2012**, *45* (2), 1118–1121.

(21) Reisberg, S. H.; Hurley, H. J.; Mathers, R. T.; Tanski, J. M.; Getzler, Y. D. Y. L. Lactide Cyclopolymerization Kinetics, X-Ray Structure, and Solution Dynamics of (ᵗBu-SalAmEE)Al and a Cautionary Tale of Polymetalate Formation. *Macromolecules* **2013**, *46* (9), 3273–3279.

(22) Wongmahasirikun, P.; Prom-on, P.; Sangtrirutnugul, P.; Kongsaeree, P.; Phomphrai, K. Synthesis of Cyclic Polyesters: Effects of Alkoxy Side Chains in Salicylaldiminato Tin(II) Complexes. *Dalt. Trans.* **2015**, *44*, 12357–12364.

(23) Cao, P. F.; Mangadlao, J. D.; De Leon, A.; Su, Z.; Advincula, R. C. Catenated Poly(∈-Caprolactone) and Poly(l-Lactide) via Ring-Expansion Strategy. *Macromolecules* **2015**, *48* (12), 3825–3833.

(24) Cao, P. F.; Rong, L. H.; Mangadlao, J. D.; Advincula, R. C. Synthesizing a Trefoil Knotted Block Copolymer via Ring-Expansion Strategy. *Macromolecules* **2017**, *50* (4), 1473–1481.

(25) Bonnet, F.; Stoffelbach, F.; Fontaine, G.; Bourbigot, S. Continuous Cyclo-Polymerisation of L-Lactide by Reactive Extrusion Using Atoxic Metal-Based Catalysts: Easy Access to Well-Defined Polylactide Macrocycles. *RSC Adv.* **2015**, *5* (40), 31303–31310.

(26) Bielawski, C. W.; Benitez, D.; Grubbs, R. H. An " Endless " Route to Cyclic Polymers. *Science.* **2002**, *297*, 2041–2045.

(27) Bielawski, C. W.; Benitez, D.; Grubbs, R. H. Synthesis of Cyclic Polybutadiene via Ring-Opening Metathesis Polymerization : The Importance of Removing Trace Linear Contaminants. *J. Am. Chem. Soc.* **2003**, *125*, 8424–8425.

(28) Gonsales, S. A.; Kubo, T.; Flint, M. K.; Abboud, K. A.; Sumerlin, B. S.; Veige, A. S. Highly Tactic Cyclic Polynorbornene : Stereoselective Ring Expansion Metathesis

Polymerization of Norbornene Catalyzed by a New Tethered Tungsten-Alkylidene Catalyst. *J. Am. Chem. Soc.* **2016**, *138*, 4996–4999.

(29)   Nadif, S.; Kubo, T.; Gonsales, S. A.; Venkatramani, S.; Ghiviriga, I.; Sumerlin, B. S.; Veige, A. S. Introducing " Ynene " Metathesis: Ring-Expansion Metathesis Polymerization Leads to Highly Cis and Syndiotactic Cyclic Polymers of Norbornene. *J. Am. Chem. Soc.* **2016**, *138*, 6408–6411.

(30)   Roland, C. D.; Li, H.; Abboud, K. A.; Wagener, K. B.; Veige, A. S. Cyclic Polymers from Alkynes. *Nat. Chem.* **2016**, *8*, 791–796.

(31)   He, T.; Zheng, G. H.; Pan, C. Y. Synthesis of Cyclic Polymers and Block Copolymers by Monomer Insertion into Cyclic Initiator by a Radical Mechanism. *Macromolecules* **2003**, *36* (16), 5960–5966.

(32)   Narumi, A.; Zeidler, S.; Barqawi, H.; Enders, C.; Binder, W. H. Cyclic Alkoxyamine-Initiator Tethered by Azide/Alkyne-"click"- Chemistry Enabling Ring-Expansion Vinyl Polymerization Providing Macrocyclic Polymers. *J. Polym. Sci. Part A Polym. Chem.* **2010**, *48* (15), 3402–3416.

(33)   Narumi, A.; Hasegawa, S.; Yanagisawa, R.; Tomiyama, M.; Yamada, M.; Binder, W. H.; Kikuchi, M.; Kawaguchi, S. Ring Expansion-Controlled Radical Polymerization: Synthesis of Cyclic Polymers and Ring Component Quantification Based on SEC-MALS Analysis. *React. Funct. Polym.* **2016**, *104*, 1–8.

(34)   Bunha, A.; Cao, P. F.; Mangadlao, J. D.; Advincula, R. C. Cyclic Poly(Vinylcarbazole) via Ring-Expansion Polymerization-RAFT (REP-RAFT). *React. Funct. Polym.* **2014**, *80* (1), 33–39.

(35)   Johnston, D. S. Macrozwitterion Polymerization. *Adv. Polym. Sci.* **1982**, *42*, 51–106.

(36)   Szwarc, M. Some Aspects of Anionic Polymerization. *Makromol. Chemie* **1960**, *35*, 132–158.

(37)   Culkin, D. A.; Jeong, W.; Csihony, S.; Gomez, E. D.; Balsara, N. P.; Hedrick, J. L.; Waymouth, R. M. Zwitterionic Polymerization of Lactide to Cyclic Poly(Lactide)

by Using N-Heterocyclic Carbene Organocatalysts. *Angew. Chemie - Int. Ed.* **2007**, *46* (15), 2627–2630.

(38)   Brown, H. A.; De Crisci, A. G.; Hedrick, J. L.; Waymouth, R. M. Amidine-Mediated Zwitterionic Polymerization of Lactide. *ACS Macro Lett.* **2012**, *1* (9), 1113–1115.

(39)   Kricheldorf, H. R.; Lomadze, N.; Schwarz, G. Cyclic Poly(Thioglycolide) and Poly(D,L-Thiolactide) by Zwitterionic Polymerization of Dithiolane-2,4-Diones. *Macromolecules* **2007**, *40* (14), 4859–4864.

(40)   Mayr, H.; Lakhdar, S.; Maji, B.; Ofial, A. R. A Quantitative Approach to Nucleophilic Organocatalysis. *Beilstein J. Org. Chem.* **2012**, *8*, 1458–1478.

(41)   Kricheldorf, H. R.; Garaleh, M.; Schwarz, G. Tertiary Amine-Initiated Zwitterionic Polymerization of Pivalolactone - A Reinvestigation by Means of MALDI-TOF Mass Spectrometry. *J. Macromol. Sci. - Pure Appl. Chem.* **2005**, *42 A* (2), 139–148.

(42)   Li, A.; Lu, L.; Li, X.; He, L. L.; Do, C.; Garno, J. C.; Zhang, D. Amidine-Mediated Zwitterionic Ring-Opening Polymerization of N-Alkyl N-Carboxyanhydride: Mechanism, Kinetics, and Architecture Elucidation. *Macromolecules* **2016**, *49* (4), 1163–1171.

(43)   Zhang, X.; Waymouth, R. M. Zwitterionic Ring Opening Polymerization with Isothioureas. *ACS Macro Lett.* **2014**, *3* (10), 1024–1028.

(44)   Stukenbroeker, T. S.; Solis-Ibarra, D.; Waymouth, R. M. Synthesis and Topological Trapping of Cyclic Poly(Alkylene Phosphates). *Macromolecules* **2014**, *47* (23), 8224–8230.

(45)   Chang, Y. A.; Rudenko, A. E.; Waymouth, R. M. Zwitterionic Ring-Opening Polymerization of N-Substituted Eight-Membered Cyclic Carbonates to Generate Cyclic Poly(Carbonate)S. *ACS Macro Lett.* **2016**, *5* (10), 1162–1166.

(46)   Asenjo-Sanz, I.; Veloso, A.; Miranda, J. I.; Pomposo, J. A.; Barroso-Bujans, F. Zwitterionic Polymerization of Glycidyl Monomers to Cyclic Polyethers with $B(C_6F_5)_3$. *Polym. Chem.* **2014**, *5* (24), 6905–6908.

(47)   Asenjo-Sanz, I.; Veloso, A.; Miranda, J. I.; Alegría, A.; Pomposo, J. A.; Barroso-Bujans, F. Zwitterionic Ring-Opening Copolymerization of Tetrahydrofuran and Glycidyl Phenyl Ether with B(C$_6$F$_5$)$_3$. *Macromolecules* **2015**, *48* (6), 1664–1672.

(48)   Kammiyada, H.; Konishi, A.; Ouchi, M.; Sawamoto, M. Ring-Expansion Living Cationic Polymerization via Reversible Activation of a Hemiacetal Ester Bond. *ACS Macro Lett.* **2013**, *2* (6), 531–534.

(49)   Kammiyada, H.; Ouchi, M.; Sawamoto, M. Ring-Expansion Living Cationic Polymerization of Vinyl Ethers: Optimized Ring Propagation. *Macromol. Symp.* **2015**, *350* (1), 105–116.

(50)   Kammiyada, H.; Ouchi, M.; Sawamoto, M. A Convergent Approach to Ring Polymers with Narrow Molecular Weight Distributions through Post Dilution in Ring Expansion Cationic Polymerization. *Polym. Chem.* **2016**, *7* (45), 6911–6917.

(51)   Kaitz, J. A.; Diesendruck, C. E.; Moore, J. S. End Group Characterization of Poly(Phthalaldehyde): Surprising Discovery of a Reversible, Cationic Macrocyclization Mechanism. *J. Am. Chem. Soc.* **2013**, *135* (34), 12755–12761.

(52)   Zhang, Y.; Miyake, G. M.; Chen, E. Y. X. Alane-Based Classical and Frustrated Lewis Pairs in Polymer Synthesis: Rapid Polymerization of MMA and Naturally Renewable Methylene Butyrolactones into High-Molecular-Weight Polymers. *Angew. Chemie - Int. Ed.* **2010**, *49* (52), 10158–10162.

(53)   Wang, Q.; Zhao, W.; He, J.; Zhang, Y.; Chen, E. Y. X. Living Ring-Opening Polymerization of Lactones by n-Heterocyclic Olefin/Al(C$_6$F$_5$)$_3$ Lewis Pairs: Structures of Intermediates, Kinetics, and Mechanism. *Macromolecules* **2017**, *50* (1), 123–136.

(54)   Piedra-Arroni, E.; Ladavière, C.; Amgoune, A.; Bourissou, D. Ring-Opening Polymerization with Zn(C$_6$F$_5$)$_2$-Based Lewis Pairs: Original and Efficient Approach to Cyclic Polyesters. *J. Am. Chem. Soc.* **2013**, *135* (36), 13306–13309.

(55)   Li, X. Q.; Wang, B.; Ji, H. Y.; Li, Y. S. Insights into the Mechanism for Ring-Opening Polymerization of Lactide Catalyzed by Zn(C$_6$F$_5$)$_2$/Organic Superbase Lewis Pairs. *Catal. Sci. Technol.* **2016**, *6* (21), 7763–7772.

(56) Geisert, D.; Hocker, H. Synthesis and Investigation of Macrocyclic Polystyrene. *Macromolecules* **1980**, *281* (13), 653–656.

(57) Hild, G.; Kohler, A.; Rempp, P. Synthesis of Ring-Shaped Macromolecules. *Eur. Polym. J.* **1980**, *16*, 525–527.

(58) Roovers, J.; Toporowski, P. M. Synthesis of High Molecular Weight Ring Polystyrenes. *Macromolecules* **1983**, *16*, 843–849.

(59) Roovers, J.; Toporowski, P. M. Synthesis and Characterization of Ring Polybutadienes. *J. Polym. Sci. Part B Polym. Phys.* **1988**, *26* (6), 1251–1259.

(60) Hogen-Esch, T. E.; Sundararajan, J.; Toreki, W. Synthesis and Characterization of Topologically Interesting Vinyl Polymers. *Makromol. Chemie. Macromol. Symp.* **1991**, *47* (1), 23–42.

(61) Madani, A. El; Favier, J.; Hemery, P.; Sigwalt, P. Synthesis of Ring-Shaped Polyisoprene. *Polym. Int.* **1992**, *27*, 353–357.

(62) Ishizu, K.; Kanno, H. Novel Synthesis and Characterization of Cyclic Polystyrenes. *Polymer.* **1996**, *37* (8), 1487–1492.

(63) Ishizu, K.; Ichimura, A. Synthesis of Cyclic Diblock Copolymers by Interfacial Condensation. *Polymer.* **1998**, *39* (25), 6555–6558.

(64) Gan, Y.; Dong, D.; Hogen-Esch, T. E. Synthesis and Characterization of a Catenated Polystyrene-Poly(2-Vinylpyridine) Block Copolymer. *Macromolecules* **2002**, *35* (18), 6799–6803.

(65) Cramail, S.; Schappacher, M.; Deffieux, A. Controlled Synthesis and Solution Behavior of Macrocyclic Poly[(Styrene)-b-(Ethylene Oxide)] Copolymers. *Macromol. Chem. Phys.* **2000**, *201* (17), 2328–2335.

(66) Yu, G. E.; Garrett, C. A.; Mai, S. M.; Altinok, H.; Attwood, D.; Price, C.; Booth, C. Effect of Cyclization on the Association Behavior of Block Copolymers in Aqueous Solution. Comparison of Oxyethylene/Oxypropylene Block Copolymers Cyclo-$P_{34}E_{104}$ and $E_{52}P_{34}E_{52}$. *Langmuir* **1998**, *14* (9), 2278–2285.

(67) Ma, J. Synthesis of Well-Defined Macrocyclic Block Copolymers Using Living Coupling Agent Method. *Macromol. Symp.* **1995**, *49*, 41–49.

(68) Yin, R.; Hogen-Esch, T. E. Synthesis and Characterization of Narrow Molecular Weight Distribution Polystyrene-Poly(Dimethylsiloxane) Macrocyclic Block Copolymers and Their Isobaric Precursors. *Macromolecules* **1993**, *26* (25), 6952–6957.

(69) Yin, R.; Amis, E. J.; Hogen-Esch, T. E. Macromol. Symp. 85,217-238 (1994). *Macromol. Symp.* **1994**, *238*, 217–238.

(70) Oike, H.; Imaizumi, H.; Mouri, T.; Yoshioka, Y.; Uchibori, A.; Tezuka, Y. Designing Unusual Polymer Topologies by Electrostatic Self-Assembly and Covalent Fixation. *J. Am. Chem. Soc.* **2000**, *122* (40), 9592–9599.

(71) Oike, H.; Imamura, H.; Imaizumi, H.; Tezuka, Y. Tailored Synthesis of Branched and Network Polymer Structures by Electrostatic Self-Assembly and Covalent Fixation with Telechelic Poly(THF) Having AT-Phenylpyrrolidinium Salt Groups. *Macromolecules* **1999**, *32* (15), 4819–4825.

(72) Oike, H.; Hamada, M.; Eguchi, S.; Danda, Y.; Tezuka, Y. Novel Synthesis of Single- and Double-Cyclic Polystyrenes by Electrostatic Self-Assembly and Covalent Fixation with Telechelics Having Cyclic Ammonium Salt Groups. *Macromolecules* **2001**, *34* (9), 2776–2782.

(73) Stanford, M. J.; Pflughaupt, R. L.; Dove, A. P. Synthesis of Stereoregular Cyclic Poly(Lactide)s via "Thiol-Ene" Click Chemistry. *Macromolecules* **2010**, *43* (16), 6538–6541.

(74) Sun, P.; Chen, J.; Liu, J.; Zhang, K. Self-Accelerating Click Reaction for Cyclic Polymer. *Macromolecules* **2017**, *50* (4), 1463–1472.

(75) Sun, P.; Zhu, W.; Chen, J.; Liu, J.; Wu, Y.; Zhang, K. Synthesis of Well-Defined Cyclic Polyesters via Self-Accelerating Click Reaction. *Polymer.* **2017**, *121*, 196–203.

(76) Qu, L.; Sun, P.; Wu, Y.; Zhang, K.; Liu, Z. Efficient Homodifunctional Bimolecular Ring-Closure Method for Cyclic Polymers by Combining RAFT and Self-

Accelerating Click Reaction. *Macromol. Rapid Commun.* **2017**, *38* (15), 1–6.

(77)   Li, Z.; Qu, L.; Zhu, W.; Liu, J.; Chen, J. Q.; Sun, P.; Wu, Y.; Liu, Z.; Zhang, K. Self-Accelerating Click Reaction for Preparing Cyclic Polymers from Unconjugated Vinyl Monomers. *Polymer.* **2018**, *137*, 54–62.

(78)   Liu, X.; Chen, J. Q.; Zhang, M.; Wu, Y.; Yang, M.; Zhang, K. A Versatile Method for Cyclic Polymers from Conjugated and Unconjugated Vinyl Monomers. *J. Polym. Sci. Part A Polym. Chem.* **2019**, *57* (17), 1811–1820.

(79)   Zhang, M.; Wu, Y.; Liu, Z.; Li, J.; Huang, L.; Zhang, K. An Efficient Ring-Closure Method for Preparing Well-Defined Cyclic Polynorbornenes. *Macromol. Rapid Commun.* **2020**, *41* (4), 1900598.

(80)   Tezuka, Y.; Komiya, R. Metathesis Polymer Cyclization with Telechelic Poly(THF) Having Allyl Groups. *Macromolecules* **2002**, *35* (23), 8667–8669.

(81)   Hayashi, S.; Adachi, K.; Tezuka, Y. An Efficient Route to Cyclic Polymers by ATRP-RCM Process. *Chem. Lett.* **2007**, *36* (8), 982–983.

(82)   Quirk, R. P.; Wang, S. F.; Foster, M. D.; Wesdemiotis, C.; Yol, A. M. Synthesis of Cyclic Polystyrenes Using Living Anionic Polymerization and Metathesis Ring-Closure. *Macromolecules* **2011**, *44* (19), 7538–7545.

(83)   Xie, M.; Shi, J.; Ding, L.; Li, J.; Han, H.; Zhang, Y. Cyclic Poly(e-Caprolactone) Synthesized by Combination of Ring-Opening Polymerization with Ring-Closing Metathesis, Ring Closing Enyne Metathesis, or '"Click"' Reaction. *J. Polym. Sci. Part A Polym. Chem.* **2009**, *47*, 3022–3033.

(84)   Ding, L.; Lu, R.; An, J.; Zheng, X.; Qiu, J. Cyclic Polyphosphoesters Synthesized by Acyclic Diene Metathesis Polymerization and Ring Closing Metathesis. *React. Funct. Polym.* **2013**, *73* (9), 1242–1248.

(85)   Chen, C. W.; Cheng, C. C.; Dai, S. A. Reactive Macrocyclic Ether - Urethane Carbodiimide (MC - CDI): Synthesis, Reaction, and Ring-Opening Polymerization (ROP). *Macromolecules* **2007**, *40* (23), 8139–8141.

(86)   Voter, A. F.; Tillman, E. S. An Easy and Efficient Route to Macrocyclic Polymers via Intramolecular Radical-Radical Coupling of Chain Ends. *Macromolecules* **2010**, *43* (24), 10304–10310.

(87)   Voter, A. F.; Tillman, E. S.; Findeis, P. M.; Radzinski, S. C. Synthesis of Macrocyclic Polymers Formed via Intramolecular Radical Trap-Assisted Atom Transfer Radical Coupling. *ACS Macro Lett.* **2012**, *1* (8), 1066–1070.

(88)   Schappacher, M.; Deffieux, A. Synthesis of Macrocyclic Poly(2-Chloroethyl Vinyl Ether)S. *Die Makromol. Chemie, Rapid Commun.* **1991**, *12*, 447–453.

(89)   Rique-Lurbet, L.; Schappacher, M.; Deffieux, A. A New Strategy for the Synthesis of Cyclic Polystyrenes: Principle and Application. *Macromolecules* **1994**, *27* (22), 6318–6324.

(90)   Schappacher, M.; Deffieux, A. α-Acetal-ω-Bis(Hydroxymethyl) Heterodifunctional Polystyrene: Synthesis, Characterization, and Investigation of Intramolecular End-to-End Ring Closure. *Macromolecules* **2001**, *34* (17), 5827–5832.

(91)   Kubo, M.; Hayashi, T.; Kobayashi, H.; Tsuboi, K.; Itoh, T. Synthesis of α-Carboxyl, ω-Amino Heterodifunctional Polystyrene and Its Intramolecular Cyclization. *Macromolecules* **1997**, *30* (9), 2805–2807.

(92)   Lepoittevin, B.; Perrot, X.; Masure, M.; Hemery, P. New Route to Synthesis of Cyclic Polystyrenes Using Controlled Free Radical Polymerization. *Macromolecules* **2001**, *34* (3), 425–429.

(93)   O'Bryan, G.; Ningnuek, N.; Braslau, R. Cyclization of α, ω Heterotelechelic Polystyrene Prepared by Nitroxide-Mediated Radical Polymerization. *Polymer.* **2008**, *49* (24), 5241–5248.

(94)   Hoskins, J. N.; Grayson, S. M. Synthesis and Degradation Behavior of Cyclic Poly(ε-Caprolactone). *Macromolecules* **2009**, *42* (17), 6406–6413.

(95)   Hideki, M.; Ryohei, K.; Chunhong, Z.; Ryosuke, S.; Toshifumi, S.; Toyoji, K. Synthesis of Well-Defined Macrocyclic Poly(δ-Valerolactone) by & QuotClick

Cyclization". *Macromolecules* **2009**, *42* (14), 5091–5096.

(96)   Josse, T.; De Winter, J.; Dubois, P.; Coulembier, O.; Gerbaux, P.; Memboeuf, A. A Tandem Mass Spectrometry-Based Method to Assess the Architectural Purity of Synthetic Polymers: A Case of a Cyclic Polylactide Obtained by Click Chemistry. *Polym. Chem.* **2015**, *6* (1), 64–69.

(97)   Qiu, X. P.; Tanaka, F.; Winnik, F. M. Temperature-Induced Phase Transition of Well-Defined Cyclic Poly(N-Isopropylacrylamide)s in Aqueous Solution. *Macromolecules* **2007**, *40* (20), 7069–7071.

(98)   Goldmann, A. S.; Quémener, D.; Millard, P. E.; Davis, T. P.; Stenzel, M. H.; Barner-Kowollik, C.; Müller, A. H. E. Access to Cyclic Polystyrenes via a Combination of Reversible Addition Fragmentation Chain Transfer (RAFT) Polymerization and Click Chemistry. *Polymer.* **2008**, *49* (9), 2274–2281.

(99)   Hossain, M. D.; Valade, D.; Jia, Z.; Monteiro, M. J. Cyclic Polystyrene Topologies via RAFT and CuAAC. *Polym. Chem.* **2012**, *3* (10), 2986–2995.

(100)   Eugene, D. M.; Grayson, S. M. Efficient Preparation of Cyclic Poly (Methyl Acrylate) - Block -Poly (Styrene) by Combination of Atom Transfer Radical Polymerization and Click Cyclization. *Macromolecules* **2008**, *41*, 5082–5084.

(101)   Ge, Z.; Zhou, Y.; Xu, J.; Liu, H.; Chen, D.; Liu, S. High-Efficiency Preparation of Macrocyclic Diblock Copolymers via Selective Click Reaction in Micellar Media. *J. Am. Chem. Soc.* **2009**, *131* (5), 1628–1629.

(102)   Touris, A.; Hadjichristidis, N. Cyclic and Multiblock Polystyrene-Block-Polyisoprene Copolymers by Combining Anionic Polymerization and Azide/Alkyne "Click" Chemistry. *Macromolecules* **2011**, *44* (7), 1969–1976.

(103)   Zhang, B.; Zhang, H.; Li, Y.; Hoskins, J. N.; Grayson, S. M. Exploring the Effect of Amphiphilic Polymer Architecture: Synthesis, Characterization, and Self-Assembly of Both Cyclic and Linear Poly(Ethylene Gylcol)- B -Polycaprolactone. *ACS Macro Lett.* **2013**, *2* (10), 845–848.

(104)   Diels, O.; Alder, K. Synthesen in Der Hydroaromatischen Reihe. *Liebigs Ann. der*

Chemie **1928**, *98*, 460.

(105) Taticchi, A.; Fringuelli, F. *The Diels Alder Reaction Selected Practical Methods*, John Wiley.; Baffins Lane, 2002.

(106) Mizawa, T.; Takenaka, K.; Shiomi, T. Synthesis of α-Maleimide-ω-Dienyl Heterotelechelic Poly(Methyl Methacrylate) and Its Cyclization by the Intramolecular Diels-Alder Reaction. *J. Polym. Sci. Part A Polym. Chem.* **2000**, *38* (1), 237–246.

(107) Durmaz, H.; Dag, A.; Gurkan, H.; Tunca, U. Cyclic Homo and Block Copolymers Through Sequential Double Click Reactions. *J. Polym. Sci. Part A Polym. Chem.* **2010**, *48*, 5083.

(108) Glassner, M.; Blinco, J. P.; Barner-Kowollik, C. Diels-Alder Reactions as an Efficient Route to High Purity Cyclic Polymers. *Macromol. Rapid Commun.* **2011**, *32* (9–10), 724–728.

(109) Taticchi, A.; Fringuelli, F. Diels-Alder Reaction Facilitated by Special Physical and Chemical Methods. In *The Diels Alder Reaction Selected Practical Methods*; Taticchi, A., Fringuelli, F., Eds.; Baffins Lane, 2002.

(110) Josse, T.; Altintas, O.; Oehlenschlaeger, K. K.; Dubois, P.; Gerbaux, P.; Coulembier, O.; Barner-Kowollik, C. Ambient Temperature Catalyst-Free Light-Induced Preparation of Macrocyclic Aliphatic Polyesters. *Chem. Commun.* **2014**, *50* (16), 2024–2026.

(111) Porter, G.; Tchir, M. F. Flash Photolysis of an Ortho- Alkyl-Benzophenone. *Chem. Commun.* **1967**, *26*, 1372.

(112) Glassner, M.; Oehlenschlaeger, K. K.; Gruendling, T.; Barner-Kowollik, C. Ambient Temperature Synthesis of Triblock Copolymers via Orthogonal Photochemically and Thermally Induced Modular Conjugation. *Macromolecules* **2011**, *44* (12), 4681–4689.

(113) Tang, Q.; Wu, Y.; Sun, P.; Chen, Y.; Zhang, K. Powerful Ring-Closure Method for Preparing Varied Cyclic Polymers. *Macromolecules* **2014**, *47* (12), 3775–3781.

(114) Josse, T.; De Winter, J.; Altintas, O.; Dubois, P.; Barner-Kowollik, C.; Gerbaux, P.; Coulembier, O. A Sunlight-Induced Click Reaction as an Efficient Route to Cyclic Aliphatic Polyesters. *Macromol. Chem. Phys.* **2015**, *216* (11), 1227–1234.

(115) Lu, D.; Jia, Z.; Monteiro, M. J. Synthesis of Alkyne Functional Cyclic Polymers by One-Pot Thiol-Ene Cyclization. *Polym. Chem.* **2013**, *4* (6), 2080–2089.

(116) Liu, B.; Wang, H.; Zhang, L.; Yang, G.; Liu, X.; Kim, I. A Facile Approach for the Synthesis of Cyclic Poly(N-Isopropylacrylamide) Based on an Anthracene-Thiol Click Reaction. *Polym. Chem.* **2013**, *4* (8), 2428–2431.

(117) Long, S.; Tang, Q.; Wu, Y.; Wang, L.; Zhang, K.; Chen, Y. A Method for Preparing Water Soluble Cyclic Polymers. *React. Funct. Polym.* **2014**, *80* (1), 15–20.

(118) Tang, Q.; Zhang, K. A Method for Cyclic and Tadpole-Shaped Polymers. *Polym. Int.* **2015**, *64* (8), 1060–1065.

(119) Sletten, E. M.; Bertozzi, C. R. From Mechanism to Mouse: A Tale of Two Bioorthogonal Reactions. *Acc. Chem. Res.* **2011**, *44* (9), 666–676.

(120) Debets, M. F.; Van Berkel, S. S.; Dommerholt, J.; Dirks, A. J.; Rutjes, F. P. J. T.; Van Delft, F. L. Bioconjugation with Strained Alkenes and Alkynes. *Acc. Chem. Res.* **2011**, *44* (9), 805–815.

(121) Sun, P.; Tang, Q.; Wang, Z.; Zhao, Y.; Zhang, K. Cyclic Polymers Based on UV-Induced Strain Promoted Azide-Alkyne Cycloaddition Reaction. *Polym. Chem.* **2015**, *6* (22), 4096–4101.

(122) Dong, J.; Sharpless, K. B.; Kwisnek, L.; Oakdale, J. S.; Fokin, V. V. SuFEx-Based Synthesis of Polysulfates. *Angew. Chemie - Int. Ed.* **2014**, *53* (36), 9466–9470.

(123) Liu, W.; Zhang, S.; Liu, S.; Wu, Z.; Chen, H. Efficient Heterodifunctional Unimolecular Ring-Closure Method for Cyclic Polymers by Combining RAFT and SuFEx Click Reactions. *Macromol. Rapid Commun.* **2019**, *40* (20), 1–7.

MALDI-ToF MS analysis of poly(glycidyl

phenyl ether) initiated by water / t-BuP$_4$

During MALDI-ToF MS characterization of poly(glycidyl phenyl ether) (PGPE) initiated with water / phosphazene base, the presence of an unknown mass population was observed. Initially, the peak mass could not be assigned to any structure. One hypothesis was that polymer chains underwent elimination or fractionation and formed stable ionized species.[1] To clarify this, a series of MALDI-ToF MS data were recorded by changing the ionizing agent.

A water-initiated PGPE (Table 1, Entry 1, Chapter IV) was mixed with a cationizing agent, sodium, potassium or lithium, for MALDI-ToF MS measurements (Figure 1a to 1c respectively). *Trans*-2-[3-(4-*tert*-Butylphenyl)-2-methyl-2-propenylidene]malononitrile (DCTB) was used as matrix, and a laser power of 50 % was used to ionize the samples. In the three measurements, two mass populations were observed. For the first population, the mass peaks depended on the mass of the cation used during sample preparation, as expected. This set of peaks was assigned to water-initiated polymer (PGPE-OH) ionized with the corresponding cation. However, the second population did not exhibit any mass shifts when using different cations. This result proves the presence of an additional ion source independent of the cation used for measurements. Interestingly, when the polymer sample was mixed with t-BuP$_4$ before measurements, only a mass distribution attributed to the second population was observed (named P$_4$-PGPE in Figure 1d). Therefore, the unassigned peak distribution can be assigned to that produced upon laser ionization of polymer chains in the presence of residual phosphazene base.
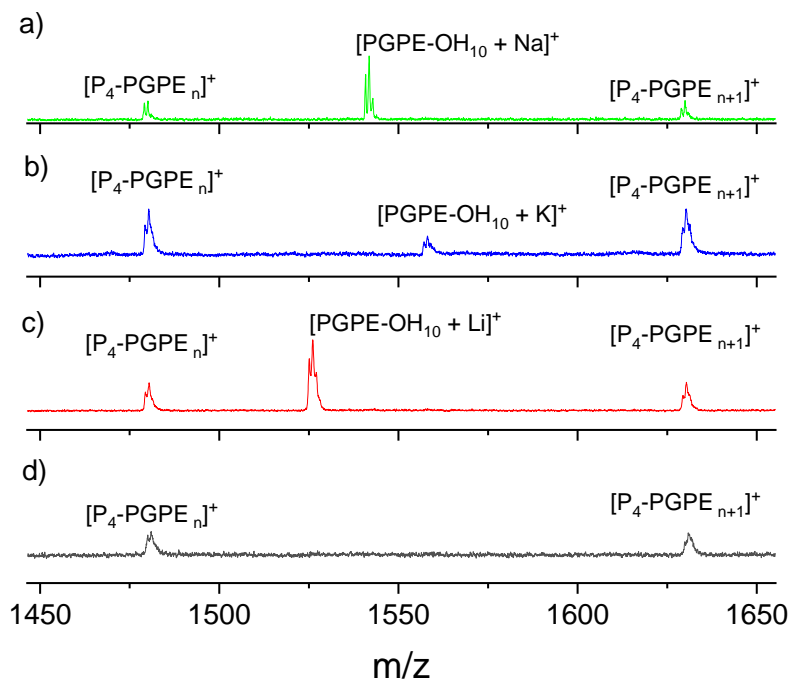
Figure 1. MALDI-ToF MS of water-initiated PGPE in the presence of a) sodium, b) potassium, c) lithium and d) t-BuP$_4$

In general, it is recommended to use low laser power during MALDI-ToF MS measurements to avoid ionization of potential impurities present at low percentage, or to avoid fractionation of polymer chains. A water-initiated PGPE sample was measured using different laser power with sodium as ionizing agent (Figure 2). When reducing the laser power during MALDI-ToF MS measurement, the intensity of the P$_4$-PGPE signal was observed to decrease drastically.
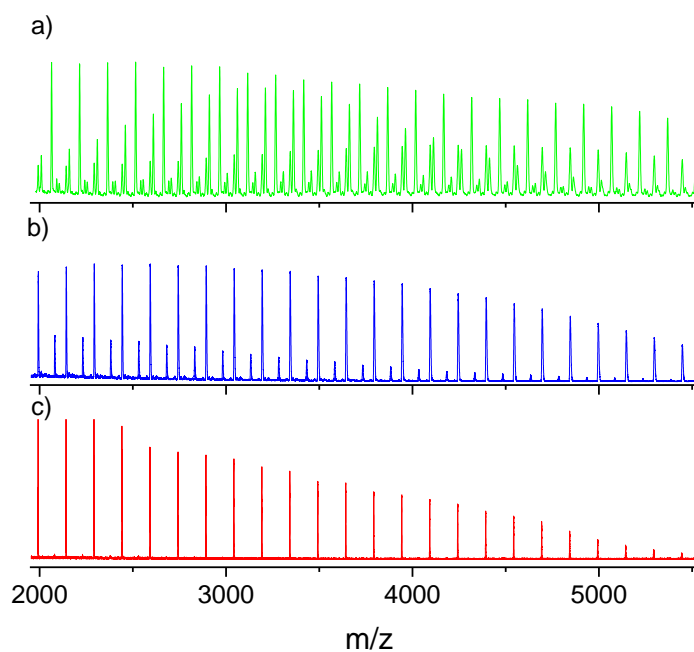
Figure 2. MALDI-ToF MS of water-initiated PGPE in the presence of sodium using a laser power of a) 80 % b) 50 % and c) 30 %

Therefore, it can be concluded that the P_4-PGPE species is not representative of the polymer sample and it is observed due to residual phosphazene base. Moreover, it is overrepresented when using high laser power.

The use of DCTB as a matrix, sodium as ionizing agent and a laser power of 30 % gave the best results for the MALDI-ToF MS analysis of PGPE samples prepared in the presence of phosphazene base.

<u>Reference</u>

(1)   Li, Y.; Hoskins, J. N.; Sreerama, S. G.; Grayson, M. A.; Grayson, S. M. The Identification of Synthetic Homopolymer End Groups and Verification of Their Transformations Using MALDI-TOFmass Spectrometry. *J. Mass Spectrom.* **2010**, *45* (6), 587–611.

List of acronyms and abbreviations

ε*	complex permittivity
[η]	intrinsic viscosity
τ	relaxation time
ω	radial frequency
ALK	alkyne group
ATRP	atom transfer radical polymerization
BDS	broadband dielectric spectroscopy
Br	bromide
c-1a-polymer	cyclic 1-arm polymer
c-2a-polymer	cyclic 2-arm polymer
Cu	copper
CuAAC	copper(I)-catalyzed alkyne-azide cycloaddition
Đ	polydispersity index
DBU	1,8-Diazabicyclo[5.4. 0]undec-7-ene
DCM	dichloromethane
DCTB	trans-2-[3-(4-tert-Butylphenyl)-2-methyl-2- propenylidene]malononitrile
DMSO	dimethyl sulfoxide
DSC	differential scanning calorimetry
DSPAAC	double strain-promoted azide–alkyne cycloaddition
EZROP	electrophilic zwitterionic ring opening polymerization

FTIR	Fourier-transform infrared spectroscopy
GPC	gel permeation chromatography
GPE	glycidyl phenyl ether
HN	Havriliak-Negami
l-1a-polymer	linear 1-arm polymer
l-2a-polymer	linear 2-arm polymer
LS	light scattering
MALDI-ToF MS	matrix assisted laser desorption ionization - time of flight mass spectrometry
MALS	multi-angle light scattering
Mn	number-average molar mass
Mw	weight-average molar mass
N_3	azide group
Na	sodium
NaOH	sodium hydroxide
NM	normal mode
NMP	nitroxide-mediated polymerization
NMR	nuclear magnetic resonance
OH	hydroxy group
PB	phosphazene base
PGPE	poly(glycidyl phenyl ether)
POx	propylene oxide
RAFT	reversible addition–fragmentation chain-transfer
RCM	ring closure metathesis
ROMP	ring-opening metathesis polymerization

RTA-ATRC	radical trap-assisted atom transfer radical coupling
SEC	size exclusion chromatography
t-BuP$_4$	1-tert-Butyl-4,4,4-tris(dimethylamino)-2,2-bis[tris(dimethylamino)-phosphoranylidenamino]-2λ5,4λ5-catenadi(phosphazene)
T$_g$	glass transition temperature
THF	tetrahydrofuran
VFT	Vogel-Tamman-Fulcher
WLF	Williams-Lander-Ferry
ZROP	zwitterionic ring opening polymerization

List of publications and conference participations

Part of the results presented in this thesis has been published and can be found in the following references:

1. **Ochs, J**.; Veloso, A.; Martínez-Tong, D. E.; Alegria, A.; Barroso-Bujans, F. An Insight into the Anionic Ring-Opening Polymerization with Tetrabutylammonium Azide for the Generation of Pure Cyclic Poly(Glycidyl Phenyl Ether). *Macromolecules* **2018**, *51* (7), 2447–2455.

2. **Ochs, J**.; Martínez-Tong, D. E.; Alegria, A.; Barroso-Bujans, F. Dielectric Relaxation as a Probe To Verify the Symmetrical Growth of Two-Arm Poly(Glycidyl Phenyl Ether) Initiated by t-BuP$_4$ /Ethylene Glycol. *Macromolecules* **2019**, *52*, 2083–2092.

3. Martínez-Tong, D. E.; **Ochs, J**.; Barroso-Bujans, F.; Alegria, A. Broadband Dielectric Spectroscopy to Validate Architectural Features in Type-A Polymers: Revisiting the Poly(Glycidyl Phenyl Ether) Case. *Eur. Phys. J. E* **2019**, *42*, 93.

4. **Ochs, J**.; Alegría, A.; Gónzalez de San Román, E.; Grayson, S. M.; Barroso-Bujans, F. Synthesis of Macrocyclic Poly(Glycidyl Phenyl Ether) with a Dipole-Inverted Microstructure via Ring Closure of Two-Arm Linear Precursors Obtained by Initiation with t-BuP$_4$ /Water (submitted).

Part of this thesis results has been presented in international conferences and seminars.

Oral presentation

1. **Ring opening polymerization and CuAAC reaction for the synthesis of pure monocyclic polyethers** <u>Jordan Ochs</u>, Daniel E. Martinez-Tong, Angel Alegria and Fabienne Barroso-Bujans. 6th Young Polymer Scientists Conference, San Sebastian, Spain, 2018.

2. **Ring opening polymerization and CuAAC reaction for the synthesis of pure monocyclic polyethers** <u>Jordan Ochs</u>, Daniel E. Martinez-Tong, Angel Alegria and Fabienne Barroso-Bujans. Polymers and Soft Matter Group seminar, Centro de Física de Materiales, San Sebastian, Spain 2018.

3. **Synthesis and characterization of cyclic poly(glycidyl phenyl ether) with controlled dipolar microstructure** <u>Jordan Ochs</u>, Angel Alegria and Fabienne Barroso-Bujans. PhD seminar series, Centro de Física de Materiales, San Sebastian, Spain 2020.

Poster presentations

1. **Synthesis of regio-regular cyclic poly(glycidyl phenyl ether)** Jordan Ochs, and Fabienne Barroso-Bujans. Ring Polymers Workshop: Future Research Perspectives, Hersonissos, Greece, 2017.

2. **Insight into the anionic ring-opening polymerization with tetrabutylammonium azide to produce cyclic polyethers** Jordan Ochs, Antonio Veloso and Fabienne Barroso-Bujans. 255th ACS National Meeting & Exposition, New Orleans, USA, 2018.

3. **Synthesis of azide-terminated polyethers with tetrabutylammonium azide for generating pure rings** Jordan Ochs, Angel Alegria and Fabienne Barroso-Bujans. Bordeaux Polymer Conference, Bordeaux, France, 2018. (Wiley-VCH prize for best poster)

4. **Ring opening polymerization and CuAAC reaction for the synthesis of pure monocyclic polyethers** Jordan Ochs, Daniel E. Martinez-Tong, Angel Alegria and Fabienne Barroso-Bujans. 10th ECNP International Conference on Nanostructured Polymers and Nanocomposites, San Sebastian, Spain, 2018.

5. **Synthesis of poly(glycidyl phenyl ether) with precise topology and dipolar microstructure confirmed by MALDI-ToF MS and Broadband Dielectric Spectroscopy** Jordan Ochs, Scott M. Grayson, Angel Alegria and Fabienne Barroso-Bujans. Applied Polymer Technology Extension Consortium Annual Meeting, Baton Rouge, USA, 2019.